UC Davis

UC Davis Electronic Theses and Dissertations

Title

Assessing the impact of novel persistent parvoviruses in free-ranging and zoo-housed wildlife

Permalink

https://escholarship.org/uc/item/26m791f5

Author

Alex, Charles E.

Publication Date

2022

Peer reviewed|Thesis/dissertation

eScholarship.org Powered by the California Digital Library
University of California

Assessing the impact of novel persistent parvoviruses in free-ranging and zoo-housed wildlife

By

CHARLES EVERETT ALEX

DISSERTATION

Submitted in partial satisfaction of the requirements for the degree of

DOCTOR OF PHILOSOPHY

in

INTEGRATIVE PATHOBIOLOGY

in the

OFFICE OF GRADUATE STUDIES

of the

UNIVERSITY OF CALIFORNIA

DAVIS

Approved:

Patricia A. Pesavento, Chair

Brian G. Murphy

Simon J. Anthony

Committee in Charge

2022

Abstract

Until recently, the genus *Amdoparvovirus* (family: *Parvoviridae*) was considered monotypic, comprising only a single recognized viral species. Aleutian Mink Disease Virus (AMDV), the type species, emerged as a significant pathogen on mink farms in the 1950s, and has been relatively well studied due to its economic importance. Despite decades of AMDV research, the pathogenesis and determinants of disease manifestation are still incompletely understood, and no effective treatment or preventative (vaccine) exists. New Amdoparvoviruses have since been discovered in several additional small carnivore species, primarily among the Mustelidae, Canidae, and Ailuridae. These discoveries have indicated a broad range of potentially susceptible host species, but the epidemiology and pathologic consequences of these infections are not well understood.

Skunk Amdoparvovirus (SKAV) was first reported in free-ranging striped skunks (*Mephitis Mephitis*) in Canada in 2017, and Red Panda Amdoparvovirus (RPAV) was first reported in a cohort of endangered western red pandas (*Ailurus fulgens*) at a zoological institution in the USA in 2018. These novel viruses offer unique opportunities to examine the impact of Amdoparvovirus infections across species, and outside of the context of a mink farm. We undertook a series of studies to evaluate the impact of SKAV and RPAV in their respective hosts.

We evaluated the prevalence of Amdoparvovirus infections in these heretofore unrecognized hosts by prospective sampling of tissues from necropsied animals and feces from living zoo-housed red pandas. The long-term management of red pandas in zoos also provided an opportunity evaluate evidence of viral persistence in individual animals based on detection and quantitation in fecal samples, which were collected prospectively over a six-year timespan. To

understand the relationships among Amdoparvoviruses within and between host species, we performed phylogenetic analyses on viral sequences obtained from prevalence studies. Finally, we evaluated tissue targets and the spectrum of Amdoparvovirus-associated lesions using *in situ* hybridization assays to localize viral nucleic acid in archived, formalin-fixed, paraffin-embedded tissues collected during necropsies.

SKAV appears to be an ancient but previously unrecognized virus in striped skunks, with infections detectable across their North American range and significant sequence variation largely attributable to geographic origin of samples. RPAV was likewise detected in zoological collections across the United States, and exhibits marked sequence variation. Three distinct clades of RPAV appear to circulate in the North American zoo-housed population, and are likely transmitted among cohorts by inter-institutional transfers for breeding or management purposes. Both SKAV and RPAV appear to infect a variety of host cell targets, including epithelium, endothelium, and leukocytes, and although asymptomatic infections appear to be common, both viruses were associated with lesions in some cases, including tubulointerstitial nephritis, myocarditis, and arteritis. We conclude that persistent Amdoparvovirus infections, while previously unrecognized, are widespread and potentially important pathogens in these hosts.

An additional study to evaluate potential viral etiologies in cases of encephalitis in American black bears (*Ursus americanus*) is also described in this thesis. Novel viruses – including a novel circovirus and a novel Chapahamaparvovirus – were detected in this study, although a specific etiologic association with lesions was not definitively identified. The approach to evaluating clinical significance of a novel and potentially pathogenic virus is the same, underscoring the importance of retrospective and prospective evaluations and the challenges associated with establishing disease causality in the context of persistent viruses.

Acknowledgements

This work would not have been possible but for the devotion and generosity of so many passionate and dedicated teachers, mentors, collaborators, and colleagues who have helped me along the way.

At VMRCVM, Drs. Tom Cecere and Tanya LeRoith, for putting me on my path.

At UC Davis, the entire faculty and staff of the VMTH Anatomic Pathology Service, for making me the pathologist I am today. Drs. Sebastian Carrasco and Sarah Cook, for the friendships and solidarity that sustained me through our residencies, and Dr. Cook especially for the camaraderie that was so vital these last few years.

At the San Diego Zoo, the entire Disease Investigations team, for showing me the power and possibilities in this work. In particular, Dr. Steve Kubiski, who has been a patient and generous mentor from the very beginning of all of this.

My qualifying exam committee: Drs. Lark Coffey, Jonna Mazet, Simon Anthony, and Brian Murphy, for their thoughtful insight into this project.

In the Pesavento lab, I am indebted to Ken Jackson for his expertise and saintly patience in the lab, to Terza Brostoff for her relentless enthusiasm and encouragement, and to Tiffany Tse, Joie Lin, Maya Schlesinger, and Eric Stubbs, who taught me so much.

Most especially, I am immensely grateful to Dr. Patricia Pesavento, for everything. It has been such an incredible privilege to observe your curiosity, passion, creativity, and compassion for the better part of a decade.

And to my family, for their endless support. Thank you.

Dedication

This is dedicated to the folks who are in it to save species, against all odds.

Table of contents

CHAPTER 1:

Introduction: Assessing the impact of novel persistent parvoviruses in free-ranging and zoo-housed wildlife

Charles E. Alex, DVM, DACVP

The family *Parvoviridae*

The family *Parvoviridae*, first established in 1975, is so-named for the miniscule, ~25-nm-diameter virions of its members.[1] The unencapsulated and notoriously durable virions contain single copies of a spartan genome, just ~4-6 kilobases in length, composed of linear, single-stranded DNA.[2,3] Genomes are organized into central coding regions flanked by non-coding terminal repeats. The coding region includes two main gene cassettes: an open reading frame (ORF) on the 5' ("left") end of the positive-sense genome encodes replication-associated non-structural (NS) proteins, and a 3' ("right") ORF encodes proteins that compose the virion shell (VP). Each gene cassette can encode multiple proteins by alternative splicing. The terminal, non-coding regions consist of imperfect palindromic repeats that fold into three-dimensional 'hairpin' structures integral for replication. Viral genome replication is initiated by NS proteins and occurs by 'rolling hairpin replication,' wherein hairpin structures prime DNA replication by host DNA polymerase, and single DNA strands are displaced and subsequently encapsidated.[2,4] The hairpin sequences are characterized as homotelomeric (the same on both ends) or heterotelomeric (differing at the 3' and 5' ends), driving minor, genus-specific differences in replication strategies.[3]

Despite their small size and simple genomic organization, the *Parvoviridae* have been tremendously successful in targeting hosts across the animal kingdom.[5] The family was

previously divided into subfamilies *Parvovirinae* and *Densovirinae* on the basis of their tropism for vertebrate or invertebrate hosts, respectively.[1] *Parvovirinae* have been detected in nearly all vertebrate clades, and the Densoviruses infect a wide variety of invertebrates including arthropods, mollusks, and echinoderms, and possibly cnidarians.[6] A taxonomic reorganization of the family was undertaken in 2020, in part to account for a growing number of divergent, vertebrate-infecting "Chapparvoviruses" that appear more closely related to some Densoviruses than *Parvovirinae*; current recommendations now recognize a third sub-family, *Hamaparvovirinae*, including the vertebrate "Chapparvoviruses" and their closely related, invertebrate-infecting phylogenetic neighbors.[7]

Phylogenetic categorization of parvoviruses is primarily based on amino acid (aa) sequence homology in the main replication-associated (NS-1) protein.[3,7] Viruses of a given genus typically share *≥35% sequence similarity, and viruses sharing ≥85% sequence identity are considered members of the same viral species. The current taxonomic organization recognizes ten genera of vertebrate-infecting Parvovirinae, eight genera of invertebrate-infecting Densovirinae, and five genera in the newly created subfamily Hamaparvovirinae, including two genera infecting vertebrates and three genera of invertebrate viruses.[7]*

The genus *Amdoparvovirus*

Within *Parvovirinae*, the genus *Amdoparvovirus* comprises a growing roster of viruses infecting small carnivores. Their ~4.7kb, heterotelomeric genomes exhibit typical parvoviral organization, with a 5' NS ORF encoding several nonstructural proteins and a 3' capsid ORF encoding 'minor' (VP1) and 'major' (VP2) capsid proteins.[8] Notably, unlike most other *Parvoviridae*, the N-terminal region of the VP-1 protein lacks a phospholipase A2 (PLA2)

domain.[4,8,9] The PLA2 domain facilitates viral escape from the endosome during infection, and its absence in the Amdoparvoviruses suggests that an alternative mechanism of endosome escape is utilized, but the details of intracellular trafficking are not well understood.

The type species for the genus, Aleutian Mink Disease Virus (AMDV), emerged in the mid-20th century as an economically important pathogen in the mink farming industry.[10] For nearly half a century AMDV was the only known Amdoparvovirus, but recent advances in molecular detection have spurred a rapid expansion of the genus in the past decade, and have foreshadowed the likelihood of additional species yet to be discovered.

Aleutian Mink Disease Virus (AMDV)

Discovery and establishment of the genus Amdoparvovirus

"Aleutian Disease" (AD) of American mink (*Mustela vison*) was initially observed in the mid-20th century.[10] It presented as a chronic, progressive wasting syndrome among farmed mink, primarily of the color-diluted 'Aleutian' phenotype.[11] This commercially popular fur phenotype occurs in mink homozygous for a recessive allele in a gene (LYST) linked to a lysosomal trafficking abnormality, similar to Chediak-Higashi disease in humans, that impairs destruction of phagocytized immune complexes.[12] The disease was originally considered a genetic disorder linked to the Aleutian genotype, but decades of interrogation ultimately implicated a novel parvoviral pathogen.[13,14] Finally fully sequenced in 1988, and clearly distinct from other known parvoviruses, AMDV became the solitary and eponymous constituent of the new genus *Amdovirus* (later revised to *Amdoparvovirus*).[15]

AMDV-associated disease

Aleutian Disease in mink primarily manifests clinically as a slowly progressive wasting syndrome, affecting mink of all color phases but particularly severely in mink of the Aleutian phenotype. Affected adult mink exhibit anorexia, cachexia, and reproductive losses.[16,17] These clinical signs are attributed to persistent infection, chronic antigenic stimulation, and an exuberant but non-neutralizing humoral immune response.[18,19] Clinicopathologic evaluation typically reveals plasmacytosis and profound hypergammaglobulinemia. Disease results from antigen-antibody complex deposition in tissues (type 3 hypersensitivity), most often manifesting as proliferative glomerulonephritis and arteritis. Typical gross findings include lymphadenomegaly, splenomegaly, hepatomegaly, mucosal ulceration, hemorrhages, and renal changes that vary from swelling and petechiation to atrophy and fibrosis depending on chronicity. Microscopically, lesions are attributed to marked plasmacytic infiltration of multiple tissues, mucosal inflammation, and membranoproliferative glomerulonephritis and interstitial nephritis. Amphophilic to basophilic intranuclear inclusion bodies in infected cells are variably reported.

In mink kits, a distinct presentation occurs due to permissive, cytolytic viral replication in pneumocytes.[20] Affected kits become dyspneic or die suddenly, and at necropsy their lungs are congested and fail to collapse. The histopathologic lesion is acute interstitial pneumonia, with pneumocyte necrosis, intra-alveolar fibrin exudation, hemorrhage, type 2 pneumocyte hyperplasia, and intra-epithelial intranuclear inclusions.

The immunologically driven pathogenesis of AD provides the basis for its diagnosis and frustrates efforts to control it. Presumptive diagnosis of AD is typically based on compatible clinical signs and clinicopathologic findings of plasmacytosis and hypergammaglobulinemia.

More specific diagnosis has historically been achieved via detection of anti-AMDV antibodies using counter-immunoelectrophoresis (CIEP) or ELISA. These methods can strongly support a diagnosis of amdoparvoviral disease, but may be cross-reactive across multiple viral species – a fact that has led to significant ambiguity in interpretation of serological studies, particularly outside of the captive (farm) setting. Control of AD on farms has posed a significant challenge. Vaccine efforts have been unsuccessful because disease is driven by the humoral response, and vaccines designed to promote humoral immunity therefore have the effect of exacerbating disease.[21–23] Treatment of individual cases focuses on supportive care and immune suppression to abrogate antigen-antibody complex formation and tissue deposition.[24,25]

Molecular epidemiology of AMDV

AMDV is believed to have originated in American mink and dispersed globally via the mink farming industry.[26] Due to its profound economic impact, extensive studies of AMDV epidemiology have been undertaken in mink farming regions (North America, Europe, China). The resulting wealth of seroprevalence and sequence data from these regions have led to significant insights into viral diversity, evolution, and spread.[8,26,27] Eradication from farms remains an elusive goal, however, and genetic determinants of virulence are still poorly understood. Fewer studies have focused on the dispersal and genetic characterization of AMDV in free-ranging mink and other species.

AMDV strains exhibit remarkable genetic diversity. Enigmatically, sequence variation is highest in the replication-associated proteins encoded by the nonstructural ORF, while capsid-coding sequences are relatively conserved.[8] It has been suggested that higher purifying pressures in the capsid gene are a reflection of a tendency toward antibody-dependent enhancement (ADE)

of infection, (i.e., that stability of epitope sequences promotes immune recognition and persistent infection of phagocytes), but this is entirely speculative.[8]

A recent global phylogenetic analysis demonstrated variation of up to 77% in the species-determining NS-1 aa sequence, prompting a recent proposal to sub-divide AMDV into at least three distinct species (AMDV-1, -2, and -3) based on taxonomic criteria for the *Parvoviridae*.[7,27] This proposed division likely reflects the historical dispersal of multiple "AMDV" variants, possibly from mink originating from disparate regions of North America. These variants are all now distributed widely and, while particular strains can be tracked in localized outbreaks, individual variants are not strictly correlated with global patterns of spread.[26]

The spread of AMDV to free-ranging animals in farming regions has been a concern, particularly in the context of endangered species. In the critically endangered European mink (*Mustela lutreola*), for example, serological studies identified putative AMDV infections in up to 32% of animals tested, although specific viral identification by sequencing was not performed.[28–31] Indeed, the historical reliance on serological methods, or on PCR detection without sequencing, complicate the interpretation of AMDV epidemiology in wildlife. Previous reports detected apparent AMDV infections by such methods in a wide variety of species, including weasels, skunks, otters, raccoons, bobcats, polecats, martens, genets, and badgers, but without correlating sequence data, and especially in the context of an increasing diversity of Amdoparvoviruses, these results cannot be definitively attributed to AMDV.[32–34]

Novel Amdoparvoviruses

Amdoparvovirus was a monotypic genus – containing only AMDV – for decades. But beginning in 2011, the genus has undergone a rapid expansion, spurred largely by advances in

sequencing technologies. It has since become clear that diverse Amdoparvoviruses infect a wide range of host species, but in most cases the significance of these infections remains unclear. Several of the newly discovered Amdoparvoviruses have been speculatively associated with disease, but rigorous studies of pathogenesis and disease association have been lacking. Following is a summary of newly discovered Amdoparvoviruses, their epidemiology, and evidence for their association with disease.

Gray Fox Amdovirus

In 2011, a novel Amdoparvovirus was identified in tissues from a gray fox (*Urocyon cinereoargenteus*) in Sonoma County, California, USA.[35] The index case was one of a group of free-ranging gray foxes that presented with gait abnormalities and myositis. Viral metagenomics, performed on tissue from the spleen, yielded a novel parvovirus with typical Amdoparvoviral features, including the apparent absence of a PLA2 domain in the VP-1 protein, and shared ~67% aa sequence identity with AMDV. The new virus was named Gray Fox Amdovirus (GFAV) – having been reported prior to a renaming of the genus from *Amdovirus* to *Amdoparvovirus* – and is recognized by ICTV under the species name *Carnivore Amdoparvovirus 2*.[7]

After its initial detection in spleen tissue, GFAV was subsequently detected in heart and lung tissue from the same animal by PCR. Subsequent PCR testing of various tissues from additional gray foxes exhibiting similar clinical signs demonstrated GFAV in heart tissue from one additional animal. Nine animals were PCR-negative, although the authors conceded that there was inconsistency in the types of tissues tested. No efforts to localize virus in tissues are reported, and no association with clinical disease was made.

Raccoon Dog and Fox Amdoparvovirus

Shortly after the discovery of GFAV, a novel Amdoparvovirus was discovered in captive raccoon dogs (*Nyctereutes procyondoides*) and Arctic foxes (*Vulpes lagopus*) in six fur farms in northeastern China.[36] Clinical signs were reported among young animals – beginning at 40 days of age – and were progressive over the course of several months. Reported signs included anorexia, emaciation, growth retardation, polydipsia, chronic diarrhea, and unkempt fur coats. Necropsy findings included splenomegaly, lymphadenomegaly, and renal congestion and "brittleness." Histopathologic lesions were not described.

Serum samples from affected animals were positive for "AMDV-specific" CIEP, and tissue samples tested by PCR demonstrated the presence of Amdoparvovirus in 90% and 100% of raccoon dogs tested, respectively. In arctic foxes from one affected farm, virus was detected in tissue, urine, or fecal samples from several arctic foxes with chronic diarrhea. Using an indirect immunofluorescence assay targeting AMDV antigen, virus was demonstrated in smears of spleen and kidney tissue of diseased raccoon dogs, but not from healthy animals. Viral cultures in Crandall-Rees Feline Kidney (CRFK) cells yielded viral particles, detected by transmission electron microscopy, that were compatible with a parvovirus. Amdoparvovirus was also reportedly detected at high rates in deep sequencing of "lesion tissues," although the specific tissues tested by this method were not reported. Amdoparvovirus was not detected by any method in any samples from reported healthy animals of either species.

Four near-full-length Amdoparvovirus genomes were obtained in this study, sharing approximately 76.7% aa sequence identity with AMDV. Phylogenetic analyses placed the new Raccoon Dog and Fox Amdoparvovirus (RDFV) in an intermediate position between AMDV

and GFAV, and this virus has officially been recognized by ICTV as *Carnivore Amdoparvovirus 3*.[7]

Skunk Amdoparvovirus

Due to their close taxonomic relationship with mink, North American striped skunks (*Mephitis mephitis*) were among the earliest subjects in experimental AMDV studies.[37,38] The first report of naturally occurring 'Aleutian Disease' in this species was published in 1986, and sporadic case reports or series in subsequent years had suggested that the presence of an AMDV-like virus in skunks was responsible for AD-like lesions.[39–43] Additionally, several sero-positivity studies in pursuit of alternative hosts for AMDV identified striped skunks as a likely reservoir.[37,38,44–46] Confirmatory DNA sequencing in these earlier reports was inconsistent, and in most cases seropositivity was interpreted as specific to AMDV, and results from DNA sequencing, where performed, were taken to indicate divergent strains of AMDV.

In 2017, the full genetic sequences of naturally occurring Amdoparvoviruses in striped skunks were reported and, for the first time, were characterized as a novel viral species.[47] Skunk Amdoparvovirus (SKAV), designated as *Carnivore Amdoparvovirus 4*, and was detected in 44 skunks found dead in Vancouver, British Columbia, Canada.[3] Strains of the novel virus shared ~80.4% aa sequence identity with AMDV in the NS-1 gene, fulfilling criteria for recognition as a distinct species. The authors additionally analyzed sequences from "AMDV-like" viruses from striped skunks in Ontario (Eastern Canada) and California, USA, and determined that these partial sequences were in fact variants of SKAV, rather than AMDV as had been previously assumed.[41,46] These preliminary findings suggested a widespread distribution of SKAV across North America, but its prevalence and impact on the species were not well understood.

Red Panda Amdoparvovirus

In 2018, we reported a novel Amdoparvovirus in zoo-housed Western red pandas (*Ailurus fulgens*) from Sacramento, California, USA.[48] Red Panda Amdoparvovirus (RPAV, ICTV designation: *Carnivore Amdoparvovirus 5*), was initially detected by metagenomics analyses of tissues from a geriatric animal that died with pyogranulomatous lesions. The novel virus shared approximately 75% aa sequence identity with AMDV. Using conventional PCR, RPAV was subsequently detected in or feces of all four co-housed red pandas from the same collection. Two of these cohort-mates, both geriatric, died shortly thereafter, and RPAV was detected in tissues of all three necropsied animals by in situ hybridization using RPAV-specific probes. In the same study, tissues from a retrospective case that died in 2003 were also tested by RPAV ISH. The finding of specific probe hybridization in this retrospective case suggested that RPAV may have been present in this collection for over a decade prior to its detection. Lesions putatively attributed to RPAV are described in detail in the original description of viral discovery.[48]

In 2022, several divergent genomes most closely related to RPAV were reported in Chinese red pandas (*Ailurus styani*) from a giant panda breeding center in China.[49] These viruses shared <80% aa sequence identity in NS1 with the RPAV sequences originally reported, indicating that these may represent a distinct viral species. Tentatively designated RpAPV-2, the virus was detected in multiple tissues from 32 dead red pandas tested, and >50% of fecal samples from primarily asymptomatic red pandas, suggesting a high prevalence, at least among captive animals housed in close proximity. Clinical disease or lesions associated with RpAPV-2 infection, if any, were not reported.

Unclassified Amdoparvoviruses

Criteria for official recognition of novel parvoviruses are fairly stringent. Specifically, proposed species must have been isolated and sequenced, or must be sequenced from samples derived from a "likely host" and reported in a peer-reviewed publication. Contiguous sequence of the full coding region must include both the major nonstructural protein, NS-1 (bearing an SF3 helicase domain that is well-conserved among the Parvoviridae), and the capsid-coding (VP) gene. Other genomic motifs and size constraints (~4-6kb) must also be met. Proposed species are then subject to independent verification by the ICTV Parvoviridae Study Group before an official designation is bestowed.[7] Because of these criteria, and the time taken for independent verification, the list of ICTV-recognized Amdoparvoviruses represent only a subset of the species that are likely to exist. 'Unofficial' Amdoparvoviruses, including those that fail some criteria for recognition or are pending ICTV review, are listed in the table below. The detection of apparent endogenous amdoparvoviral elements in the genome of a rodent (the Transcaucasian mole vole, *Ellobius lutescens*) provides additional support for a likely larger-than-appreciated host range for diverse Amdoparvoviruses.[52,53,54]

Virus name	**Abbreviation**	**ICTV status**	**Putative maintenance host**	**Reference**
British Columbia Amdoparvovirus	BCAV	Pending recognition	Mink	[27]
Labrador Amdoparvovirus 1	LaAV-1	Pending recognition	Martens	[50]
Labrador Amdoparvovirus 2	LaAV-2	Not eligible (partial sequence)	Fox	[50]
Red Panda Amdoparvovirus 2	RpAPV-2	Pending recognition	Chinese red panda	[49]
Red Fox Fecal Amdovirus	RFFAV	Not eligible (partial sequence)	Red fox	[51]
Rattus nitidus parvovirus	RtRn-ParV	Not eligible (partial sequence)	Rat	[52]

Rhinolophus Lepidus parvovirus	BtRl-PV	Not eligible (partial sequence)	Horseshoe bat	[53]
Rhinolophus pusillus parvovirus	Rp-BtAMDV1	Not eligible (partial sequence)	Horseshoe bat	[54]

Objectives of the thesis

The studies included in this dissertation focus on two recently discovered Amdoparvoviruses: Skunk Amdoparvovirus (SKAV) and Red Panda Amdoparvovirus (RPAV). These novel viruses – in, respectively, an exceedingly common wildlife species and an exceedingly rare, endangered species – are of particular concern, and offer unique opportunities to understand Amdoparvovirus epidemiology and disease. Both viruses have been detected among asymptomatic animals, but have also been linked to significant, even fatal disease.[42,48] Striped skunks, ubiquitous throughout North America, have the potential to disseminate infections widely, including at the busy wildlife-domestic animal interface of suburbia where they thrive. Red pandas, native to temperate forest of the Himalayas, are a species of significant conservation concern, with population estimates of <10,000 animals remaining in the wild.[55] Zoo populations are a critical safeguard for the survival of the species, and the discovery of a novel potential pathogen in this species necessitates a thorough investigation into the consequences of infection. Moreover, this zoo-housed population is subject to careful medical attention and deceased animals are nearly always necropsied, providing unique opportunities to evaluate viral persistence and disease association.

The epidemiology and phylogenetic relationships among these novel Amdoparvoviruses are not well understood, and few studies have substantively examined the pathogenesis of amdoparvoviral disease in species other than mink. This is critical information for determining

the possible impact of these infections in their retrospective hosts and – at least for the endangered red panda – whether intervention may be necessary to mitigate losses. To begin to address this gap in knowledge, the objectives of this thesis were to (1) determine the prevalence of Amdoparvovirus infections in free-ranging striped skunks and zoo-housed red pandas in North America; (2) characterize phylogenetic relationships among Amdoparvoviruses in striped skunks and red pandas; and (3) identify potential manifestations of Amdoparvovirus-associated disease in these species.

Underscoring the ubiquity of novel, enigmatic ssDNA viruses – and the need for fulsome studies of potential roles in disease – a fourth objective of this thesis is to characterize possible viral etiologies for a syndrome of idiopathic encephalitis observed in Northern California black bears (*Ursus americanus*), with particular attention to a novel Circovirus and a novel Chapahamaparvovirus (subfamiliy: *Hamaparvovirinae*).

References

1. Cotmore, S. F. *et al.* The family Parvoviridae. *Arch. Virol.* **159**, 1239–1247 (2014).
2. Kerr, J., Cotmore, S. & Bloom, M. E. *Parvoviruses*. (CRC Press, 2005).
3. Cotmore, S. F. *et al.* ICTV Virus Taxonomy Profile: Parvoviridae. *J. Gen. Virol.* **100**, 367–368 (2019).
4. Cotmore, S. F. & Tattersall, P. Parvoviruses: Small Does Not Mean Simple. *Annu Rev Virol* **1**, 517–537 (2014).
5. Jager, M. C., Tomlinson, J. E., Lopez-Astacio, R. A., Parrish, C. R. & Van de Walle, G. R. Small but mighty: old and new parvoviruses of veterinary significance. *Virol. J.* **18**, 210 (2021).
6. Pénzes, J. J., Pham, H. T., Yu, Q., Bergoin, M. & Tijssen, P. Parvoviruses of Invertebrates (Parvoviridae)1. in *Encyclopedia of Virology (Fourth Edition)* (eds. Bamford, D. H. & Zuckerman, M.) 835–848 (Academic Press, 2021).
7. Pénzes, J. J. *et al.* Reorganizing the family Parvoviridae: a revised taxonomy independent of the canonical approach based on host association. *Arch. Virol.* **165**, 2133–2146 (2020).
8. Canuti, M. *et al.* Driving forces behind the evolution of the Aleutian mink disease parvovirus in the context of intensive farming. *Virus Evol* **2**, vew004 (2016).
9. Zádori, Z. *et al.* A viral phospholipase A2 is required for parvovirus infectivity. *Dev. Cell* **1**, 291–302 (2001).
10. Hartsough, G. R. & Gorham, J. R. Aleutian disease in mink. *National Fur News* **28**, 10–11 (1956).

11. Russell JD, Bennett JR, Hancock, BB. The etiology and pathogenesis of Aleutian disease in mink. *Lab. Anim. Care* **13**, (1963).
12. Anistoroaei, R., Krogh, A. K. & Christensen, K. A frameshift mutation in the LYST gene is responsible for the Aleutian color and the associated Chédiak-Higashi syndrome in American mink. *Anim. Genet.* **44**, 178–183 (2013).
13. Hahn, E. C., Ramos, L. & Kenyon, A. J. Expression of Aleutian mink disease antigen in cell culture. *Infect. Immun.* **15**, 204–211 (1977).
14. Porter, D. D., Larsen, A. E., Cox, N. A., Porter, H. G. & Suffin, S. C. Isolation of Aleutian disease virus of mink in cell culture. *Intervirology* **8**, 129–144 (1977).
15. Bloom, M. E., Alexandersen, S., Perryman, S., Lechner, D. & Wolfinbarger, J. B. Nucleotide sequence and genomic organization of Aleutian mink disease parvovirus (ADV): sequence comparisons between a nonpathogenic and a pathogenic strain of ADV. *J. Virol.* **62**, 2903–2915 (1988).
16. Eklund, C. M., Hadlow, W. J., Kennedy, R. C., Boyle, C. C. & Jackson, T. A. Aleutian disease of mink: properties of the etiologic agent and the host responses. *J. Infect. Dis.* **118**, 510–526 (1968).
17. Karstad, L. Aleutian disease--an example of slowly-progressive infectious disease. *Can. Vet. J.* **11**, 36–38 (1970).
18. Bloom, M. E., Race, R. E., Hadlow, W. J. & Chesebro, B. Aleutian disease of mink: the antibody response of sapphire and pastel mink to Aleutian disease virus. *J. Immunol.* **115**, 1034–1037 (1975).

19. Porter, D. D., Larsen, A. E. & Porter, H. G. The pathogenesis of Aleutian disease of mink. I. In vivo viral replication and the host antibody response to viral antigen. *J. Exp. Med.* **130**, 575–593 (1969).

20. Larsen, S., Alexandersen, S., Lund, E., Have, P. & Hansen, M. Acute interstitial pneumonitis caused by Aleutian disease virus in mink kits. *Acta Pathol. Microbiol. Immunol. Scand. A* **92A**, 391–393 (2009).

21. Porter, D. D., Larsen, A. E. & Porter, H. G. The pathogenesis of Aleutian disease of mink. II. Enhancement of tissue lesions following the administration of a killed virus vaccine or passive antibody. *J. Immunol.* **109**, 1–7 (1972).

22. Bloom, M. E. *et al.* Identification of aleutian mink disease parvovirus capsid sequences mediating antibody-dependent enhancement of infection, virus neutralization, and immune complex formation. *J. Virol.* **75**, 11116–11127 (2001).

23. Best, S. M. & Bloom, M. E. Pathogenesis of aleutian mink disease parvovirus and similarities to b19 infection. *J. Vet. Med. B Infect. Dis. Vet. Public Health* **52**, 331–334 (2005).

24. Cheema, A., Henson, J. B. & Gorham, J. R. Aleutian disease of mink. Prevention of lesions by immunosuppression. *Am. J. Pathol.* **66**, 543–556 (1972).

25. Alexandersen, S., Storgaard, T., Kamstrup, N., Aasted, B. & Porter, D. D. Pathogenesis of Aleutian mink disease parvovirus infection: effects of suppression of antibody response on viral mRNA levels and on development of acute disease. *J. Virol.* **68**, 738–749 (1994).

26. Zaleska-Wawro, M., Szczerba-Turek, A., Szweda, W. & Siemionek, J. Seroprevalence and Molecular Epidemiology of Aleutian Disease in Various Countries during 1972-2021: A Review and Meta-Analysis. *Animals (Basel)* **11**, (2021).

27. Canuti, M., Pénzes, J. J. & Lang, A. S. A new perspective on the evolution and diversity of the genus Amdoparvovirus (family Parvoviridae) through genetic characterization, structural homology modeling, and phylogenetics. *Virus Evol* **8**, veac056 (2022).
28. Mañas, S. *et al.* Aleutian mink disease parvovirus in wild riparian carnivores in Spain. *J. Wildl. Dis.* **37**, 138–144 (2001).
29. Mañas, S. *et al.* PREVALENCE OF ANTIBODY TO ALEUTIAN MINK DISEASE VIRUS IN EUROPEAN MINK (MUSTELA LUTREOLA) AND AMERICAN MINK (NEOVISON VISON) IN SPAIN. *J. Wildl. Dis.* **52**, 22–32 (2016).
30. Sánchez-Migallón Guzmán, D. *et al.* Aleutian disease serology, protein electrophoresis, and pathology of the European mink (Mustela lutreola) from Navarra, Spain. *J. Zoo Wildl. Med.* **39**, 305–313 (2008).
31. Maran, T., Skumatov, D., Gomez, A., Põdra, M., Abramov, A.V. & Dinets, V. Mustela lutreola. *The IUCN Red List of Threatened Species 2016: e.T14018A45199861.* (2016) doi:10.2305/IUCN.UK.2016-1.RLTS.T14018A45199861.en.
32. Fournier-Chambrillon, C. *et al.* Antibodies to Aleutian mink disease parvovirus in free-ranging European mink (Mustela lutreola) and other small carnivores from southwestern France. *J. Wildl. Dis.* **40**, 394–402 (2004).
33. Farid, A. H. Aleutian mink disease virus in furbearing mammals in Nova Scotia, Canada. *Acta Vet. Scand.* **55**, 10 (2013).
34. Knuuttila, A. *et al.* Aleutian mink disease virus in free-ranging mustelids in Finland - a cross-sectional epidemiological and phylogenetic study. *J. Gen. Virol.* **96**, 1423–1435 (2015).
35. Li, L. *et al.* Novel amdovirus in gray foxes. *Emerg. Infect. Dis.* **17**, 1876–1878 (2011).

36. Shao, X.-Q. *et al.* Novel amdoparvovirus infecting farmed raccoon dogs and arctic foxes. *Emerg. Infect. Dis.* **20**, 2085–2088 (2014).

37. Oie, K. L. *et al.* The relationship between capsid protein (VP2) sequence and pathogenicity of Aleutian mink disease parvovirus (ADV): a possible role for raccoons in the transmission of ADV infections. *J. Virol.* **70**, 852–861 (1996).

38. Kenyon, A. J., Kenyon, B. J. & Hahn, E. C. Protides of the Mustelidae: immunoresponse of mustelids to Aleutian mink disease virus. *Am. J. Vet. Res.* **39**, 1011–1015 (1978).

39. Woolf, A. & Gremillion-Smith, C. Pathologic findings in rabies-suspect, random-source, and accidentally killed skunks. *J. Am. Vet. Med. Assoc.* **189**, 1089–1091 (1986).

40. Pennick, K. E., Latimer, K. S., Brown, C. A., Hayes, J. R. & Sarver, C. F. Aleutian disease in two domestic striped skunks (Mephitis mephitis). *Vet. Pathol.* **44**, 687–690 (2007).

41. Allender, M. C. *et al.* Infection with Aleutian disease virus-like virus in a captive striped skunk. *J. Am. Vet. Med. Assoc.* **232**, 742–746 (2008).

42. LaDouceur, E. E. B. *et al.* Aleutian Disease: An Emerging Disease in Free-Ranging Striped Skunks (Mephitis mephitis) From California. *Vet. Pathol.* **52**, 1250–1253 (2015).

43. Giannitti, F., Sadeghi, M., Delwart, E., Schwabenlander, M. & Foley, J. ALEUTIAN DISEASE VIRUS-LIKE VIRUS (AMDOPARVOVIRUS SP.) INFECTING FREE-RANGING STRIPED SKUNKS (MEPHITIS MEPHITIS) IN THE MIDWESTERN USA. *J. Wildl. Dis.* **54**, 186–188 (2018).

44. Ingram, D. G. & Cho, H. J. Aleutian disease in mink: virology, immunology and pathogenesis. *J. Rheumatol.* **1**, 74–92 (1974).

45. Britton, A. P. *et al.* Beyond Rabies: Are Free-Ranging Skunks (Mephitis mephitis) in British Columbia Reservoirs of Emerging Infection? *Transbound. Emerg. Dis.* **64**, 603–612 (2017).

46. Nituch, L. A., Bowman, J., Wilson, P. J. & Schulte-Hostedde, A. I. Aleutian mink disease virus in striped skunks (Mephitis mephitis): evidence for cross-species spillover. *J. Wildl. Dis.* **51**, 389–400 (2015).

47. Canuti, M., Doyle, H. E., P Britton, A. & Lang, A. S. Full genetic characterization and epidemiology of a novel amdoparvovirus in striped skunk (Mephitis mephitis). *Emerg. Microbes Infect.* **6**, e30 (2017).

48. Alex, C. E. *et al.* Amdoparvovirus Infection in Red Pandas (Ailurus fulgens). *Vet. Pathol.* **55**, 552–561 (2018).

49. Zhao, M. *et al.* Viral metagenomics unveiled extensive communications of viruses within giant pandas and their associated organisms in the same ecosystem. *Sci. Total Environ.* **820**, 153317 (2022).

50. Canuti, M. *et al.* Multi-host dispersal of known and novel carnivore amdoparvoviruses. *Virus Evol* **6**, (2020).

51. Bodewes, R., van der Giessen, J., Haagmans, B. L., Osterhaus, A. D. M. E. & Smits, S. L. Identification of multiple novel viruses, including a parvovirus and a hepevirus, in feces of red foxes. *J. Virol.* **87**, 7758–7764 (2013).

52. Wu, Z. *et al.* Comparative analysis of rodent and small mammal viromes to better understand the wildlife origin of emerging infectious diseases. *Microbiome* **6**, 178 (2018).

53. Wu, Z. *et al.* Deciphering the bat virome catalog to better understand the ecological diversity of bat viruses and the bat origin of emerging infectious diseases. *ISME J.* **10**, 609–620 (2016).

54. Lau, S. K. P. *et al.* Bats host diverse parvoviruses as possible origin of mammalian dependoparvoviruses and source for bat-swine interspecies transmission. *J. Gen. Virol.* (2017) doi:10.1099/jgv.0.000969.

55. Glatston, A., Wei, F., Than Zaw (IUCN SSC Cat SG / Wildlife Conservation Society (WCS), Myanmar Program, Yangon, Myanmar) & Sherpa, A. P. IUCN Red List of Threatened Species: Ailurus fulgens. *IUCN Red List of Threatened Species* (2015).

CHAPTER 2:

Amdoparvovirus infections are prevalent, persistent, and genetically diverse in zoo-housed red pandas (*Ailurus fulgens*)

Charles E. Alex, DVM, DACVP, Kenneth A Jackson, MS, Steven V. Kubiski, DVM, PhD, DACVP, Raymund F. Wack, DVM, DACZM, DECZM, and Patricia A. Pesavento, DVM, PhD, DACVP

Published in:
Journal of Zoo and Wildlife Medicine (2022) 53(1):83-91. doi: 10.1638/2021-0082.

Abstract:

Red pandas (*Ailurus fulgens*) are a globally endangered small carnivoran species, and subjects of a robust *ex situ* conservation effort that includes animal housed in zoos. In 2018, Red Panda Amdoparvovirus (RPAV) was discovered by metagenomics analyses of tissues from two geriatric red pandas, and in one case associated with significant lesions. Because RPAV was discovered in a single zoo cohort, it was unclear whether these infections represent a widely distributed, enzootic virus of red pandas or a localized 'spillover' from a different host species into this collection. The first goal of this study was to estimate the prevalence of RPAV in US zoos. We amplified RPAV from feces of 104 individual red pandas from 37 US zoos, and the virus was detected in 52/104 samples (50.0%), and detectable in feces from clinically normal animals throughout the 4.5-year sampling period. Next, to establish persistence of infection in individual animals, we tested serial samples in a single cohort over a 4.5-year period and virus was consistently shed by infected animals. Finally, full viral coding sequences were amplified and sequenced from 3 cases, and partial sequences of both the nonstructural (NS) and capsid (VP) genes were obtained for an additional 19 cases. RPAV is a genetically diverse but monophyletic viral species, and multiple viral lineages are present in US zoo-housed red pandas. Although the origins of these infections remain to be determined, we conclude that RPAV is widespread in red pandas in the United States, and that infections are persistent—presumably for the lifetime of the animal—and generally asymptomatic.

Introduction:

Red pandas (*Ailurus sp.*) are small carnivorans native to temperate forests in the Himalayas and western China, and are the only extant members of the family *Ailuridae*. With wild populations estimated at fewer than 10,000, they are classified as endangered by the International Union for Conservation of Nature (IUCN) and are listed as Appendix 1 species according to the Convention on International Trade in Endangered Species of Wild Fauna and Flora (CITES).[5,10] Two genetically distinct subpopulations exist: the Himalayan red panda (*Ailurus fulgens*), whose native range includes parts of Nepal, northern India, Tibet, Myanmar, Bhutan and far-western China, and the Chinese red panda (*Ailurus styani*), native to parts of Yunnan and Sichuan provinces in western China. These were historically regarded as subspecies (*Ailurus fulgens fulgens* and *Ailurus fulgens styani*, respectively), but there is increasing genetic evidence and support for their recognition as two separate species.[8,16] The strategy for survival of the species includes an *ex situ* conservation effort that (as of March 3, 2021) relies on 850 individuals housed in zoos worldwide, 218 of which are in the United States and carefully managed by a Species Survival Plan.[28] Red Pandas are charismatic and popular attractions in zoos and serve critical functions for education and as safeguards for the continuity of the species. Understanding disease threats to the captive and free-ranging populations is imperative to ensuring their welfare and continued sustainability.

The Amdoparvoviruses (APVs) are a genus in the family *Parvoviridae*.[7,24] They have a simple, small genome that is linear, single-stranded DNA, and approximately 5000 nucleotides long, with two open reading frames (ORFs) flanked by non-coding terminal hairpins.[7] A 5' nonstructural (NS) ORF encodes proteins that function in replication, and a 3' capsid (VP) ORF encodes two proteins that comprise the virion.[6,15,25] For over 50 years, studies on genetics,

pathogenesis of infection, and clinical impact of Amdoparvoviruses were limited to Aleutian Mink Disease Virus (AMDV), which was first recognized in the 1950s as a cause of a chronic, progressive disease (Aleutian disease) in farmed mink (*Mustela vison*).[11,12] Recently, however, advances in sequencing technology and sensitive detection methods have facilitated a rapid expansion of the Amdoparvovirus genus, with novel members discovered in the past ten years in gray fox[21], raccoon dog and arctic fox[26], and skunks.[2] Aside from AMDV, which is a significant cause of morbidity and mortality in mink, very little is known about the pathogenesis of Amdoparvovirus infections in carnivores. Significant lesions have been attributed to Skunk Amdoparvovirus infections in striped skunks (*Mephitis mephitis*), and disease association has been suspected but not well established for other members of the genus.[20,21,26]

In 2018, we reported the discovery of an Amdoparvovirus infecting red pandas from a zoological collection.[1] Species demarcation criteria in the *Parvoviridae* indicate a threshold of <85% amino acid sequence identity in the major nonstructural (NS1) protein for recognition of a novel viral species.[24] Red Panda Amdoparvovirus (RPAV) shares approximately 75% amino acid sequence identity in this protein with other members of the genus, and was thus recognized as a novel species.[24] RPAV was detected by metagenomic analyses of tissues from two geriatric animals that died within a 1-year period (2015-2016), and was detected during that same timespan by PCR in fecal samples from all four healthy co-housed members of the cohort. Based on histopathology and *in situ* hybridization (ISH) analyses, RPAV was abundant, strongly associated with inflammation, and considered the cause of death in at least one of the deceased pandas.

Taken together, findings indicated that RPAV is a novel and potentially pathogenic virus in this endangered species. Amdoparvoviruses are recognized as multi-host pathogens,[3,4] and it

was unclear whether RPAV is native to red pandas or a spillover into this collection from a different host species. Establishing the epidemiological context, including prevalence, shedding (possible transmission), and viral genetic characteristics, is critical for interpreting the significance of infection in individual cases and for understanding the possible impact of RPAV on the health of zoo-housed red pandas at the individual and population level. To this end, we report a cross-sectional study among zoological collections in the US, and a single-institution longitudinal study with the goals of (1) estimating the prevalence of fecal shedding (potential transmission), (2) establishing the persistence of infection over a five-year timespan in individual animals within a single cohort, and (3) characterizing the phylogenetic relationships and genetic diversity of RPAV. These studies are fundamental to our estimation of the clinical impact of RPAV infection.

Materials and methods:

Animals and samples:

Fecal samples (~50-200 grams) from 104 red pandas were collected by staff at participating institutions, labeled with the date of collection and identifying information (name, institutional identification number, and/or international studbook number), and shipped on ice to our laboratory. Samples were stored frozen at -20C until use. Information on sex, subspecies, and dates of birth for each red panda were obtained from the Zoological Information Management System[28] database based on identifying information provided by submitting zoos. Depending on the volume of submitted feces, 1-6 separate 1-gram samples from each submission were collected and processed for DNA extraction. Extractions were performed either using a

commercial kit (DNEasy Blood and Tissue Kit) according to protocols for tissue DNA extraction, or were performed by a commercial laboratory (Idexx, West Sacramento).

PCR Detection:

The target for PCR detection was a 154-nucleotide-long amplicon from the nonstructural gene, as previously described.[1] The 25 µL PCR reactions contained 12.5 µL Apex Hot Start Taq BLUE Master Mix, 0.5 µM of each primer, and approximately 100 ng of purified DNA. Reactions were performed in a C1000 Touch Thermal Cycler (BioRad) with an initial activation step at 95C for 15 minutes followed by 35-40 cycles of denaturation at 95C for 30 seconds, annealing at 54C for 30 seconds, and elongation at 72C for 30 seconds, with a final elongation at 72C for 10 minutes. Primers are given in Table 2.1. Amplicons were evaluated by 1.4% agarose gel electrophoresis. Purified DNA from previously identified, PCR-confirmed RPAV cases were used as positive controls in each amplification, and negative (no template) controls were also included in each run. Samples were considered positive if at least one 1g extraction yielded a detectable band of the correct size.

Sequencing:

Various PCR reactions were used to amplify RPAV genomes in overlapping segments from positive samples. All reaction mixtures were composed as described above, with the exception that for degenerate primers 1.0 µM were used. Primers used to generate amplicons for sequencing are included in Table 2.1. In most cases, PCR products were purified using either ExoSap-IT PCR Product Cleanup Reagent (ThermoFisher) or the QiaQuick PCR Purification Kit (Qiagen). In some cases, PCR products were cloned into TA TOPO cloning vectors

(ThermoFisher) and transformed into One Shot Top10 Chemically Competent E. coli (ThermoFisher) and cultured overnight in liquid media, then prepared for sequencing using the QiaPrep Spin MiniPrep kit (Qiagen). Samples were submitted for bi-directional Sanger sequencing at the UC DNA Sequencing Facility (UC Davis).

Phylogenetic analysis:

Sanger sequence traces were inspected, manually edited as necessary, and primer sequences were trimmed. Sequences were aligned in Geneious[18] using the MUSCLE algorithm[9] with default settings. For amino acid sequence comparisons in NS1, we reproduced splice patterns in silico based on experimental evidence from AMDV and predictions from SKAV.[2,25] The full NS1 amino acid sequences were compared to previously published RPAV sequences, representative sequences from other Amdoparvoviruses, and a Canine Parvovirus-2 outgroup obtained from GenBank. Sequences used for these comparisons are listed in Table 2.2. We also analyzed partial nucleotide sequences in the NS and VP ORFs from 19 additional cases. Optimal substitution models for each nucleotide data set were determined using the Model Selection function in MEGAX,[19,27] and Maximum Likelihood phylogenies were generated in MEGAX with 500 bootstrap replicates.

Statistical Analysis:

Statistical analyses were performed in JMP.[17] Fisher's Exact tests were used to evaluate the correlation between infection status and subspecies and sex. A Wilcoxon Rank Sum test was used to evaluate the correlation between infection status and age. P values ≤ 0.05 were considered statistically significant.

Results:

Prevalence:

We had previously established that RPAV was detectable in the gastrointestinal tissues and feces of animals in a single zoo cohort. We collected fecal samples were collected from 104 red pandas representing 37 zoological collections. RPAV was detected in feces from 52/104 animals (50.0%), representing 25/37 zoos tested (67.6%). Results and distributions by subspecies, sex, and age for the animals included in this study are shown in Table 2.3. Infection status was significantly associated with subspecies, with infections detected in 47/78 (60.3%) Himalayan red pandas (*A. fulgens*) and 5/26 (19.2%) Chinese red pandas (*A. styani*) (p=0.0005). There was no significant difference in infection status by sex (p=0.70). There was a trend toward increased infections in older animals, but this did not reach statistical significance (p=0.13).

Persistence:

To evaluate the persistence of fecal RPAV shedding, we collected 422 samples from six *A. fulgens* PCR-tested serial samples from animals in a single zoo cohort between 15 January 2016 and 13 July 2020, for a total sampling period of 4.5 years. Six animals were included in this study. Cases 1 and 2 were geriatric females that died during the sample collection period. Cases 3 and 4 were an 8-year-old male and a 5-year-old female, respectively, that remained clinically healthy throughout the sampling period. Cases 5 and 6 were a 1-year-old female and a 2-year-old male that were introduced to the cohort during year 2 of sample collection. The subset of samples tested, and their PCR results, are summarized in Table 2.4.

RPAV was consistently detectable in feces from cases 1-4 throughout the sampling period. Samples from cases 5 and 6 were PCR-negative prior to their introduction to the collection, and RPAV was not detected in their fecal samples collected during their first 2 months of cohabitation with infected animals (0/23 and 0/32 for cases 5 and 6, respectively). When was resumed approximately 1 year later both introduced animals were infected, and RPAV was detectable in serial fecal samples (5/10 and 8/10 for cases 5 and 6, respectively).

Genetic Diversity:

Phylogenetic analysis based on complete NS1 amino acid sequences demonstrated clear monophyletic clustering of RPAV sequences (Figure 2.1). Pairwise distances among RPAV sequences approached but did not exceed the species demarcation threshold, with up to 12.3% divergence between the two most divergent RPAV sequences.[24] RPAV amino acid sequences were between 62.0-74.4% similar to other members of the Amdoparvovirus genus. Thus, despite the remarkable sequence diversity among red panda samples, RPAV sequences are members of a single viral species based on established criteria for *Parvoviridae*.

We next amplified partial sequences from the NS and VP ORFs from 19 additional cases. The resulting Sanger traces were trimmed for read quality, resulting in an 852-nucleotide-long segment in NS and a 515-nucleotide-long segment of the VP gene with high quality reads that were used for phylogenetic analyses. Phylogeny based on partial NS sequences demonstrated substantial genetic diversity in both genes and evidence of three genetically distinct RPAV clades (Figure 2.3A). Notably, multiple clades were sometimes detectable from animals at the same institution (Figure 2.3B). For most cases clade groupings were consistent in both genome

segments, but there were several instances in which NS and VP sequences obtained from individual samples belonged to different RPAV clades.

Discussion:

We demonstrated that RPAV infections are highly prevalent (50%) among zoo-housed red pandas. We consider the prevalence to be a minimum estimate of the prevalence in this population for several reasons. Firstly, feces from an individual bowel movement were voluminous (30-200 grams) and the extracted sample represented only a fraction (1 g) of a sample at a single point in time. Either low quantities of viral shedding or uneven viral distribution in fecal samples may have led to missed cases. Secondly, quantities of shed virus are likely to be variable depending on diet, behavior, illness, stage of infection, the natural history of the virus, or other factors. Although shedding was consistently detectable among several persistently infected red pandas, negative samples were obtained from at least one animal known to be infected. Thus, sporadic negative samples in infected animals can occur, and clarification of the viral 'life cycle,' including identification of sites of persistence and frequency and quantitation of shed virus, are needed to determine optimal samples and sampling schedules for the most accurate detection of infected animals.

Lastly, given the degree of sequence diversity observed in RPAV, we recognize that although we targeted a relatively conserved portion of the genome, cases may have been missed due to sequence variation in the primer binding sites of our screening assay. We therefore suggest that RPAV may be even more widespread in this population than our results indicate.

The longitudinal cohort study demonstrates that RPAV is persistently (at least >4 years) shed by healthy red pandas. Red pandas are frequently transferred among US zoos frequently for breeding or management purposes, and we suggest that these movements are a mechanism by which infections are propagated throughout the zoo-housed population. Indeed, we demonstrated two putative new infections after previously PCR-negative red pandas were introduced to an infected cohort. The trend toward increased infections in older animals may thus reflect a higher number of cumulative exposures over the course of a lifetime, and/or an increase in viral production/shedding due to age-related immune senescence. Because infection is present most often in healthy animals, the detection of RPAV must be interpreted cautiously with respect to clinical significance.

Our phylogenetic analyses indicate that the infections detected represent diverse variants of a single viral species. Because the origins of these infections are unknown, this is critical information for evaluating whether RPAV originated in wild-caught ancestors of the current zoo population or spilled over from a different host into red pandas in zoos. Although this question remains unresolved, the widespread distribution and monophyly of RPAV suggests that RPAV is likely either a native virus of red pandas or spilled over many years ago and spread through the zoo population. Either scenario could plausibly explain the significantly higher proportion of cases detected in Himalayan red pandas relative to Chinese red pandas. These populations are maintained separately in zoos, with limited opportunities for contact between them. Thus, if RPAV infections are native to or spilled over into Himalayan red pandas, the Chinese red panda subpopulation may have been relatively protected by their separate management. There are instances in which individual zoos have housed both species, however, and given the remarkable durability of parvoviruses in the environment, there may have been rare opportunities for

crossover between subpopulations. A limitation of this study is that all sequences obtained were from Himalayan red pandas, so phylogenetic relationships between viral variants infecting the two subpopulations are unknown.

Our growing database of RPAV sequence data, including the identification of multiple distinct clades, provide an important starting point for molecular epidemiological studies in this population. More detailed phylogenetic characterizations, including recombination analyses, coupled with medical records, pedigrees, and detailed historical records of movements among zoo populations, will facilitate a better understanding of the transmission dynamics and risk factors for infection in this population, to better inform management decisions. Further research should also be focused on determining the prevalence and phylogenetic relationships of RPAV in other zoo cohorts and in free-ranging animals, including longitudinal comparative studies of the two subpopulations, to better understand the natural history of these infections.

Finally, while it must be emphasized that infections are prevalent in clinically normal animals, the consequences of infection are not well understood. In our longitudinal cohort, two pandas that died within the study period had virus widely distributed in tissues, in one case clearly associated with inflammation. Other Amdoparvoviruses are known to be pathogenic in small carnivores, and the possibility that RPAV may be contributing to morbidity or mortality in red pandas must be carefully evaluated.

Acknowledgements:

The authors thank Dr. Simon Anthony and Dr. Terza Brostoff for thoughtful review and critique of the manuscript. We thank Dr. Marta Canuti and Dr. Andrew Lang for helpful discussions and

advice for sequencing strategies. We thank the veterinary and husbandry staff at participating institutions for their assistance with sample acquisition: Binder Park Zoo, Battle Creek, Michigan; Birmingham Zoo, Birmingham, Alabama; Blank Park Zoo, Des Moines, Iowa; Brandywine Zoo, Wilmington, Delaware; Cape May County Park and Zoo, Cape May Court House, New Jersey; Cincinnati Zoo and Botanical Garden, Cincinnati, Ohio; Columbus Zoo and Aquarium, Powell, Ohio; Denver Zoo, Denver, Colorado; Detroit Zoo, Royal Oak, Michigan; Elmwood Park Zoo, Norristown, Pennsylvania; Essex County Turtle Back Zoo, West Orange, New Jersey; Franklin Park Zoo, Boston, Massachusetts; Great Plains Zoo & Delbridge Museum of Natural History, Sioux Falls, South Dakota; Happy Hollow Park & Zoo, San Jose, California; Henry Vilas Zoo, Madison, Wisconsin; Idaho Falls Zoo at Tautphaus Park, Idaho Falls, Idaho; Indianapolis Zoo, Indianapolis, Indiana; Kansas City Zoo, Kansas City, Missouri; Mesker Park Zoo, Evansville, Indiana; Milwaukee County Zoo, Milwaukee, Wisconsin; Minnesota Zoo, Apple Valley, Minnesota; NEW Zoo & Adventure Park, Green Bay, Wisconsin; Oglebay Good Zoo, Wheeling, West Virginia; Potawatomi Zoo, South Bend, Indiana; Potter Park Zoo, Lansing, Michigan; Pueblo Zoo, Pueblo, Colorado; Sacramento Zoo, Sacramento, California; San Diego Zoo Wildlife Alliance, San Diego, California; Sedgwick County Zoo, Wichita, Kansas; Seneca Park Zoo, Rochester, New York; Sequoia Park Zoo, Eureka, California; Smithsonian National Zoological Park, Washington, DC; Smithsonian Conservation Biology Institute, Front Royal, Virginia; Saint Louis Zoo, St. Louis, Missouri; Trevor Zoo at Millbrook School, Millbrook, New York; Tulsa Zoo, Tulsa, Oklahoma; ZooMontana, Billings, Montana. Special thanks are owed to the veterinary and husbandry staff at the Sacramento Zoo for their continued support in a years-long sampling effort. This project is supported in part by a philanthropic grant from the McBeth Foundation via San Diego Zoo Wildlife Alliance.

References:

1. Alex CE, Kubiski SV, Li L, Sadeghi M, Wack RF, McCarthy MA, Pesavento JB, Delwart E, Pesavento PA. 2018. Amdoparvovirus Infection in Red Pandas (*Ailurus fulgens*). Vet Pathol. 55(4):552–561.
2. Canuti M, Doyle HE, P Britton A, Lang AS. 2017. Full genetic characterization and epidemiology of a novel amdoparvovirus in striped skunk (*Mephitis mephitis*). Emerg Microbes Infect. 6(5):e30.
3. Canuti M, McDonald E, Graham SM, Rodrigues B, Bouchard É, Neville R, Pitcher M, Whitney HG, Marshall HD, Lang AS. 2020. Multi-host dispersal of known and novel carnivore amdoparvoviruses. Virus Evol. 6(2). doi:10.1093/ve/veaa072. [accessed 2021 Mar 24]. https://academic.oup.com/ve/article/6/2/veaa072/5912945.
4. Canuti M, Todd M, Monteiro P, Van Osch K, Weir R, Schwantje H, Britton AP, Lang AS. 2020. Ecology and Infection Dynamics of Multi-Host Amdoparvoviral and Protoparvoviral Carnivore Pathogens. Pathogens. 9(2). doi:10.3390/pathogens9020124.
5. CITES. Appendices I, II, and III. [accessed 2021 May 14]. https://cites.org/eng/app/appendices.php.
6. Clemens DL, Wolfinbarger JB, Mori S, Berry BD, Hayes SF, Bloom ME. 1992. Expression of Aleutian mink disease parvovirus capsid proteins by a recombinant vaccinia virus: self-assembly of capsid proteins into particles. J Virol. 66(5):3077–3085.
7. Cotmore SF, Agbandje-McKenna M, Canuti M, Chiorini JA, Eis-Hubinger A-M, Hughes J, Mietzsch M, Modha S, Ogliastro M, Pénzes JJ, et al. 2019. ICTV Virus Taxonomy Profile: Parvoviridae. J Gen Virol. 100(3):367–368.

8. Dalui S, Khatri H, Singh SK, Basu S, Ghosh A, Mukherjee T, Sharma LK, Singh R, Chandra K, Thakur M. 2020. Fine-scale landscape genetics unveiling contemporary asymmetric movement of red panda (Ailurus fulgens) in Kangchenjunga landscape, India. Sci Rep. 10(1):15446.
9. Edgar RC. 2004. MUSCLE: a multiple sequence alignment method with reduced time and space complexity. BMC Bioinformatics. 5:113.
10. Glatston A, Wei F, Than Zaw (IUCN SSC Cat SG / Wildlife Conservation Society (WCS), Myanmar Program, Yangon, Myanmar), Sherpa AP. 2015 Apr 11. IUCN Red List of Threatened Species: Ailurus fulgens. IUCN Red List of Threatened Species. [accessed 2021 Mar 15]. https://www.iucnredlist.org/species/714/110023718.
11. Gorham JR, Leader RW, Henson JB. 1964. The experimental transmission of a virus causing hypergammaglobulinemia in mink: Sources and modes of infection. J Infect Dis. 114:341–345.
12. Hartsough GR G JR. 1956. Aleutian disease in mink. Nat Fur News. 28:10–11.
13. Hasegawa M, Kishino H, Yano T. 1985. Dating of the human-ape splitting by a molecular clock of mitochondrial DNA. J Mol Evol. 22(2):160–174.
14. Huang Q, Deng X, Best SM, Bloom ME, Li Y, Qiu J. 2012. Internal polyadenylation of parvoviral precursor mRNA limits progeny virus production. Virology. 426(2):167–177.
15. Huang Q, Luo Y, Cheng F, Best SM, Bloom ME, Qiu J. 2014. Molecular characterization of the small nonstructural proteins of parvovirus Aleutian mink disease virus (AMDV) during infection. Virology. 452-453:23–31.

16. Hu Y, Thapa A, Fan H, Ma T, Wu Q, Ma S, Zhang D, Wang B, Li M, Yan L, et al. 2020. Genomic evidence for two phylogenetic species and long-term population bottlenecks in red pandas. Sci Adv. 6(9):eaax5751.
17. JMP. Version 15. SAS Institute Inc., Cary, NC, 1989-2019.
18. Kearse M, Moir R, Wilson A, Stones-Havas S, Cheung M, Sturrock S, Buxton S, Cooper A, Markowitz S, Duran C, et al. 2012. Geneious Basic: an integrated and extendable desktop software platform for the organization and analysis of sequence data. Bioinformatics. 28(12):1647–1649.
19. Kumar S, Stecher G, Li M, Knyaz C, Tamura K. 2018. MEGA X: Molecular Evolutionary Genetics Analysis across Computing Platforms. Mol Biol Evol. 35(6):1547–1549.
20. LaDouceur EEB, Anderson M, Ritchie BW, Ciembor P, Rimoldi G, Piazza M, Pesti D, Clifford DL, Giannitti F. 2015. Aleutian Disease: An Emerging Disease in Free-Ranging Striped Skunks (Mephitis mephitis) From California. Vet Pathol. 52(6):1250–1253.
21. Le SQ, Gascuel O. 2008. An improved general amino acid replacement matrix. Mol Biol Evol. 25(7):1307–1320.
22. Li L, Pesavento PA, Woods L, Clifford DL, Luff J, Wang C, Delwart E. 2011. Novel amdovirus in gray foxes. Emerg Infect Dis. 17(10):1876–1878.
23. Parrish CR. 1991. Mapping specific functions in the capsid structure of canine parvovirus and feline panleukopenia virus using infectious plasmid clones. Virology. 183(1):195–205.

24. Pénzes JJ, Söderlund-Venermo M, Canuti M, Eis-Hübinger AM, Hughes J, Cotmore SF, Harrach B. 2020. Reorganizing the family Parvoviridae: a revised taxonomy independent of the canonical approach based on host association. Arch Virol. 165(9):2133–2146.
25. Qiu J, Cheng F, Burger LR, Pintel D. 2006. The transcription profile of Aleutian mink disease virus in CRFK cells is generated by alternative processing of pre-mRNAs produced from a single promoter. J Virol. 80(2):654–662.
26. Shao X-Q, Wen Y-J, Ba H-X, Zhang X-T, Yue Z-G, Wang K-J, Li C-Y, Qiu J, Yang F-H. 2014. Novel amdoparvovirus infecting farmed raccoon dogs and arctic foxes. Emerg Infect Dis. 20(12):2085–2088.
27. Stecher G, Tamura K, Kumar S. 2020. Molecular Evolutionary Genetics Analysis (MEGA) for macOS. Mol Biol Evol. 37(4):1237–1239.
28. ZIMS. 2021. Species360 Zoological Information Management System, ZIMS. [accessed 2021].

Tables and figures:

Table 2.1. PCR primers used for RPAV detection and sequencing.

Purpose	Target region[a]	Amplicon size (nt)	Primers	Binding site	Sequence
Screening assay	956-1069	154	RP Amdo NSF2	936-955	CGCCAAAACCAACCGACCAA
			RP Amdo NSR2	1069-1089	AACACGCCCTTAGCTGTGCT
Full coding sequence	53-478	467	Amdo30F	32-52	TGGAATGMGGAAGTKCTRGTG
			Amdo392R	479-498	CCHAMSMAACARTGRATATG
	256-1107	893	AmdoNS1.130F	236-255	AAACCAACCAMAGMAACACC
			AmdoNS1.1058R	1108-1128	TCTTCTGGAGTAAAGCAACCA
	970-1980	1052	Amdo948F	950-969	GACCAAACTGACTCAGCAAC
			Amdo1999R	1981-2001	GTGAGCTGCCAGAACTCTTGT
	1591-2228	677	Amdo4F	1572-1590	AAGCYATTACTGGAGGWGG
			Amdo5R	2229-2248	TTGCTGRATAAAYACGTGTC
	2112-2825	754	Amdo5F	2094-2111	AAGAGACCTCGGCATGAG
			Amdo2844R	2826-2847	CCTGTAACGACGCAGTTAAGTC
	2648-3307	660	SKAV1F	2636-2647	CCAACAAGTAATGACACCWTGG
			SKAVR1	3308-3324	TCACCCCAAAAGTGACC
	3201-3984	827	Amdo8Fb	3181-3200	CCAAAGTACACGTTGCTTGG
			Amdo4692R	3985-4009	CAGTGAGGTTCTCTGTTAGTTTAAC
	3928-4307	422	Amdo4556F	3906-3927	CTGATGTGGACCACAAACCTAG
			Amdo8R	4308-4329	GGTTRTTCACTDTTYATGTAAC

[a]All nucleotide positions refer to the previously published genome NC_031751.

Table 2.2. Published sequences used for phylogenetic comparisons.

Viral Species	GenBank accession number	Reference
Canine Parvovirus	M38245	23
Aleutian Mink Disease Virus	JN040434	14
Gray Fox Amdovirus	NC_038533	22
Raccoon Dog and Arctic Fox Amdoparvovirus	KJ396347	26
Skunk Amdoparvovirus	KX981920	2
Red Panda Amdoparvovirus (CA1)	NC_031751	1
Red Panda Amdoparvovirus (CA2)	KY564173	1

Table 2.3. Results of PCR screening of feces from US zoo-housed red pandas.

Category	Total tested	Positive	Negative
All	104	52	52
Species			
A. fulgens	78	47	31
A. styani	26	5	21
Sex			
Male	51	24	27
Female	53	28	25
Age (years)			
0-1	8	4	4
1-2	20	7	13
3-5	33	16	17
6-9	20	11	9
10+	23	14	9

Table 2.4. RPAV detection in serial samples (samples positive/samples tested)

Case	2016	2017	2019	2020	Total
1	8/10[a]				8/10
2	10/10[a]				10/10
3	7/7	23/23	10/10	2/2	42/42
4	8/8	23/23	11/11	2/2	44/44
5		0/23[b]	5/5	1/2	6/30
6		0/32[b]	8/8[c]		8/40

[a]Cases 1 and 2 were geriatric animals that died in 2016.

[b]Cases 5 and 6 were introduced to the collection in 2017. Samples collected before their introduction were PCR-negative for RPAV.

[c]Cases 6 was transferred to a different collection in 2019.

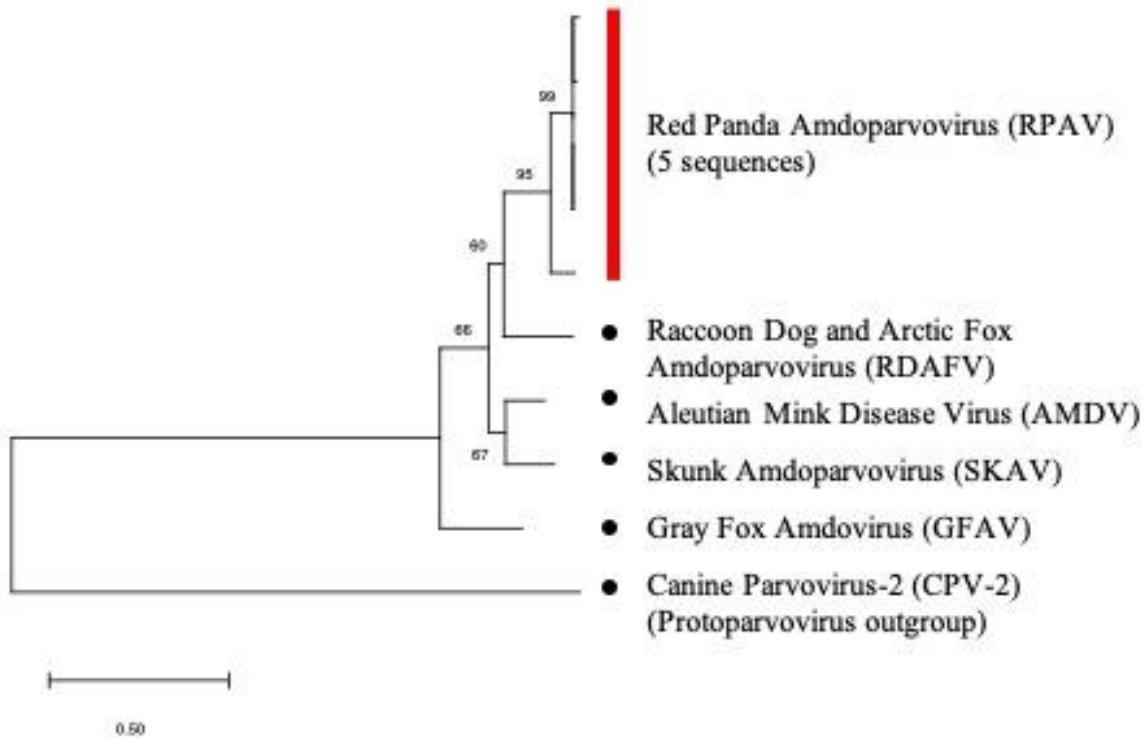

Figure 2.1: Phylogenetic analysis based on full amino acid sequences of the NS1 gene. Sequences isolated from red panda samples cluster as a monophyletic Amdoparvovirus lineage. The Maximum Likelihood method and Le Gasquel model were used and the tree with the highest log likelihood (-6678.69) is shown.[21] A discrete Gamma distribution was used to model evolutionary rate differences among sites (+G, 4 categories, parameter = 1.2784). 500 bootstrap replicates were performed, and bootstrap support values are shown next to nodes.

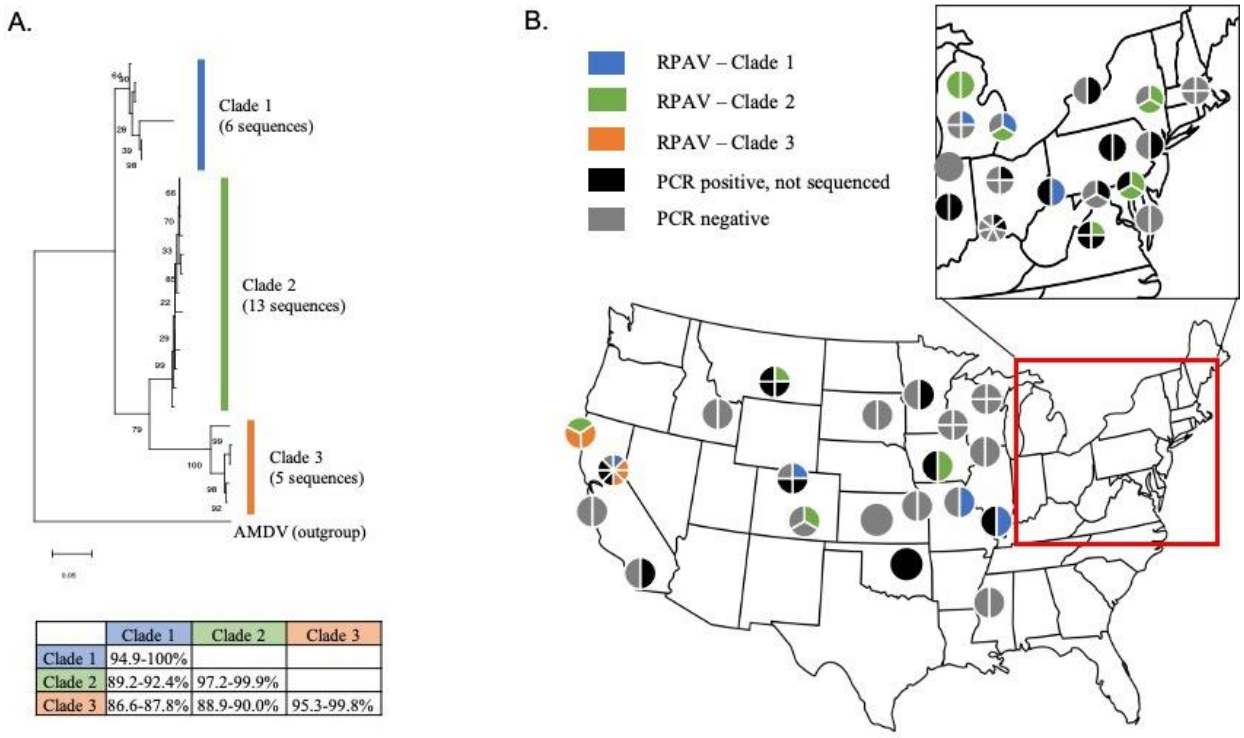

	Clade 1	Clade 2	Clade 3
Clade 1	94.9-100%		
Clade 2	89.2-92.4%	97.2-99.9%	
Clade 3	86.6-87.8%	88.9-90.0%	95.3-99.8%

Figure 2.2: (A) Phylogenetic analysis based on 852 nucleotides in the NS gene. RPAV sequences form three distinct clades. The range of percent identity within and between groups based on pairwise comparisons is shown. For phylogeny, the Maximum Likelihood method and Hasegawa-Kishino-Yano model were used, and the tree with highest log likelihood (-3183.46) is shown.[13] A discrete Gamma distribution was used (+G, parameter=0.4382), and 500 bootstrap replicates were performed. Bootstrap support values are shown next to nodes.

(B) Map of testing and results. Each pie chart represents a zoo cohort, and segments represent individual animals. One to eight animals were present in the cohorts tested. RPAV lineages (blue, green, and orange) were determined based on partial NS1 sequence.

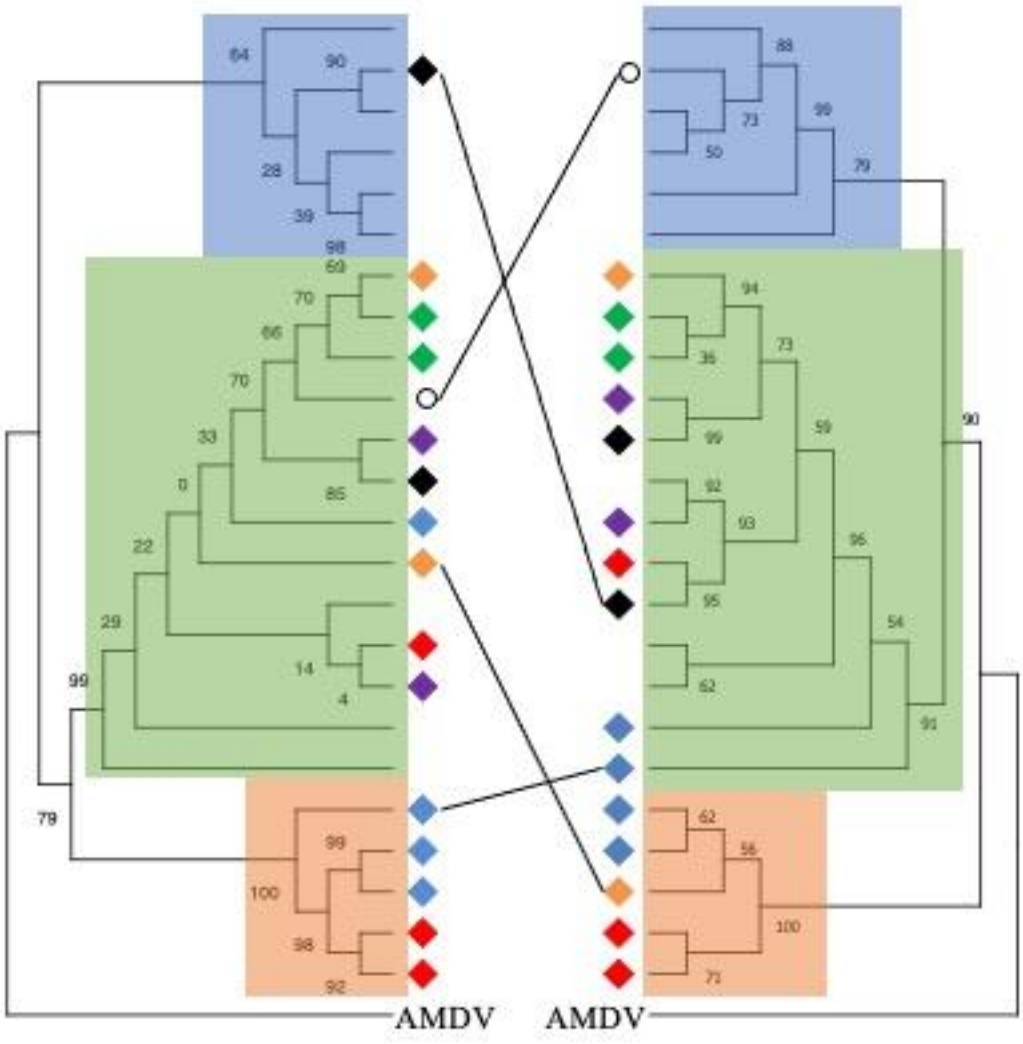

Figure 2.3: Maximum likelihood trees of partial NS (left) and VP (right) sequences. Diamond tip markers indicate zoos from which the sequences originated (grouped by color). Tips without markers were the only sequences obtained from their respective institutions. Several zoos (black, red, blue) had multiple RPAV lineages represented in their collections. Clade grouping is generally maintained between trees, but in several cases (black lines) sequences from individual animals shift clades depending on the segment examined. The empty circle is the only sequence from its institution, but is marked to show the shift in clade grouping.

The NS tree is the same as that shown in Figure 2.2, with transformed branches. The Maximum Likelihood VP tree (left) was generated from 563 nucleotides in the capsid coding sequence using the Hasegawa-Kishino-Yano model with a discrete gamma distribution (parameter = 0.6857) and allows for invariant sites (+*I*, 63.25%).[13] 500 bootstrap replicates were performed. Branches were transformed, and bootstrap support values are shown next to nodes.

CHAPTER 3:

Natural disease and evolution of an amdoparvovirus endemic in striped skunks (*Mephitis mephitis*)

Charles E. Alex, DVM, DACVP, Marta Canuti, PhD, Maya S. Schlesinger, DVM, Kenneth A. Jackson, MS, David Needle, DVM, DACVP, Claire Jardine, DVM, PhD, Larissa Nituch, MS, Laura Bourque, DVM, Andrew S. Lang, PhD, Patricia A. Pesavento, DVM, PhD, DACVP

Published in:

Transboundary and Emerging Diseases (2022) 1-10. doi: 10.1111/tbed.14511

Abstract:

Striped skunks (*Mephitis mephitis*) densely populate the human-animal interface of suburbia throughout North America. Skunks share that habitat with numerous related mesocarnivores, where increased contact, competition for shared food and water sources, and other stressors contribute to increased exposure and susceptibility to viral infection. The recently identified skunk amdoparvovirus (SKAV) has been detected at high prevalence in skunks and occasionally in mink, but its distribution in North America is unknown. To understand the impact of SKAV in striped skunks and the risk posed to related species, we investigated the geographic distribution of SKAV, analyzed its genetic diversity and evolutionary dynamics, and evaluated viral distribution in tissues of infected animals to identify possible mechanisms of transmission. SKAV was detected in 72.5% (37/51) skunks and was present at high rates at all locations tested across North America. Analysis of the complete genomic sequence of 29 strains showed a clear geographic segregation, frequent recombination, and marked differences in the evolutionary dynamics of the major structural (VP2) and non-structural (NS1) proteins. NS1 was characterized by a higher variability and a higher percentage of positively selected codons. This could indicate that antibody-mediated enhancement of infection occurs in SKAV, an infection strategy that may be conserved across amdoparvoviruses. Finally, *in situ* hybridization revealed virus in epithelium of the gastrointestinal tract, urinary tract, and skin, indicating that viral transmission could occur via oronasal, fecal and/or urinary secretions, as well as from skin and hair. The endemicity of SKAV over large geographic distances and its high genetic diversity suggest a long-term virus-host association. Persistent shedding and high environmental stability likely contribute to efficient viral spread, simultaneously offering opportunities for cross-species transmission with consequent risk to sympatric species, including domestic animals and wildlife.

Introduction:

Amdoparvovirus is a rapidly growing genus within the viral family *Parvoviridae* comprising several important pathogens of carnivorans.[18,22,76] The best-known and prototypical amdoparvovirus is Aleutian mink disease virus (AMDV, species *Carnivore amdoparvovirus 1*), which causes persistent infections in mink (family Mustelidae) and related species. Clinical outcomes range from subclinical infection to fatal inflammatory disease, but the genetic determinants of host tropism and disease manifestations are not entirely characterized [18]. For decades after its discovery in the mid-20th century AMDV was the only recognized amdoparvovirus (former genus *Amdovirus*), but advances in viral detection and sequencing have led to a considerable expansion of the genus in the past decade.[4,17,18,59,82]

Most known amdoparvoviruses infect carnivorans of the superfamily Musteloidea or family Canidae. The genus now includes five officially recognized members: AMDV, Gray fox amdovirus (GFAV) [59], Racoon dog and fox amdoparvovirus (RDFV) [82], Skunk amdoparvovirus (SKAV) [17], and Red panda amdoparvovirus (RPAV) [4], classified as *Carnivore amdoparvovirus 2* through *5*, respectively [23,76]. Additional amdoparvoviruses have been identified in foxes (red fox fecal amdovirus [14]) and foxes and martens (Labrador Amdoparvovirus 1 and 2[18]) and recent studies suggest that bats and rodents can also be amdoparvovirus hosts [57,75,87,88]. Members of the genus possess a small (~5kb) single-stranded DNA genome that includes two main coding cassettes, one containing information for the three non-structural proteins NS1-3 and one coding for the two capsid proteins VP1-2 [19]. The two coding regions are characterized by different evolutionary dynamics, and, unlike other parvoviruses, the VP open reading frame (ORF) is more genetically conserved than the NS ORF [17,69] and this also true when comparing viruses from different species [18]. This antigenic stability is likely linked to the fact that antibodies

directed against the viral capsid can enhance viral uptake by circulating macrophages, a known cellular target for viral replication [11]. This mechanism, known as antibody dependent enhancement (ADE), has been described for AMDV[11,46] but is also presumed to occur for other amdoparvoviruses. Besides AMDV, little is known about the pathogenicity and the evolutionary dynamics that characterize viruses in this genus.

AMDV infection in farm-raised mink is associated with significant disease, but the prevalence and impact of amdoparvovirus infections in free-ranging populations of any species have not been well characterized [4,54,82]. Amdoparvoviruses lack strict host specificity and are known to infect multiple hosts [18,21,22,82]. This plasticity in host range, coupled with the crowding of susceptible species in and around urban environments and the notorious durability of parvoviral virions in the environment, could allow for frequent exposures of potentially susceptible hosts. Very little is known about the behavior of amdoparvoviruses in novel hosts, or in situations of co-infection by multiple amdoparvoviral species. These circumstances could lead to outbreaks in previously uninfected species, novel disease presentations, or the emergence of novel recombinant genotypes with alterations in virulence and host tropism. Phylogenetic and epidemiological data are therefore imperative for understanding the impact of amdoparvoviral infections in their primary hosts and the risks posed to related species.

Striped skunks (*Mephitis mephitis*) are ubiquitous in North America where they share dens, food, and water sources with multiple other animals, and as such they are poised to play an important role as reservoirs and spreaders of viral infections among wildlife and domestic animals [81]. SKAV was recognized as a distinct viral species in 2017 and has been detected with remarkably high prevalence in striped skunks from British Columbia (86%) and California (65%), and while subclinical infections appear to be common, infections have been associated

with disease in some cases [15,17,32]. Moreover, SKAV has been shown to infect mink, and AMDV has, in turn, been found in skunks [70], but the consequences of these infections and the potential for co-infections are unknown. While SKAV has been identified in multiple sites across North America, its current geographic range is not known, and its genetic variability is not well characterized. Additionally, the basic natural history of the virus, such as potential routes of transmission and tissue tropism, has not been characterized. This context is critical for understanding the impact of SKAV infections in skunks, and the risks posed to other potentially susceptible hosts. Therefore, the objectives of this study were to investigate the geographic distribution of SKAV in striped skunks across North America, assess the range of genetic diversity and regional variation in SKAV by analyzing sequences from disparate sites, study SKAV's evolutionary dynamics, and investigate tissue distribution of SKAV in infected skunks to increase our understanding of its pathology and identify potential sources of shedding and transmission routes.

Materials and Methods:

Animals and samples:

Spleen samples were collected from striped skunks that died or were euthanized for purposes unrelated to this study. For the California cohort, samples were taken from skunks that died or were euthanized at a wildlife rescue organization, all of which originated from within an approximately 20-mile radius around Sonoma County, CA. Ten samples from skunks from Ontario were received from the Ontario Ministry of Northern Development, Mines, Natural Resources (OMNDMNRF) and were collected in 2020 as part of a rabies surveillance program in the Golden Horseshoe area of Southern Ontario (all were rabies-negative). From Nova Scotia,

samples originated from a trapped and euthanized skunk which had been exhibiting signs of disease and poor doing for several weeks prior to euthanasia. The three samples from British Columbia originated from cases that were initially reported in a previous publication [17]. From New England (New Hampshire, Vermont, and Maine), samples originated from licensed trappers collecting nuisance animals during the 2019-2020 harvest. Animals were collected in Durham, Pembroke, Lebanon, and Canaan NH; St. Johnsbury and Burton, VT; and Greene and Waterville, ME. DNA was extracted from approximately 10 mg of tissue using the DNEasy Blood and Tissue Kit (Qiagen) and eluted in 100 µL elution buffer.

Handling of samples at Memorial University of Newfoundland was done under Animal Use Protocols 15-04-AL and 20-04-AL.

Detection of SKAV and sequence amplification:

All samples originating from the USA were screened for SKAV using primers SKAV-F1 (AGAGCAACCAAACCACCC) and SKAV-R1 (TCACCCCAAAAGTGACC), targeting a 365-nucleotide long segment of the VP ORF.[7] PCR products were examined by agarose gel electrophoresis. Samples yielding bands of the expected size were purified using the QIAquick PCR purification kit (Qiagen) or ExoSAP-IT PCR Product Clean-up Reagent (ThermoFisher) and Sanger-sequenced to confirm identity. All samples originating from Canada were screened using previously described protocols [17–19]. From a selection of positive samples, we chose randomly among PCR-positive cases to represent each investigated area and among the two previously reported lineages identified in BC (Canuti et al., 2017), and whole viral coding regions were generated by PCR amplification of overlapping fragments and Sanger sequencing. All primers used for genome amplifications are available upon request.

Sequence and phylogenetic analysis:

Amplicon sequences were inspected for quality, manually edited as necessary, and assembled to generate full coding sequences using Geneious R11 (Biomatters). Sequences from this study were then compared to near-full genomic sequences of seven previously published SKAV sequences originating from British Columbia [17]. Splice sites for NS2, NS3, and VP1 were determined based on previous predictions for SKAV [17], splice patterns were reproduced *in silico*, and the resulting protein-coding sequences were used to predict protein sequences. Nucleotide and protein alignments were performed using ClustalW 2.0 [55], optimal substitution models for genetic distance estimates were determined by the lowest Bayesian information criterion (BIC) with the ModelFinder function in IQ-TREE 2 [45,65], and maximum likelihood phylogenetic trees were generated with IQ-TREE 2. Branch support was assessed with both ultrafast bootstrap approximation (ufBoot [40]) and SH-like approximate likelihood ratio test (SH-aLRT [35]). Three AMDV strains were used as outgroup in each tree. The obtained trees were annotated in MEGA X [53] and final figures prepared with INKSCAPE (https://inkscape.org/, downloaded on 19 June 2020). Pairwise sequence identities were calculated as a percentage value of 1 – p-distance.

Recombination and selection pressure analyses

Full-length alignments were evaluated for recombinant genomes as previously described [19] by using all methods included in the RDP 5.5 [63] package and only events detected by at least 3 methods with $p<0.05$ were considered. Additionally, a breakpoint analysis was also performed with GARD [52] through Datamonkey 2.0 [85].

Sites under positive and purifying selection were assessed with Fixed Effect Likelihood (FEL [51]) and Fast Unconstrained Bayesian Approximation for inferring selection (FUBAR [66])

while episodic positive or diversifying selection was assessed by Mixed Effects Model of Evolution (MEME [67]) using default parameters through Datamonkey.

In situ hybridization:

We performed colorimetric *in situ* hybridization to demonstrate the presence of viral genomic DNA in tissue sections from selected cases from the California cohort. The assay was performed on 5-μm thick sections of formalin-fixed, paraffin-embedded tissues on Superfrost Plus slides (Fisher Scientific). We designed a set of 20 ZZ-paired probes spanning the VP ORF of SKAV (probe set V-SK23-VP1, Advanced Cell Diagnostics, Inc.), corresponding to nucleotide positions 2066-4186 of a reference genome (accession number KX981923). To evaluate likely pathways of viral shedding, selected tissues included sections of the gastrointestinal tract, urinary tract, and integument. Tissue sections were pre-treated with protease for 2 hours at 40 °C prior to hybridization, assayed using the RNAscope 2.5 Red Assay Kit (Advanced Cell Diagnostics, Inc.), counterstained with hematoxylin and mounted with EcoMount (Biocare Medical). Serial sections were also tested using an unrelated, GC-content-matched probe as a negative control.

Data availability:

All sequences obtained in this study have been deposited in GenBank under accession numbers OL889855-OL889879.

Results:

Amdoparvovirus detection and molecular typing:

We detected SKAV infections in regions where skunk amdoparvoviruses have not previously been reported (Maine, Vermont, and New Hampshire) and in areas where AMDV or

SKAV were previously detected (California, Ontario and Nova Scotia) [19,30,69] (Table 3.1). Although limited numbers of samples were available for each investigated region, viral detection rate was high in all locations. Excluding samples reported in a previous study [15], 72.5% (37/51) of investigated samples were positive, indicating amdoparvoviral endemicity in these areas.

All PCR-positive samples were confirmed to be infected by SKAV by sequencing, and we amplified complete or near-complete amdoparvoviral coding sequences from a selection of samples across the study area. The final dataset included novel sequences from seven animals from California, seven animals from Ontario, five animals from northeastern North America (two from Maine, two from New Hampshire, and one from Nova Scotia), and three additional animals from British Columbia from a previously investigated cohort [17]. Three additional VP sequences were obtained from animals from California. Genomes were 91.8-98% identical to each other and the genome organization was identical for all strains and consistent with amdoparvoviral genome structure. All sequences obtained in this study were most closely related to seven previously published complete genomic sequences of SKAV from British Columbia [17], which were therefore included in all following analyses, and they all belonged to the species *Carnivore amdoparvovirus 4* with pairwise amino acid identities of 84.6-100% among all 36 complete NS1 sequences.

Recombination analysis:

Since parvoviruses are known to increase their genetic variability through recombination [19,23], a search for chimeric genomes and breakpoint predictions were performed with RDP and GARD. Both methods provided evidence for multiple possible recombination events in the evolutionary history of these viruses. Specifically, over the complete genome, RDP detected 10

potential recombination events and GARD inferred 11 different breakpoints (Supplementary Table S3.1). All potential recombinant sequences detected in RDP were from BC or Ontario. As expected, both methods also showed phylogenetic discordance between the NS1 and VP2 regions. Since amdoparvoviral structural and nonstructural proteins experience different evolutionary constraints, discordant topologies of trees constructed with these two regions can be linked to different selection pressure dynamics and evolutionary rates as well as to recombination [19] For these reasons, the two ORFs were also examined separately.

Since some methods, like GARD, are known to overestimate recombination, especially in cases of asymmetric tree topology [9], we elected to explore in more detail only highly supported potential breakpoints that were detected in multiple events and by both methods on alignments of the whole genome as well as both ORFs separately. Four of the six events involving NS1 detected by RDP were caused by a breakpoint at nt ~850-950 that roughly divides NS1 ORF in two parts, and a breakpoint in this region was also detected by GARD. This is similar to what was previously identified for AMDV [19]. Possibly because of a higher sequence homogeneity and consequent difficulty in determining breakpoints and obtaining supported clades, fewer recombination events were detected for VP2. However, both methods identified a hotspot of potential breakpoints located between nt 500-800 of the VP2 ORF. The occurrence of recombination was further confirmed by phylogenetic analyses.

Phylogenetic analysis

To study the molecular epidemiology of SKAV in North America, maximum likelihood phylogenetic trees were built with all nucleotide sequences of the full NS1 and VP2 ORFs separately, as well as with portions of these genes from between identified breakpoints (Fig. 3.1). The trees built with the full ORFs (left panels) showed a clear segregation of strains depending

on sampling sites but with inconsistent clustering. Strain clustering within the NS1 tree mirrored the geography of sample collection locations, with a clade including all sequences from the West Coast (British Columbia and California) and another containing eastern sequences (Ontario, Nova Scotia, Maine, Vermont, New Hampshire). However, the tree built with VP2 ORF showed the presence of three separate clades, one single-sequence clade formed by the strain from Nova Scotia, one including sequences from California and Ontario, and one containing all other sequences. Additional differences between the two trees included the presence of three distinct sub-groups of sequences from British Columbia in the NS1 tree but not in the VP2 tree, different sub-groups of sequences from Ontario in the two trees, and the presence of a clade including sequences from Maine, Vermont, and New Hampshire in the NS1 tree but not in the VP2 tree.

The presence of these groups and sub-groups was also confirmed by sequence identities within the detected groups (Supplementary Table S3.2), considering a cut-off of within-group identity of at least 94%. These results confirmed a different evolutionary history for the two genes and an overall higher sequence identity for VP2 (92.1-99.8%) compared to NS1 (90.6-98.4%).

Finally, trees built with portions of the two genes determined by the main predicted potential breakpoints showed further inconsistencies (Figure 3.1, middle and right panels). In each of these trees the geographic segregation was only partially preserved, with both sequences from British Columbia and Ontario, identified as recombinant by RDP, sometimes segregating into different clades. This pattern confirms that recombination is a frequent occurrence for these viruses, as was previously shown for AMDV [19]. Additionally, since inconsistencies involved both closely related and distant sequences, we can hypothesize that this pattern was a result of both old and more recent recombination events.

Site-by-site selection pressure analysis:

Since selection pressure estimates are affected by recombination, which can cause an overestimation of positive selection pressure [8], this analysis was performed on both genes separately by splitting the alignments according to identified breakpoints and by removing additional potential recombinant sequences until RDP found no evidence for recombination in the alignments. This resulted in two alignments (nt 1-849 and 850-1926) of 25 sequences for NS1 (sequences removed: BC_SK29, BC_SK24, BC_SK10, and ON_SSK6) and in one alignment of 29 sequences for VP2 (sequences removed: BC_SK1, BC_SK29, ON_SSK7). While the percentage of negatively selected sites detected by FEL was similar for the 2 ORFs (21.8% vs. 20.3% for NS1 and VP2, respectively) and the percentage of negatively selected sites detected by FUBAR was higher for VP2 compared to NS1 (23.4% vs. 15.1%), the percentage of positively selected sites was higher for NS1 compared to VP2 with all used methods (FEL: 2.2% vs. 0.9%; FUBAR: 4.7% vs. 1.9%; MEME: 5.9% vs. 2.3%), confirming that different selective forces act on the two proteins, as also previously observed for AMDV [19]. A list of sites under episodic and pervasive diversifying and purifying selection found by all methods is available in Supplementary Table S3.3.

As this high antigenic stability, could be linked to ADE, we specifically evaluated selection pressure at residues within predicted SKAV immunogenic loops. Linear epitopes of AMDV that were experimentally determined to be immunogenic were used as references and a high sequence conservation between the VP2 of SKAV and AMDV allowed us to easily identify these regions in SKAV (resides 84-102, 224-247, 307-322, and 438-497 with respect to the VP2 ORF of strain CA_S5) [11,12,61,64]. Interestingly, while positively selected sites could be identified in all four immunogenic loops, no positively selected sites were found in the epitope between

residues 427 and 445. This region has been experimentally determined to be highly immunogenic in AMDV and antibodies recognizing this epitope were capable of aggregating virus particles into immune complexes, mediating ADE and neutralizing virus infectivity *in vitro* [11,12]. In this region of SKAV VP2, there were three variable sites, most of them found in sequences from Ontario, and no residues under diversifying selection were found whereas 26% (FEL) or 37% (FUBAR) of the sites were under negative selection pressure (Supplementary Figure S3.1). These results show that immune response against SKAV and AMDV could involve the same VP2 epitopes and that the same immunogenic regions are likely involved in SKAV and AMDV immune-mediated pathogenicity.

Tissue distribution and pathways of transmission

To identify possible routes of viral shedding, we evaluated histologic sections of the urinary tract, gastrointestinal tract, and integument from representative cases by *in situ* hybridization (ISH). We detected SKAV in all three systems evaluated (Figure 3.2). In the urinary tract, the kidney was a site of infection, with SKAV detectable in renal tubular epithelial cells, protein casts within renal tubules, and in infiltrating interstitial inflammatory cells of animals with chronic tubulointerstitial nephritis (presumed macrophages, lymphocytes, and/or plasma cells). The gastrointestinal tract was a site of infection at multiple levels. Robust signal was detected in the basal epithelium of the tongue and in the gastric epithelium. In the small intestine, SKAV nucleic acid was identified in scattered individual cells in the epithelium and lamina propria (presumed phagocytized epithelial cells and/or infiltrating inflammatory cells). In the skin, signal was localized to the basal epidermis, follicular epithelial cells, and scattered cells in the superficial sub-epithelial stroma (presumed to represent infiltrating inflammatory cells).

Discussion:

SKAV, like other amdoparvoviruses, is a multi-host pathogen, and is apparently capable of causing disease in skunks and mink, but its full host spectrum remains unknown. Furthermore, given the recent definition of this virus as a distinct species, SKAV dispersal in its maintenance host and mechanisms of viral spread, such as transmission routes and tissue tropism, are still largely unexplored. In this study, we provide evidence that SKAV is likely widespread across North America and identify aspects of virus biology and evolution that could favor efficient viral transmission and perpetuation.

Distribution, diversity, and evolutionary dynamics of SKAV:

Our screening efforts allowed us to detect SKAV in various and distant areas of North America, from British Columbia (Canada) and California (USA) on the west coast, Ontario (Canada), and multiple sites from northeastern North America (New Hampshire, Vermont, and Maine, USA, and Nova Scotia, Canada), corroborating results of previous investigations [17,32,69] and adding new sites to the known geographic range of SKAV. Additionally, although sample sizes were generally too small for accurate assessment of prevalence, viral detection rates in areas where multiple samples were available was high, confirming the high prevalence reported by other studies [32,69]. It is highly likely that SKAV, like its close relative AMDV, causes persistent infections and accumulates in spleens, allowing the virus to reach such high prevalence. Nonetheless, although more samples collected in areas not considered in this study need to be investigated, the detection of SKAV in disparate geographic regions suggests that infections are likely endemic in striped skunks across their entire North American range.

Overall, we found high genetic diversity and observed several different viral clades that, for the most part, reflected the geographic origin of the strains, suggesting local diversification due to genetic drift. Interestingly, however, while region-specific sub-clades were found in trees built with both the NS1 and VP2 genes, the overall tree topology was not conserved across phylogenies. The most striking discrepancy was the presence of two clear clades corresponding to viruses from the west and the east in the tree built with NS1, which were missing from the tree built with VP2. This reflects different evolutionary dynamics in the two ORFs, further demonstrated by the fact that NS1 was less conserved (90-98% identity) than VP2 (92-99% identity).

These inconsistencies can also be linked to recombination since our analysis uncovered frequent recombination in the evolutionary history of SKAV. In fact, we identified the presence of multiple phylogenetically supported breakpoints throughout the genome, which were mainly localized within three breakpoint hot spots. Interestingly, sequences from British Columbia and Ontario were those detected as recombinant, while sequences from California and the northeastern USA consistently clustered into separate clades. Since inconsistencies occurred both at the level of main branches as well as within internal clades (i.e., within region-specific clades) we can presume that recombination was and still is important in shaping the genetic make-up of these viruses.

Our selection pressure analyses confirmed that different evolutionary forces act on the structural and non-structural proteins of SKAV. In fact, while the number of sites predicted to be negatively selected by various methods was similar for the two proteins, or even higher for VP2, each method consistently identified a higher percentage of positively selected sites in NS1. This, combined with the higher sequence conservation of the VP proteins, is inconsistent with

diversifying pressure on the capsid proteins as a mechanism to escape detection by the host immune system. Rather, it is suggestive of the possible involvement of ADE in the pathogenesis of the virus, as previously observed for AMDV [19]. In support of this, we also observed that a region experimentally determined to mediate ADE and virus neutralization in AMDV [11,12] was very conserved between the two viral species. This fragment also showed very little variation within SKAV strains, no residues under diversifying selection pressure, and approximately 30% of sites under purifying selection pressure. These results indicate that immune response and immune-mediated pathogenicity likely involve the same sites in both viruses.

The many similarities between the evolution of SKAV and AMDV, including local genetic drift, frequent recombination with similar breakpoint hot spots, and the different evolutionary forces acting on the two proteins, suggest that the two viruses also have similar biological behaviors.

Tissue distribution, pathogenicity, and spread:

To evaluate how widespread viral distribution is linked to viral transmission, we performed ISH to evaluate cell and tissue sources of viral shedding. AMDV can be shed in feces, urine, blood, and saliva of infected mink [33,34,48], and we suspected that a similar distribution would occur for SKAV in skunks. Indeed, the observed tissue distribution of viral nucleic acid demonstrated in this study confirms that SKAV in some individuals is present in, and potentially shed in oral/nasal secretions, feces, urine, as well as sloughed skin. Although presence of virus in hair itself could not be evaluated due to technical limitations of the hydrophobic hair follicle, we identified SKAV in the root sheath follicular epithelial cells, which suggests that shed hairs may also be coated with virus and/or contain sloughed viral laden keratinocytes as a potential route of

shedding and transmission. Because parvoviruses are very resilient in the environment [29,41], transmission via direct or indirect (contaminated food, water, or environment) contacts are both possible. We did not have opportunities to evaluate transplacental transmission as a mechanism of spread among skunks, although the placenta has been shown to be a site of virus replication and possible *in utero* transmission for AMDV in mink [15,16,32]. Additionally, tissue-distribution analyses were limited to a small number of individuals and follow-up studies are required to assess whether there is variability between infected animals and quantify viral presence in each tissue.

Clinical and pathological data are scarce, but preliminary investigations showed that SKAV infection can result in a similar range of clinical presentations as those observed in AMDV-positive mink. Few studies to date have evaluated pathology associated with SKAV infections, and such an evaluation was outside the scope of this study. However, similar to what has been reported for mink, lesions associated with SKAV have included multisystemic lymphoplasmacytic inflammation, glomerulonephritis, vasculitis/arteritis, and cerebral microangiopathy [15,32,54]. The presence of plasma cell-rich inflammatory lesions coupled with arteritis/vasculitis, microangiopathy, and glomerulonephritis suggests the possible involvement of immunocomplexes in virus pathogenesis and therefore provides additional support for our hypothesis that ADE can contribute to maintenance and exacerbation of infection. Overall, however, subclinical infections seem predominant [15,32]. The high frequency of mild or inapparent disease, the likely persistence of infections, and chance of viral transmission to occur through many possible different routes are all factors contributing to efficient viral spread, which enabled SKAV to become enzootic across North America, and also support the conclusion that the virus

has been circulating in skunks for a long time. This is also substantiated by its high genetic diversity and by the evidence that recombination has occurred in ancestral strains.

Although skunks are the viral reservoir and maintenance host for SKAV, spillover infections have been found in mink [19,70] and we can presume that other carnivorans are also susceptible to infection, just as other amdoparvoviruses have been shown to infect a broad range of species [58,82]. Because of persistent viral shedding and high environmental stability, large quantities of virions might remain viable in the environment for a long time, offering opportunities for cross-species transmission to sympatric species through habitat sharing or niche overlap. Additionally, spillover to bigger animals through carnivory, as hypothesized for other amdoparvoviruses [18], is also possible and could pose a risk for infection in domestic animals, since skunks are frequently found in urban and suburban environments.

Finally, to the best of our knowledge, there is no evidence of SKAV infections in mink farms. We can safely conclude, therefore, that this virus has originated in North America like its close relative AMDV. Furthermore, its presence in wild animals can be reasonably defined as autochthonous, as opposed to AMDV strains from wild animals that are frequently of farm-origin. This is well demonstrated by geographical clustering of strains. SKAV therefore offers a better model than AMDV to study amdoparvovirus evolution and transmission dynamics in wildlife. Further studies should examine more hosts and geographic locations to characterize the full genetic diversity of this virus and evaluate its cross-species transmission potential.

Conclusions:

In this study, we established that SKAV is endemic in striped skunks, with a high rate of infections in multiple sites across North America. This apparently high prevalence and the long-

term persistence of subclinical infections, likely intensified by ADE, promotes opportunities for infection with multiple strains and subsequent recombination, a mechanism frequently used by parvoviruses to further increase genetic diversity. Persistent infections, low viral pathogenicity, and high genetic diversity with local diversification due to genetic drift suggest a long-term virus-host association. The environmental stability typical of parvoviruses combined with a persistent and efficient viral shedding, which can occur though many possible transmission routes, likely contributed to the successful spread of this virus over large distances. High genetic diversity and efficient, persistent shedding also offer opportunities for cross-species transmission to potentially susceptible sympatric species that can acquire the infection by habitat sharing, predation, or close contact. As our knowledge about these viruses grow, future studies will clarify whether other members of the genus *Amdoparvovirus* possess similar biological and genetic characteristics and whether they are as broadly dispersed as SKAV and AMDV.

Conflict of Interest Statement:

The authors declare no conflict of interest.

Ethics Statement:

The authors confirm that the ethical policies of the journal, as noted on the journal's author guidelines page, have been adhered to. This study used samples collected opportunistically from dead animals. No ethical approval was required.

Acknowledgements:

We gratefully acknowledge the wildlife rescue centers, OMNDMNRF rabies program staff, and Drs. Andrew Cartoceti (Smithsonian National Zoological Park) and Megan Jones (Canadian Wildlife Health Cooperative), who contributed samples to this study. This project was supported in part by the Karen C. Drayer Wildlife Health Center, School of Veterinary Medicine, University of California, Davis.

References:

1. Alex CE, Kubiski SV, Li L, et al. Amdoparvovirus Infection in Red Pandas (Ailurus fulgens). *Vet Pathol*. 2018;**55**(4):552–561.

2. Allender MC, Schumacher J, Thomas KV, et al. Infection with Aleutian disease virus-like virus in a captive striped skunk. *J Am Vet Med Assoc*. 2008;**232**(5):742–746.

3. Anisimova M, Nielsen R, Yang Z. Effect of recombination on the accuracy of the likelihood method for detecting positive selection at amino acid sites. *Genetics*. 2003;**164**(3):1229–1236.

4. Bay RA, Bielawski JP. Recombination detection under evolutionary scenarios relevant to functional divergence. *J Mol Evol*. 2011;**73**(5–6):273–286.

5. Bloom ME, Best SM, Hayes SF, et al. Identification of aleutian mink disease parvovirus capsid sequences mediating antibody-dependent enhancement of infection, virus neutralization, and immune complex formation. *J Virol*. 2001;**75**(22):11116–11127.

6. Bloom ME, Martin DA, Oie KL, et al. Expression of Aleutian mink disease parvovirus capsid proteins in defined segments: localization of immunoreactive sites and neutralizing epitopes to specific regions. *J Virol*. 1997;**71**(1):705–714.

7. Bodewes R, van der Giessen J, Haagmans BL, Osterhaus ADME, Smits SL. Identification of multiple novel viruses, including a parvovirus and a hepevirus, in feces of red foxes. *J Virol*. 2013;**87**(13):7758–7764.

8. Britton AP, Redford T, Bidulka JJ, et al. Beyond Rabies: Are Free-Ranging Skunks (Mephitis mephitis) in British Columbia Reservoirs of Emerging Infection? *Transbound Emerg Dis*. 2017;**64**(2):603–612.

9. Broll S, Alexandersen S. Investigation of the pathogenesis of transplacental transmission of Aleutian mink disease parvovirus in experimentally infected mink. *J Virol*. 1996;**70**(3):1455–1466.

10. Canuti M, Doyle HE, P Britton A, Lang AS. Full genetic characterization and epidemiology of a novel amdoparvovirus in striped skunk (Mephitis mephitis). *Emerg Microbes Infect*. 2017;**6**(5):e30.

11. Canuti M, McDonald E, Graham SM, et al. Multi-host dispersal of known and novel carnivore amdoparvoviruses. *Virus Evol*. 2020;**6**(2).

12. Canuti M, O'Leary KE, Hunter BD, et al. Driving forces behind the evolution of the Aleutian mink disease parvovirus in the context of intensive farming. *Virus Evol*. 2016;**2**(1):vew004.

13. Canuti M, Todd M, Monteiro P, et al. Ecology and Infection Dynamics of Multi-Host Amdoparvoviral and Protoparvoviral Carnivore Pathogens. *Pathogens*. 2020;**9**(2).

14. Canuti M, Whitney HG, Lang AS. Amdoparvoviruses in small mammals: expanding our understanding of parvovirus diversity, distribution, and pathology. *Front Microbiol*. 2015;**6**:1119.

15. Cotmore SF, Agbandje-McKenna M, Canuti M, et al. ICTV Virus Taxonomy Profile: Parvoviridae. *J Gen Virol*. 2019;**100**(3):367–368.

16. Eterpi M, McDonnell G, Thomas V. Disinfection efficacy against parvoviruses compared with reference viruses. *J Hosp Infect*. 2009;**73**(1):64–70.

17. Farid AH. Aleutian mink disease virus in furbearing mammals in Nova Scotia, Canada. *Acta Vet Scand*. 2013;**55**:10.

18. Glueckert E, Clifford DL, Brenn-White M, et al. Endemic Skunk amdoparvovirus in free-ranging striped skunks (Mephitis mephitis) in California. *Transbound Emerg Dis*. 2019.

19. Gorham JR, Henson JB, Crawford TB, Padgett GA. The epizootiology of aleutian disease. *Front Biol*. 1976;**44**:135–158.

20. Gorham JR, Leader RW, Henson JB. The experimental transmission of a virus causing hypergammaglobulinemia in mink: Sources and modes of infection. *J Infect Dis*. 1964;**114**:341–345.

21. Guindon S, Dufayard J-F, Lefort V, Anisimova M, Hordijk W, Gascuel O. New algorithms and methods to estimate maximum-likelihood phylogenies: assessing the performance of PhyML 3.0. *Syst Biol*. 2010;**59**(3):307–321.

22. Hoang DT, Chernomor O, von Haeseler A, Minh BQ, Vinh LS. UFBoot2: Improving the Ultrafast Bootstrap Approximation. *Mol Biol Evol*. 2018;**35**(2):518–522.

23. Hussain I, Price GW, Farid AH. Inactivation of Aleutian mink disease virus through high temperature exposure in vitro and under field-based composting conditions. *Vet Microbiol*. 2014;**173**(1–2):50–58.

24. Kalyaanamoorthy S, Minh BQ, Wong TKF, von Haeseler A, Jermiin LS. ModelFinder: fast model selection for accurate phylogenetic estimates. *Nat Methods*. 2017;**14**(6):587–589.

25. Kanno H, Wolfinbarger JB, Bloom ME. Aleutian mink disease parvovirus infection of mink macrophages and human macrophage cell line U937: demonstration of antibody-dependent enhancement of infection. *J Virol*. 1993;**67**(12):7017–7024.

26. Kenyon AJ, Helmboldt CF, Nielsen SW. Experimental transmission of Aleutian disease with urine. *Am J Vet Res*. 1963;**24**:1066–1067.

27. Kosakovsky Pond SL, Frost SDW. Not so different after all: a comparison of methods for detecting amino acid sites under selection. *Mol Biol Evol*. 2005;**22**(5):1208–1222.

28. Kosakovsky Pond SL, Posada D, Gravenor MB, Woelk CH, Frost SDW. Automated phylogenetic detection of recombination using a genetic algorithm. *Mol Biol Evol*. 2006;**23**(10):1891–1901.

29. Kumar S, Stecher G, Li M, Knyaz C, Tamura K. MEGA X: Molecular Evolutionary Genetics Analysis across Computing Platforms. *Mol Biol Evol*. 2018;**35**(6):1547–1549.

30. LaDouceur EEB, Anderson M, Ritchie BW, et al. Aleutian Disease: An Emerging Disease in Free-Ranging Striped Skunks (Mephitis mephitis) From California. *Vet Pathol*. 2015;**52**(6):1250–1253.

31. Larkin MA, Blackshields G, Brown NP, et al. Clustal W and Clustal X version 2.0. *Bioinformatics*. 2007;**23**(21):2947–2948.

32. Lau SKP, Ahmed SS, Tsoi H-W, et al. Bats host diverse parvoviruses as possible origin of mammalian dependoparvoviruses and source for bat-swine interspecies transmission. *J Gen Virol*. 2017.

33. Leimann A, Knuuttila A, Maran T, Vapalahti O, Saarma U. Molecular epidemiology of Aleutian mink disease virus (AMDV) in Estonia, and a global phylogeny of AMDV. *Virus Res*. 2015;**199**:56–61.

34. Li L, Pesavento PA, Woods L, et al. Novel amdovirus in gray foxes. *Emerg Infect Dis*. 2011;**17**(10):1876–1878.

35. Lu T, Wang Y, Ge J, et al. Identification and characterization of a novel B-cell epitope on Aleutian Mink Disease virus capsid protein VP2 using a monoclonal antibody. *Virus Res*. 2018;**248**:74–79.

36. Martin DP, Murrell B, Golden M, Khoosal A, Muhire B. RDP4: Detection and analysis of recombination patterns in virus genomes. *Virus Evol*. 2015;**1**(1):vev003.

37. McKenna R, Olson NH, Chipman PR, et al. Three-dimensional structure of Aleutian mink disease parvovirus: implications for disease pathogenicity. *J Virol*. 1999;**73**(8):6882–6891.

38. Minh BQ, Schmidt HA, Chernomor O, et al. IQ-TREE 2: New Models and Efficient Methods for Phylogenetic Inference in the Genomic Era. *Mol Biol Evol*. 2020;**37**(5):1530–1534.

39. Murrell B, Moola S, Mabona A, et al. FUBAR: a fast, unconstrained bayesian approximation for inferring selection. *Mol Biol Evol*. 2013;**30**(5):1196–1205.

40. Murrell B, Wertheim JO, Moola S, Weighill T, Scheffler K, Kosakovsky Pond SL. Detecting individual sites subject to episodic diversifying selection. *PLoS Genet*. 2012;**8**(7):e1002764.

41. Nituch LA, Bowman J, Wilson PJ, Schulte-Hostedde AI. Aleutian mink disease virus in striped skunks (Mephitis mephitis): evidence for cross-species spillover. *J Wildl Dis*. 2015;**51**(2):389–400.

42. Nituch LA, Bowman J, Wilson P, Schulte-Hostedde AI. Molecular epidemiology of Aleutian disease virus in free-ranging domestic, hybrid, and wild mink. *Evol Appl*. 2012;**5**(4):330–340.

43. Pénzes JJ, Marsile-Medun S, Agbandje-McKenna M, Gifford RJ. Endogenous amdoparvovirus-related elements reveal insights into the biology and evolution of vertebrate parvoviruses. *bioRxiv*. 2018:224584.

44. Pénzes JJ, Söderlund-Venermo M, Canuti M, et al. Reorganizing the family Parvoviridae: a revised taxonomy independent of the canonical approach based on host association. *Arch Virol*. 2020;**165**(9):2133–2146.

45. Rosatte R LS. Skunks. Genera Mephitis, Spilogale, and Conepatus. In: Ja FGTB, ed. *Wild Mammals of North America: Biology, Management, and Conservation. Second ed.* The Johns Hopkins University Press 2003:692–707.

46. Shao X-Q, Wen Y-J, Ba H-X, et al. Novel amdoparvovirus infecting farmed raccoon dogs and arctic foxes. *Emerg Infect Dis*. 2014;**20**(12):2085–2088.

47. Weaver S, Shank SD, Spielman SJ, Li M, Muse SV, Kosakovsky Pond SL. Datamonkey 2.0: A Modern Web Application for Characterizing Selective and Other Evolutionary Processes. *Mol Biol Evol*. 2018;**35**(3):773–777.

48. Wu Z, Lu L, Du J, et al. Comparative analysis of rodent and small mammal viromes to better understand the wildlife origin of emerging infectious diseases. *Microbiome*. 2018;**6**(1):178.

49. Wu Z, Yang L, Ren X, et al. Deciphering the bat virome catalog to better understand the ecological diversity of bat viruses and the bat origin of emerging infectious diseases. *ISME J*. 2016;**10**(3):609–620.

Figures and Tables:

Table 3.1. SKAV positivity rates in each investigated region.

Region	Sample dates	Total tested	Total positive	Positivity rate
California, USA	2019-2020	23	20	87.0%
Ontario, Canada	2020	10	7	70.0%
New Hampshire, USA	2019-2020	5	1	20.0%
Maine, USA	2020	7	5	71.4%
Vermont, USA	2016-2020	5	3	60.0%
Nova Scotia, Canada	2019	1	1	100.0%
British Columbia, Canada	2011-2015	50	43	86.0% [15]
Total		101	80	79.2%

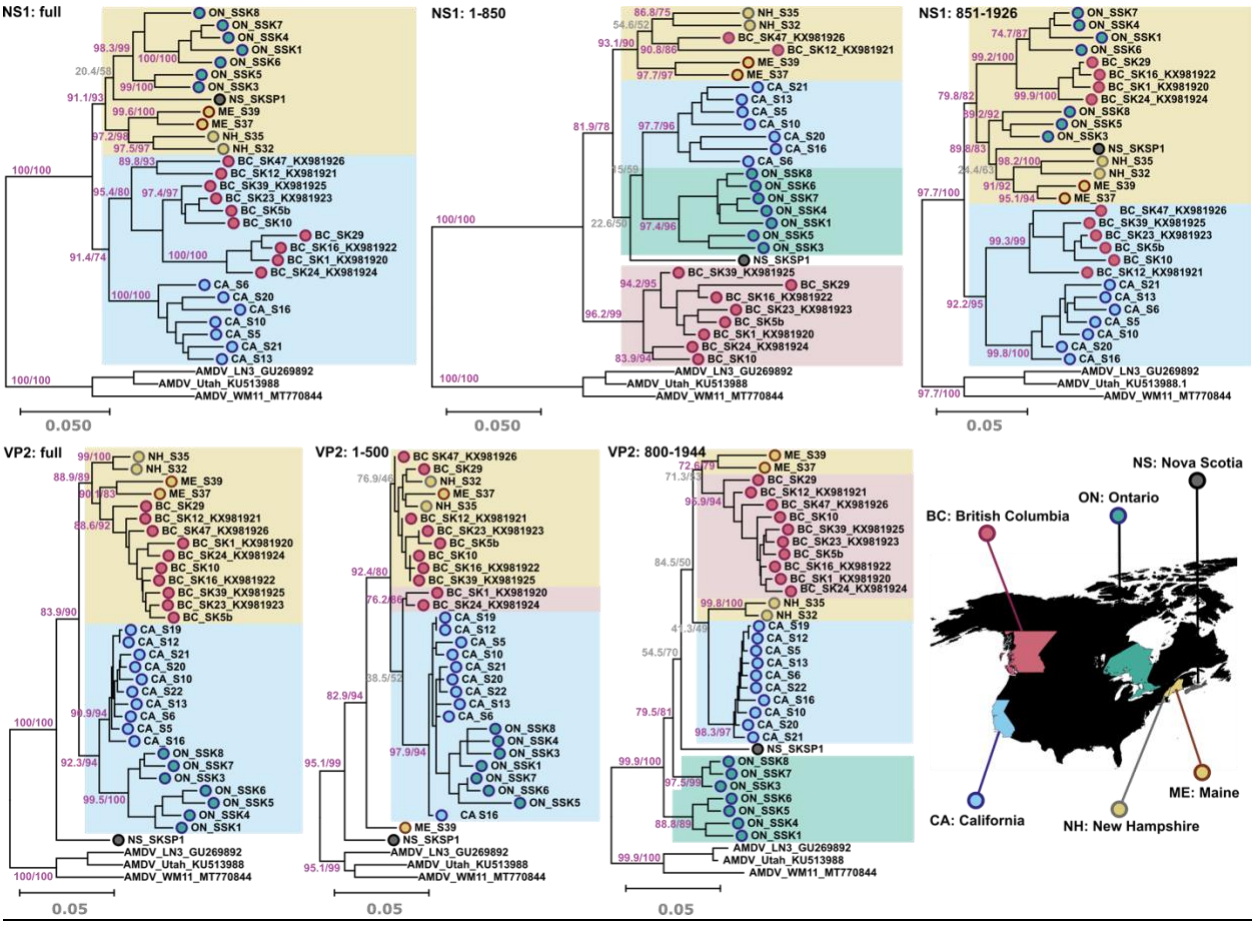

Figure 3.1. Phylogenetic analysis of SKAV strains from North America. Phylogenetic trees built with the NS1 (top) and VP2 (bottom) ORFs are shown. Analyses were performed either with the alignments of the full ORFs (left side) or sub-portions of the alignments included between recombination breakpoints (middle and left) and used nucleotide regions are indicated in tree titles. Trees were built with the maximum likelihood method with IQ-Tree based on the best models for distance estimation identified with the Model Finder function (TIM3+F+I+G4 for NS1:full, NS1:1-850, and VP2:full; TPM3+F+I+G4 for NS1:851-1926; TPM3+F+R2 for VP2:1-500; HKY+F+I+G4 for VP2:800-1944). The outcomes of the SH-aLRT and bootstrap test (1000 replicates) are shown for the main nodes (purple for statistically supported clades and gray for unsupported ones). Three AMDV strains were used as an outgroup. Strains are labelled based on collection sites, as indicated on the map at the bottom-right. The two main clades are shaded in blue (viruses from California) and yellow (viruses from Maine, Vermont, and New

Hampshire), while additional clades only present when portions of the two ORFs were used for the tree are shaded in red (viruses from British Columbia) or green (viruses from Ontario). Sequences are labelled by sampling location (BC: British Columbia, ON: Ontario, NS: Nova Scotia, CA: California, NH: New Hampshire, ME: Maine), strain name, and accession number. The map was created using Mapchart.net ©.

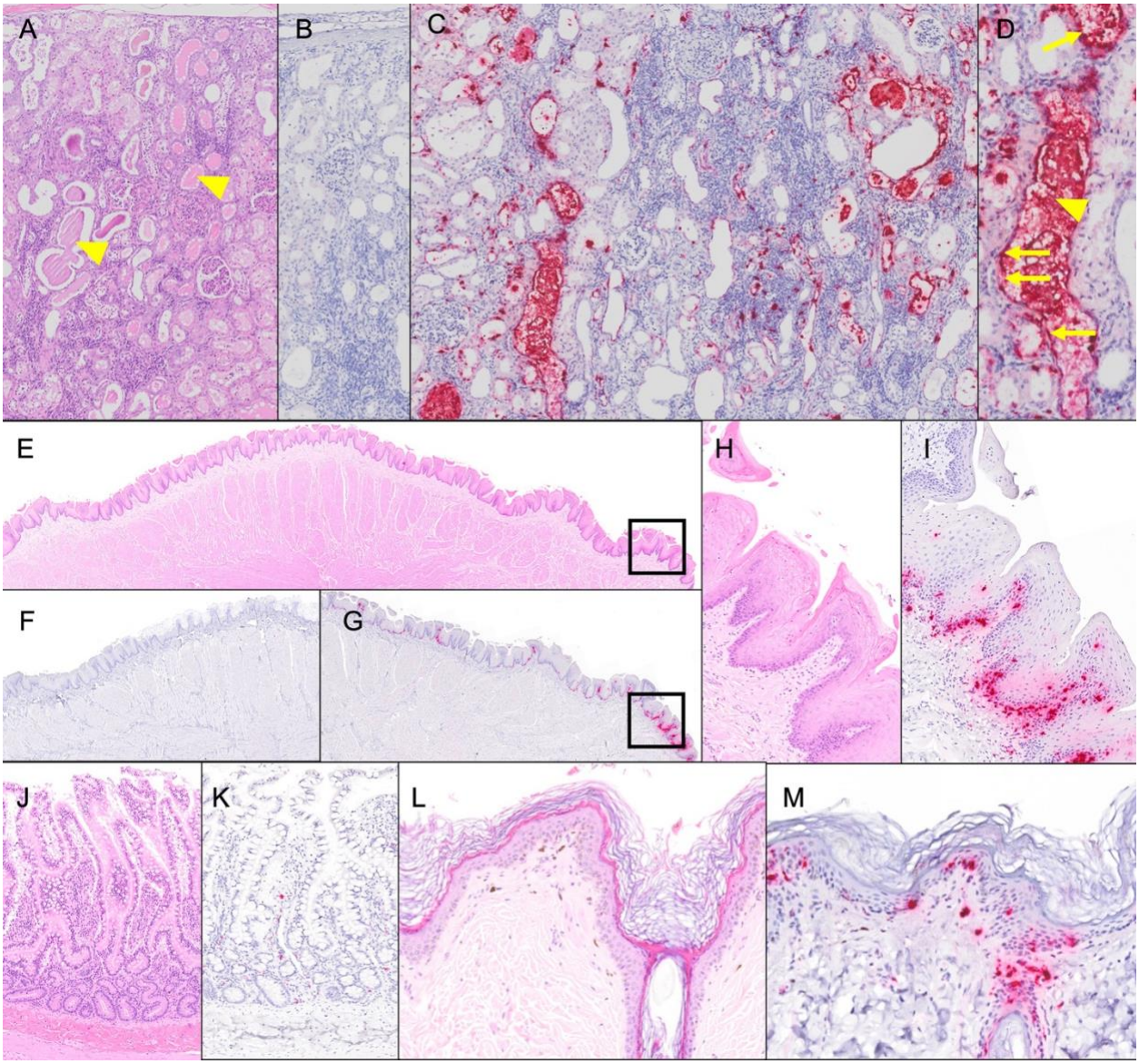

Figure 3.2. Detection of SKAV in tissues by *in situ* hybridization (ISH) demonstrates multiple potential mechanisms of shedding.

(A-C) Kidney, striped skunk. (A) Hematoxylin and eosin (H&E) staining demonstrates lesions of chronic kidney disease including lymphoplasmacytic tubulointerstitial nephritis and tubular dilation with luminal protein casts (arrowheads). (B) Negative control (DapB) ISH. No hybridization is observed. (C) ISH with SKAV-specific probes detects abundant SKAV nucleic acid (red) in the affected tissues. (D) Signal is observed in tubular epithelium (arrows) and protein casts (arrowhead). (E-J) Tongue, striped skunk. (E) H&E. (F) Negative control. (G) SKAV ISH demonstrates viral nucleic acid in lingual epithelium and

subepithelial stroma. (H) H&E, high magnification. (I) SKAV ISH, high magnification. Signal is primarily observed in basal epithelial cells, although a few individual cells are also positive at higher levels. Signal is also detected in scattered cells in the superficial submucosal stroma, presumed to be infiltrating inflammatory cells and/or capillary endothelium. (J-K) Small intestine, striped skunk. (J) H&E. (K) SKAV ISH. Scattered individual cells in the mucosal epithelium and lamina propria are positive. (L-M) Skin, striped skunk. (L) H&E. (M) SKAV ISH. Hybridization is observed primarily in the stratum basale but occurs at all levels of the epidermis. Signal is also present in epithelial lining of a hair follicle.

Table S3.1 Recombination breakpoints detected by multiple methods.

N	Breakpoint Positions		Recombinant Sequence(s)	Minor Parental Sequence(s)	Major Parental Sequence(s)	Detection Methods								
	Begin	End				RDP	GENECONV	Bootscan	Maxchi	Chimaera	SiScan	PhylPro	LARD	3Seq
1	953 (NS1)	2196 (IG)	BC_SK1	BC_SK29	BC_SK39	5.86E-14	4.86E-11	1.29E-14	7.98E-14	2.65E-13	1.57E-19	NS	NS	7.37E-15
2	853 (NS1)	2063 (IG)	BC_SK16, BC_SK24, BC_SK29	ON_SSK4	BC_SK23, BC_SK5b, BC_SK10	1.36E-05	NS	2.25E-03	9.22E-13	1.32E-09	1.99E-05	NS	NS	5.09E-10
3	900 (NS1)	1847 (NS1)	ON_SSK8	Unknown	ON_SSK7	3.93E-11	3.74E-09	1.10E-10	1.40E-12	2.81E-11	2.79E-16	NS	NS	1.81E-13
4	2775 (VP2)	3440 (VP2)	ON_SSK7	Unknown	ON_SSK4	2.08E-09	2.60E-07	3.25E-09	1.13E-04	1.51E-05	1.83E-06	NS	NS	3.48E-09
5	Beginning	844 (NS1)	ON_SSK8	ON_SSK6	ON_SSK3	1.54E-05	4.88E-04	2.09E-06	1.62E-07	7.38E-09	4.00E-08	NS	NS	4.91E-09
6	2328 (VP2)	End	ON_SSK5	ON_SSK6	ON_SSK3	7.78E-06	2.83E-02	2.53E-06	3.27E-07	5.76E-09	9.88E-10	NS	NS	4.84E-09
7	2200 (IG)	2965 (VP2)	BC_SK1	BC_SK39, BC_SK23, BC_SK5b, BC_SK10	BC_SK16	2.71E-06	8.45E-05	3.24E-05	1.87E-03	1.06E-03	4.55E-05	NS	NS	2.33E-06
8	130 (NS1)	462 (NS1)	BC_SK29	BC_SK16	Unknown	2.80E-06	7.92E-05	8.05E-06	1.62E-04	4.85E-05	5.94E-06	NS	NS	5.74E-06
9	588 (NS1)	1163 (NS1)	ON_SSK6	ON_SSK5	ON_SSK1	NS	NS	NS	1.05E-05	9.16E-03	NS	NS	NS	3.74E-02
10	3441 (VP2)	End	ON_SSK7	ON_SSK3	ON_SSK6	3.23E-03	NS	2.87E-03	3.39E-02	NS	5.13E-04	NS	NS	1.40E-04

IG: intragenic, between the stop codon of NS1 and the start codon of VP2 (~nt 2000-2200)

Table S3.2. NS1 and VP2 pairwise sequence identity ranges (percentages of 1 – p-distance) between sequences within each regional bootstrap-supported group as defined in Figure 3.1.

	ON	ON.1[1]	ON.2[2]	ON.3[3]	ON.4[4]	ME-NH-VT	NH-VT	ME	CA	BC	BC.1[5]	BC.2[6]	BC.3[7]
NS1	93.0-98.4	96.8-98.4	96.4	-	-	93.6-96.2	98.2	96.4	94.5-97.3	90.7-98.3	94.4	96.4-97.8	95.5-98.0
VP2	93.7-98.5	-	-	98.2-98.5	95.2-97.8	-	94.6	96.2	98.1-99.8	96.7-98.8	-	-	-

ON: Ontario; ME: Maine; VT: Vermont; NH: New Hampshire; CA: California; BC: British Columbia. A – indicates that the group was not identified in the tree of the corresponding ORF. [1]SSK7, SSK4, SSK1, SSK6; [2]SSK5, SSK3; [3]SSK8, SSK3, SSK7; [4]SSK6, SSK5, SSK4, SSK1; [5]SK47, SK12; [6]SK39, SK23, SK5b, SK10; [7]SK29, SK16, SK1, SK24.

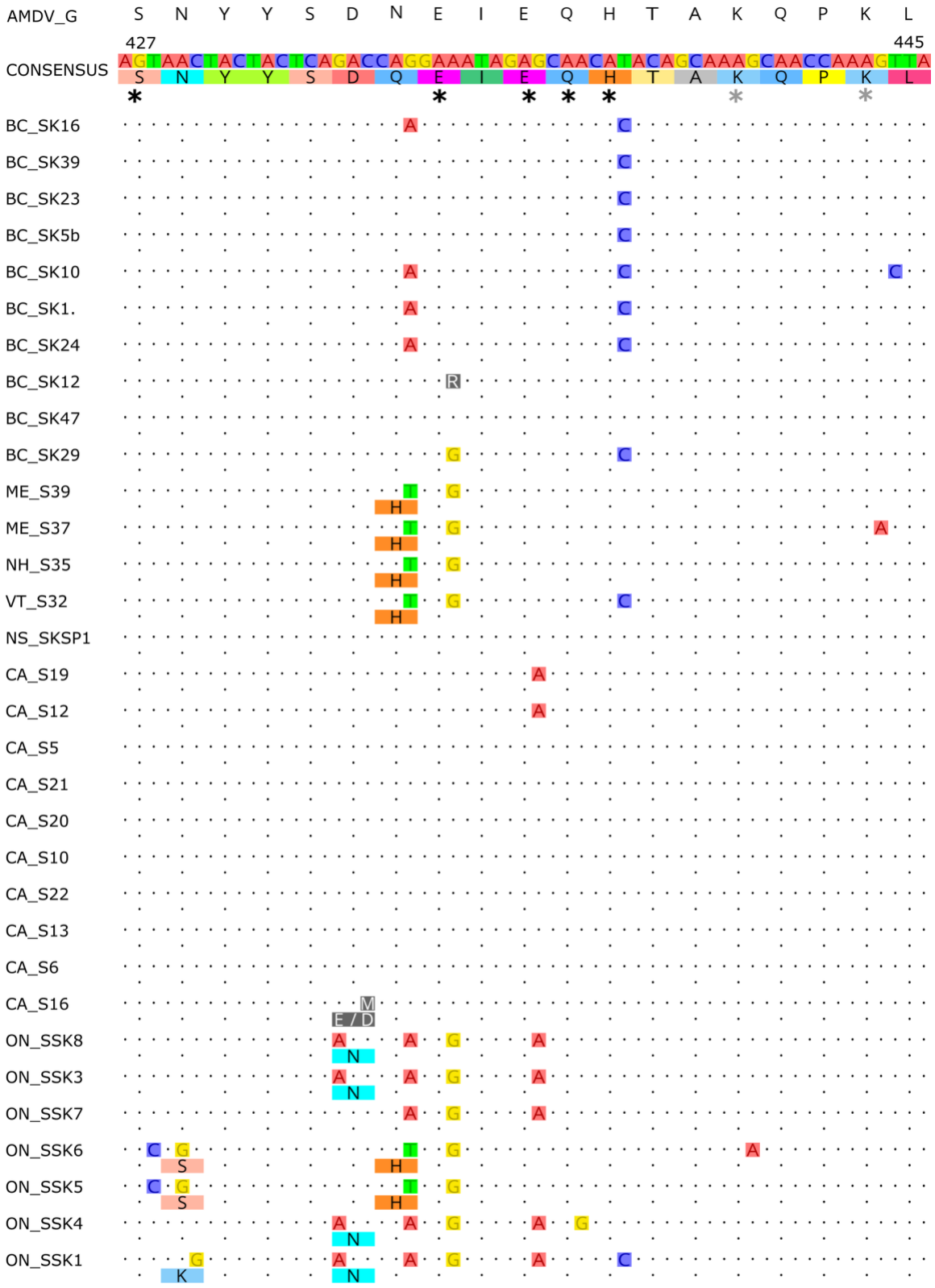

*: found under negative selection by 2 methods (FEL+FUBAR)

*: found under negative selection by 1 method (FUBAR)

Figure S3.1. Sequence variability at the level of the immunogenic epitope (amino acids 427-445 of the VP2 protein of strain CA_S5) presumed to mediate ADE. The amino acid sequence of the corresponding epitope of AMDV is reported on the top (AMDV_G, accession number: JN040434) and right below are indicated the nucleotide and amino acid consensus sequences of SKAV strains analyzed in this study. Below, for each strain, sequence variations respect to the consensus are indicated by letters, while dots indicate that the sequence in that position is identical to the consensus. Residues under purifying selection pressure are indicated by asterisks (black if found by two methods and gray if found by only one method).

Table S3.3. How many (N) and which codons of the two viral proteins NS1 and VP2 were identified to be under negative (purifying) and positive (diversifying) selection pressure by the three used methods.

Method	**Sites under purifying selection***	**Sites under diversifying selection***
NS1 (641 aa)		
FUBAR	N=97 13, 19, 35, 36, 39, 46, 50, 52, 55, 88, 90, 91, 93, 100, 102, 110, 125, 135, 136, 138, 140, 141, 143, 145, 149, 158, 168, 170, 181, 182, 187, 188, 191, 194, 199, 200, 202, 203, 211, 212, 217, 218, 223, 248, 249, 253, 254, 259, 265, 281, 294, 295, 298, 305, 308, 313, 325, 345, 352, 359, 361, 383, 384, 390, 407, 426, 427, 428, 430, 432, 433, 439, 453, 454, 468, 473, 491, 502, 507, 509, 513, 531, 532, 534, 536, 538, 539, 540, 541, 544, 559, 566, 570, 571, 573, 574, 621	N=30 6, 37, 83, 94, 163, 225, 252, 291, 310, 312, 323, 326, 332, 333, 349, 364, 381, 409, 482, 514, 521, 523, 525, 549, 557, 598, 600, 603, 604, 619
FEL	N=140 13, 19, 28, 35, 36, 39, 46, 50, 52, 55, 62, 86, 88, 90, 91, 93, 100, 102, 110, 117, 118, 124, 125, 135, 136, 137, 138, 140, 141, 143, 145, 149, 156, 158, 170, 171, 177, 181, 182, 187, 188, 191, 193, 194, 195, 199, 200, 201, 202, 203, 204, 206, 211, 212, 217, 218, 223, 245, 248, 249, 253, 254, 259, 265, 281, 294, 295, 298, 301, 305, 308, 313, 325, 343, 345, 346, 348, 352, 358, 359, 361, 367, 370, 382, 383, 384, 386, 388, 390, 405, 406, 407, 410, 423, 424, 426, 427, 428, 430, 432, 433, 439, 451,	N=14 94, 214, 225, 310, 323, 333, 349, 381, 482, 523, 525, 598, 604, 619

	453, 454, 467, 468, 469, 473, 479, 487, 491, 493, 495, 502, 505, 507, 509, 510, 513, 530, 531, 532, 534, 536, 538, 539, 540, 541, 544, 546, 548, 559, 560, 566, 570, 571, 573, 574, 621	
MEME	NA	N=38 12, 18, 21, 24, 76, 94, 109, 120, 122, 159, 183, 189, 214, 225, 264, 304, 310, 323, 333, 349, 364, 365, 381, 425, 447, 449, 450, 478, 482, 496, 523, 525, 533, 592, 598, 600, 604, 619
VP2 (646 aa)		
FUBAR	N=151 5, 6, 8, 12, 22, 24, 25, 30, 33, 44, 49, 50, 59, 65, 67, 69, 79, 88, 94, 98, 101, 107, 109, 115, 119, 129, 132, 134, 136, 148, 153, 157, 164, 174, 178, 179, 181, 185, 188, 197, 198, 211, 213, 214, 215, 218, 220, 228, 230, 244, 245, 251, 256, 259, 269, 274, 279, 283, 284, 285, 288, 290, 292, 296, 299, 306, 314, 318, 321, 327, 333, 339, 340, 343, 344, 347, 351, 353, 358, 362, 367, 368, 371, 378, 380, 383, 388, 389, 392, 402, 404, 407, 408, 416, 422, 423, 425, 426, 427, 434, 436, 437, 438, 441, 444, 448, 449, 451, 453, 454, 457, 464, 474, 476, 487, 489, 495, 496, 504, 506, 509, 517, 521, 522, 530, 534, 541, 547, 553, 556, 560, 562, 572, 579, 588, 592, 593, 596,	N=12 43, 55, 63, 89, 232, 234, 235, 258, 309, 447, 484, 628

	603, 605, 606, 607, 613, 618, 623, 634, 636, 638, 641, 642, 643, 645	
FEL	N=131 5, 6, 8, 12, 22, 25, 30, 44, 49, 50, 59, 79, 88, 94, 98, 101, 107, 109, 115, 119, 129, 132, 134, 136, 148, 153, 157, 164, 174, 178, 179, 181, 185, 188, 197, 198, 211, 213, 215, 218, 220, 228, 230, 244, 245, 251, 256, 259, 269, 274, 279, 283, 284, 285, 288, 290, 292, 296, 299, 314, 318, 326, 327, 333, 339, 340, 347, 351, 353, 358, 362, 367, 371, 380, 383, 388, 389, 392, 402, 407, 408, 416, 423, 425, 426, 427, 434, 436, 437, 438, 448, 449, 451, 454, 464, 476, 487, 488, 489, 496, 504, 506, 509, 517, 521, 522, 530, 534, 541, 547, 553, 556, 560, 562, 572, 592, 593, 596, 603, 605, 606, 607, 613, 618, 623, 634, 636, 638, 641, 642, 643	N=6 89, 232, 234, 277, 309, 628
MEME	NA	N=15 55, 60, 89, 233,234,237, 239, 306, 309, 342, 465, 484, 488, 515, 628

*Numbering was done according to protein sequences of strain CA_S5 (accession number: OL889872);

NA: not available as MEME detects only sites under positive selection pressure.

CHAPTER 4:

Amdoparvovirus-associated disease in red pandas (*Ailurus fulgens*)

Charles E. Alex, DVM, DACVP, Pavel Kvapil, DVM, Martin DM Busch, DVM, DACVP, Trine Hammer, Kenneth Conley, DVM, DACVP, Kenneth A. Jackson, MS, Eric L. Stubbs, Jenessa Gjeltema, DVM, DACZM, Michael M. Garner, DVM, DACVP, Steven V. Kubiski, DVM, PhD, DACVP, Patricia A. Pesavento, DVM, PhD, DACVP

Submitted for publication in Veterinary Pathology.

Abstract:

The roster of Amdoparvoviruses (APVs) in small carnivores is growing rapidly, but in most cases the consequences of infection are not well understood. Red Panda Amdoparvovirus (RPAV) is highly prevalent in zoo-housed red pandas and has been detected in both healthy and sick animals. Clarifying the clinical impact of RPAV in this endangered species is critical, and zoological collections offer a unique opportunity to examine viral pathogenesis and disease association in a carefully managed population. We evaluated the potential impact of RPAV in captive red pandas with a combination of prospective and retrospective analyses. First, we collected feces from two healthy animals from a single collection over a six-year period, and detected virus in 72/75 total samples, indicating that RPAV can be a long-term, asymptomatic infection. In combination, the high prevalence and evidence of persistence provided vital context for interpretation of a retrospective study on infection status and tissue distribution in necropsied animals. PCR and ISH studies of 43 necropsy cases from four zoo collections (3 US, 1 Europe, 1997-2022) demonstrated that RPAV has been present in this population for at least two decades before its discovery, and is detectable in important lesions of zoo red pandas, including myocarditis (3/3 cases), nephritis (9/10), and interstitial pneumonia (2/4). RPAV is also detectable in sporadic lesions including multisystemic pyogranulomatous inflammation, oral/pharyngeal mucosal inflammation, and dermatitis. We conclude that despite the apparently asymptomatic carriage of most infections, RPAV can have a significant impact in zoo collections.

Introduction:

Parvoviruses are small (~26nm diameter), with a ~5kb ssDNA genome encoding two open reading frames devoted to proteins for replication (2.2kb) and capsid construction (2.3kb).[9,10,26] Their small size and simple genomic organization belies a diverse, successful, and ancient family of viruses with highly variable biological behavior and host impact.[11,17] The severe and sometimes fatal disease caused by the protoparvovirus Carnivore Parvovirus-2 (CPV-2) is notorious and well-studied in several carnivores, but this type of acute, fulminant infection characterizes only a subset of the *Parvoviridae*.[17] Other, more insidious parvoviruses, such as the recently recognized Mouse Kidney Parvovirus, can cause persistent or even life-long infections, with consequences that do not coincide with initial infection, but can result in the gradual accumulation of damage over time.[29] A growing body of epidemiologic and pathologic evidence demonstrates that persistent parvovirus infections can have dire consequences for the health of the host.[8,16,29]

The prototypical and archetypical Amdoparvovirus (APV), Aleutian Mink Disease Virus (AMDV), is well known to cause persistent infections, with a wide range of clinical outcomes depending on host immunity – potentially modulated by factors such as genetics, stress, co-infections, and immunosuppression – as well as viral genotype.[8] AMDV – by. Far the best-studied APV – was discovered in the 1960s among mink housed for the fur industry and has been reviled for decades for its impact on commercial mink farming. Infections target a variety of tissues and cell types, resulting in a spectrum of acute and chronic clinical presentations including renal failure, vasculitis, neurologic disease, and/or a fatal wasting syndrome.[5,13,27] In mink kits, permissive infection of pneumocytes results in abundant virus production, cytolysis,

and fulminant, fatal interstitial pneumonia; however, adult mink pneumocytes restrict viral replication, and adults do not typically develop interstitial pneumonia.[4,22] Despite sensitive diagnostic tests and extensive research on AMDV, no effective prophylaxis is available, and mink farms continue to struggle with controlling infections.[23] AMDV was the only known APV for decades, but the genus has expanded dramatically in recent years. Novel APVs have been detected in foxes, skunks, raccoon dogs, and red pandas, but studies to date examine individual or small numbers of animals and the consequences of these infections are not well understood.[1,3,6,8,21,30]

There is urgency in identifying diseases that may be associated with the highly prevalent Red Panda Amdoparvovirus (RPAV) in zoo-housed red pandas. Estimates suggest that fewer than 10,000 red pandas (*Ailurus* spp.) remain in the wild, and ex situ conservation efforts, which include nearly 1,000 red pandas in zoos across the world, represent critical safeguards for the survival of the species.[15] The welfare and sustainability of these managed populations is paramount, and relies on understanding and mitigating disease threats. First described in 2018, RPAV shares up to 85% nucleotide identity with AMDV, and has similarities in biological behavior including high prevalence (≥50% for RPAV) and apparent long-term persistence in an individual host.[2,3] Virus can be detected in clinically normal animals, but based on viral load and co-distribution with lesions in individual cases, we postulate that RPAV is important in morbidity and mortality among zoo-housed pandas.

We previously demonstrated that several phylogenetic clades of RPAV form a single viral species that is apparently host-specific in red pandas. In this study, we evaluated the impact of RPAV infection in the zoo-housed red panda population using (1) a prospective evaluation of viral persistence (shedding in feces, collected over 6 years); (2) a retrospective assessment of

infection status in necropsied animals (43 animals, four cohorts, spanning 25 years); and (3) analysis of viral distribution in RPAV-positive animals (32/43). Drawing upon a recent comprehensive mortality review and observations of APV-associated disease in previously reported cases, we demonstrate viral association with histologic lesions known to be impactful in this population (myocardial lesions, nephritis, and interstitial pneumonia) as well as other possible manifestations of infection (multisystemic pyogranulomatous disease, mucosal inflammation, and dermatitis).[3,12]

Materials and methods:

Longitudinal study qPCR

Repeated fecal samples from two infected, un-related, co-housed red pandas[31] were collected over a six-year timespan. Samples that could confidently be attributed to individuals were collected opportunistically from enclosures by animal care staff and stored at -20C until use. Timepoints for collection each year are presented in Table S4.1. DNA extractions were performed on 1g of feces using a commercial kit (DNEasy Blood and Tissue Kit, Qiagen), with a final elution volume of 200μL. The qPCR assay was adapted from studies of related viruses to target the capsid-coding (VP) gene, using forward primer 5'-CTGTAACAGAAACCAACCAAGGTA-3' and reverse primer 5'-GGTTGGTTTGGTTGCTCTCCA-3'.[32] Samples were assayed on an ABI 7500-fast cycler (Applied Biosystems), and amplifications were performed using Maxima SYBR green with ROX as the reference dye (ThermoFisher Scientific). Each sample of extracted DNA was tested in triplicate, and the mean Ct for each sample was determined. A standard curve was generated from a segment of RPAV nucleic acid cloned into a pUC53 plasmid vector, with a lower limit

for detection of three genome copies per 5μL sample. Samples with mean copy numbers above this threshold were considered positive, and samples below this threshold were considered negative. At least six negative (no-template) control wells were placed randomly on each 96-well plate.

Case criteria for retrospective studies

Retrospective cases were identified from San Diego Zoo Wildlife Alliance (SDZWA, San Diego, CA, USA), the Sacramento Zoo (William R. Pritchard Veterinary Medical Teaching Hospital, UC Davis, Davis, CA, USA), Aalborg Zoo (Aalborg, Denmark), and Bronx Zoo (Wildlife Conservation Society, New York, NY, USA) (cohorts 1-4, respectively). All four collections had previous RPAV-positive cases detected in previous studies or in unpublished pilot studies.[2] Two additional cases from other collections were also included in order to specifically evaluate a potential association with myocarditis. Because splenic tissue has been determined to be a sensitive sample for systemic APV infection spleen was chosen to determine individual infection status.[33] Cases were excluded if fresh, frozen, or formalin-fixed, paraffin-embedded (FFPE) splenic tissue was not available.

Animal histories including birth date, death date, sex, and (sub)species were obtained from the Zoological Information Management System (ZIMS).[3] The manner of death (euthanasia or natural death) and cause of death were obtained from necropsy reports or review of histopathology.

PCR detection in retrospective cases

RPAV PCR on FFPE (n=42) or frozen (n=1) splenic tissue was performed as previously described, targeting a 187-nt segment of the viral nonstructural (NS) gene.[2,3] Cases were considered positive if a band of the correct size was obtained. PCR products were further confirmed to be RPAV by sequencing of 10 cases. Amplicons were purified with ExoSAP-IT (ThermoFisher) according to manufacturer instructions, then submitted for bidirectional Sanger sequencing at the UCDNA Sequencing Facility (UC Davis sequencing core facility).

For PCR, FFPE samples (25-μm-thick scrolls) were deparaffinized with a series of xylene and graded ethanol washes. DNA was extracted using a commercial kit (DNEasy Blood and Tissue Kit, Qiagen). PCR targeting a housekeeping gene (GAPDH) was performed on every sample to confirm DNA quality.

In situ hybridization

Colorimetric *in situ* hybridization (ISH) was performed in 29/34 PCR-positive cases. Five cases were excluded either due to autolysis, limited tissue for evaluation, or prolonged formalin fixation (>1 week). Of the 29 cases tested, select tissues were examined by ISH based on (1) lesions identified as important causes of death in zoo-housed red pandas and/or (2) lesions recognized as Amdoparvovirus-associated in other carnivores.[3,1,8]

One case of significant myocarditis was present in the collections evaluated. To evaluate a potential association of RPAV with myocarditis, we added two additional individual cases of myocarditis from other zoo collections.

To localize RPAV in tissues, we performed *in situ* hybridization using the RNAscope® 2.5 HD Reagent Kit—RED (Advanced Cell Diagnostics, Newark, CA, USA) and followed the

manufacturer's instructions to visualize the signal in FFPE tissues. A custom anti-sense probe was designed targeting the VP gene of RPAV obtained from RpAPV-CA1 (GenBank accession NC_031751).[3] To confirm adequate DNA/RNA integrity of the FFPE samples, a housekeeping gene (peptidylprolyl isomerase B) probe was applied to a subset of samples as a positive control. At least one slide with previously ISH-detected and PCR-confirmed viral nucleic acid was included in every run. Healthy red panda tissues and a probe targeting the dapB gene (Advanced Cell Diagnostics, Newark, CA, USA) were used as negative controls.

Results:

Individual red pandas can shed RPAV for >6 years

To understand patterns of RPAV shedding, we amplified RPAV DNA from feces of two live animals from one zoo collection (Collection #2) over a 6-year timespan. Viral DNA was present in 35/38 samples from case A and 37/37 samples from case B over the 6-year period (Table 4.1). Dates of collection and mean target copy numbers detected per sample are given in Supplementary Table S4.1.

Retrospective detection of RPAV in four zoo cohorts

All necropsied red pandas from cohorts 1 and 2 were evaluated (n=27). A subset of necropsied red pandas (based on available tissues) from cohorts 3 and 4 were evaluated (n=16). The entire tested population from these cohorts comprised 19 males and 24 females. Ages at death ranged from <1 day to 19 years (mean 6.5 years), and necropsies were performed between 1997-2022. A summary of cases is provided in Supplementary Table S4.2.

In total, PCR testing of splenic tissue demonstrated RPAV in 32/43 (74%) animals. This included 13/16 necropsied animals from SDZWA, 8/11 cases from Sacramento Zoo, 6/6 cases from Aalborg Zoo, and 5/10 cases from WCS. The positive cases included a wide age range from neonates to geriatric animals (mean 7.7 years) and included detection in some of the oldest necropsies available from these collections (1997). All sequenced amplicons (n=10) were phylogenetically closely related to previously identified RPAV sequences (85.8-100% identity) (Fig. 4.1).

RPAV association with diseases of red pandas

From PCR-positive cases, we evaluated viral distribution and the potential contribution of RPAV to morbidity/mortality by histopathology and ISH.

Myocarditis:

Sections of myocardium from ten cases were evaluated by ISH (Table 4.2). Five cases (cases 16, 19, 21, 26, and 35) were histologically normal. Two cases (cases 34 and 43) had endocardial and/or myocardial fibrosis with minimal inflammation. Three cases (cases 22, 44, and 45) had severe myocarditis.

All three myocarditis cases had multifocal patchy foci of inflammation with separation of cardiomyocytes by edema, plump, reactive pericytes, and infiltrating leukocytes. In affected areas, scattered cardiomyocytes were hypereosinophilic, fragmented, or replaced by eosinophilic acellular material and karyorrhectic debris. In case 22, which was previously reported, these foci were primarily centered around small-caliber blood vessels.[3] In the other two cases (cases 44 and 45), inflammation was regionally extensive and coalescing, involving large zones of the myocardium and up to ~75% of the thickness of the affected wall. There were minor differences

in the composition of the inflammatory infiltrate. In case 22, inflammation was primarily histiocytic and neutrophilic, while cases 44 and 45 were predominantly histiocytic, lymphocytic, and plasmacytic, with fewer neutrophils and eosinophils admixed.

Among the ten hearts analyzed, RPAV ISH probe hybridization was only detected in the three cases with myocarditis. The association between myocardial inflammation and RPAV detection in myocardium by ISH was statistically significant ($p=0.0083$). Signal co-localized to regions of inflammation and was not detected in the adjacent histologically normal myocardium (Fig. 4.2a-c). ISH signal was present within cells morphologically consistent with endothelial cells and macrophages (Fig. 4.2d-e).

Chronic kidney disease:

Although renal disease was not considered the primary cause of death in any case in this cohort, chronic interstitial nephritis was a common comorbidity, and kidney is a known target for APV infections in mink and skunks.[3] We tested sections of kidney from 20 cases representing a spectrum of disease. Findings grouped by histologic diagnoses are summarized in Table 4.3, and results for individual cases are presented in Supplemental Table S4.3.

Seven cases had no significant findings in the renal parenchyma. Nine cases were diagnosed with mild chronic interstitial nephritis, characterized by infiltrates of lymphocytes, plasma cells, and macrophages, with or without fibrosis, affecting <5% of the renal parenchyma in the evaluated sections. Two cases were diagnosed with moderate chronic interstitial nephritis, characterized by similar inflammatory infiltrates affecting 5-30% of the renal parenchyma. Glomeruli were normal in all but two cases – one that had mild membranoproliferative glomerulonephritis in addition to moderate chronic interstitial nephritis, and one with mild

membranoproliferative glomerulonephritis without interstitial inflammation. Arteritis was present in two cases – one with mild nephritis and one otherwise histologically normal. In these kidneys the renal or arcuate arteries were segmentally, transmurally disrupted by lymphocytes, accompanied by vacuolation and separation of smooth muscle cells and accumulation of brightly eosinophilic, acellular, fibrillar material (fibrin and/or fibrinoid necrosis). Affected arteries often had denser lymphocytic inflammation, sometimes circumferentially, at their periphery in. the region of the vasa vasorum.

In total, RPAV was detected by ISH in renal tissue in 14/20 cases tested. Among histologically normal kidneys, RPAV was detected in 2/7 cases. ISH signal in these cases was localized to the interstitium in rare, scattered individual cells which, based on morphology and location, were presumed to be endothelial cells and/or circulating leukocytes. RPAV was detected by ISH in 8/9 cases with mild chronic interstitial nephritis. In these cases, in addition to scattered individual cells throughout the interstitium, signal was present in cells within inflammatory cell aggregates (Fig. 4.2f). In two cases, signal was also detectable in tubular epithelial cells, typically adjacent to foci of interstitial inflammation. Where probe hybridization was detectable in tubular epithelium, cells exhibited features of tubular injury (karyorrhexis, necrosis, intraluminal cellular debris/casts) or epithelial attenuation. In many of these tubules ISH signal also observed in intraluminal cellular debris or casts (Fig. 4.2h-j). In both cases with moderate chronic interstitial nephritis, RPAV was similarly detected in inflammatory cell aggregates. Both cases diagnosed with membranoproliferative glomerulonephritis exhibited ISH signal in scattered cells in the interstitium, and one case additionally in the pelvic urothelium. In these two cases, probe hybridization was not detected in glomeruli.

Pneumonia:

We evaluated lung tissue by ISH from 13 red pandas: four neonates (<30d), two juveniles (30d-1yr), three adults (1-10yr), and four geriatric (>10yr) animals. No mortalities in this set were attributed to interstitial pneumonia, but pulmonary lesions were comorbidities in several cases. RPAV was detected by ISH in the lungs of 7/13 animals tested. Histologic findings and ISH results are summarized in Table 4.4.

Of the four neonates tested, one had histologically normal lungs, one had intra-alveolar hemorrhage and edema attributed to trauma, and two had regionally extensive to diffuse interstitial pneumonia. The latter was characterized by expansion of alveolar walls with edema and fibrin, intra-alveolar fibrin exudation, accumulations of intra-alveolar macrophages and cellular debris, and type 2 pneumocyte hyperplasia. RPAV was not detected in the lungs of any neonates by ISH.

Among juveniles and adults (n=5 total), three (1 juvenile, 2 adults) had histologically normal lungs, and two (1 juvenile, 1 adult) had interstitial pneumonia. RPAV was detected in the lungs by ISH in all five cases (Fig. 4.2k-n). In the normal lungs, signal was detected in rare, scattered individual cells in the alveolar walls. In both cases with interstitial pneumonia, signal was clearly localized to the sites of inflammation, and was present in type 2 pneumocytes and in intra-alveolar cells (alveolar macrophages vs. sloughed epithelial cells).

Lungs from four geriatric animals were tested. All four had pulmonary lesions, but the lesions were distinct in each case. The first (case 9) was essentially normal except for a mild, multifocal interstitial fibrosis with smooth muscle hyperplasia and mild alveolar histiocytosis. The second (case 20) had a mild suppurative bronchiolitis and mild interstitial fibrosis. The third

(case 23) had multifocal granulomatous to pyogranulomatous foci randomly distributed throughout the lungs. The fourth (case 24) had a moderate alveolar histiocytosis and prominent (subjectively increased or hyperplastic) bronchus-associated lymphoid tissue (BALT). ISH was negative in the first two geriatric cases. In the case with granulomatous/pyogranulomatous pneumonia, ISH signal was consistently detected within macrophages in granulomas. In the case with BALT hyperplasia, signal was detected in most BALT aggregates as well as segmentally in histologically normal bronchiolar epithelial cells.

Other diseases:

We previously reported a possible role of RPAV in inducing several additional lesions, including fulminant multisystemic pyogranulomatous inflammation and oral mucosal inflammation.[14] In addition, epidermis has been demonstrated as a site of APV tropism,[15] and pilot studies on red panda tissue identified dermatitis as potentially RPAV-associated. Therefore, although these are not recognized as common causes of mortality in captive red pandas, these lesions were evaluated by ISH.

Three red pandas in this study died with severe, pyogranulomatous inflammation affecting multiple organ systems. In one case (case 16), these lesions were limited to liver and spleen. In the second (case 20), pyogranulomatous lesions were present in liver, spleen, lymph nodes, lung, and bone marrow. In the third (case 22), pyogranulomatous lesions were present in liver, pancreas, intestine, urinary bladder, and epicardium/myocardium. RPAV was detected in all three cases. At least two tissues with representative lesions from each case were tested by ISH, and RPAV was consistently localized to macrophages in foci of granulomatous or pyogranulomatous inflammation (Fig. 4.3a-b).

We tested oral/pharyngeal and/or esophageal mucosal tissue from 11 cases. Five cases had evidence of RPAV in the mucosal epithelium, in a distribution similar to that which was previously reported.[7,24,25] Virus was often detectable in the basal layers of the lingual and/or oropharyngeal epithelium, with individual cells in the stratum basale and stratum spinosum exhibiting hypereosinophilia and nuclear pyknosis (presumed apoptosis), and a minimal subepithelial inflammatory infiltrate. Histologically, these sites of infection varied from essentially normal (most cases) to markedly disrupted (rare). In the most severe cases, virus was abundant throughout the oral and pharyngeal mucosa, which was multifocally ulcerated and subtended by a prominent mononuclear inflammatory infiltrate (Fig. 4.3c-f).

We tested skin tissue from eight red pandas for evidence of RPAV tropism to this tissue. These ranged from histologically unremarkable to moderately inflamed. Inflammation, where present, was characterized by scant to moderate subepithelial infiltrates of lymphocytes and plasma cells. In more heavily infiltrated sections, inflammatory cells occasionally extended into the overlying epidermis and scattered individual epithelial cells were swollen and hypereosinophilic with pyknotic nuclear material (presumed apoptosis). Four of the eight cases had detectable virus in the skin, ranging from scattered, individual epidermal cells to widespread dispersion throughout the basal epidermis, follicular epithelium, subepithelial inflammatory cells, and basal cells of sebaceous glands (Fig. 4.3g-j).

Discussion:

Healthy, sustainable zoo populations represent a critical safeguard for the survival of endangered species. Threatened by habitat loss, increasing domestic animal populations (and their communicable pathogens), and illegal trade, red pandas in the wild now number

<10,000.[8,27,28] The roughly 1000 red pandas in zoos worldwide represent approximately 10% of the overall population. Characterizing disease threats to the zoo population is imperative for the welfare and sustainability of the species. Drawing on our understanding of AMDV and the results of a recent, comprehensive red panda mortality study, this study provides information about the potential impact of RPAV infection, and characterizes widespread viral distribution, and apparent association with important inflammatory diseases of zoo-housed red pandas.[12]

A high prevalence of infection (~ 50%) based on conventional PCR and a one-time fecal sampling of the US zoo population suggests that the pathogenesis of RPAV, like AMDV includes persistent infection. This study also supports long term viral persistence with a longitudinal qPCR screening of two animals spanning over 6 years. Despite irregular (opportunistic) timespans between collections, nearly all samples (x/y) from these animals were positive, and the study was designed to cover 1/3-1/2 the lifespan of a zoo panda. We propose that, like AMDV, RPAV can be persistent and lifelong after infection. We cannot exclude the possibility that the high frequency of detection in longitudinal sampling could be sequelae to repetitive re-infection, or by environmental contamination of fecal samples, given the remarkable environmental stability of parvoviruses. Red pandas are frequently transferred between zoos for breeding or management purposes. These transfers are an essential component of a carefully managed species survival plan, but also provide opportunities for viral transmission between institutions. RPAV has been circulating among zoo-housed red pandas for decades, but we do not know whether the infection exists in the wild population.

AMDV associated diseases and tissue targets can be variable, but we have recognized for decades that mortality from plasmacytic nephritis and membranous glomerulopathy comprises the majority of the cases. This is not the case for RPAV.

Renal disease in infected red pandas was seldom a primary cause of death, although it was the single most common comorbidity in necropsied red pandas[12] and RPAV was consistently associated with interstitial inflammation and tubular necrosis. Glomerulonephropathy– characteristic of AMDV infections in mink – was rare in this study.[27] RPAV in histologically normal kidneys was detectable, albeit in scattered rare tubular epithelial cells, but was both more abundant and clearly distributed with interstitial inflammation and active tubular necrosis. Given the polyphasic nature of the renal damage in this cohort, tubular injury and parenchymal loss could accumulate piecemeal over the lifetime of the animal. For the purpose of diagnosis, this is an important difference in pathogenesis among carnivores: membranoproliferative glomerulonephritis in AMDV is attributed to an exuberant, non-neutralizing humoral immune response with antigen-antibody complex deposition, which does not play a significant role in RPAV-associated renal disease.[13]

The spectrum of lesions analyzed in this study, in addition to considering known APV related disease, relied on known causes of morbidity and mortality among zoo housed pred pandas. While active myocarditis is an uncommon diagnosis in necropsied red pandas, cardiomyopathies – and especially myocardial fibrosis – are frequent contributors to mortality in adult and geriatric animals. We found three cases with severe myocarditis, and in all three we demonstrated an abundance of RPAV nucleic acid in close association with inflammatory lesions. Myocardial fibrosis is a leading cause of morbidity/mortality in adult and geriatric red pandas, but as an end-stage lesion, the cause or causes are typically unknown. Given that RPAV is associated with myocardial inflammation, at least in these snapshots of time in individual animals, it is possible that a subset of myocardial fibrosis cases result from non-fatal episodes of RPAV associated damage.[12]

We were especially interested in the high rate of neonatal/juvenile mortalities in zoo-housed red pandas, with only ~45% of zoo housed red pandas living beyond their first year.[12] Pneumonias is the most common cause of red panda infant mortality, and these cases were additionally of interest given that AMDV is a well-recognized cause of interstitial pneumonia in mink kits.[4,12] We found no strong evidence to suggest that RPAV associated pneumonia was important in young red pandas. RPAV was present in one case of interstitial pneumonia in a juvenile. In other young pandas, RPAV was detected by ISH in scattered individual cells in the interstitium or within alveoli, in regions with no apparent damage, and although the cell target was not definitively determined, the morphology and distribution was consistent with alveolar or circulating macrophages.

We also recognized sporadic lesions in other tissues that were clearly associated with RPAV. Three animals died with severe, multisystemic pyogranulomatous disease affecting the liver, spleen, pancreas, intestinal tract, heart, and urinary bladder.[19,20,31] Virus distribution was central to inflammatory lesions by ISH, suggesting that this is a distinct presentation of RPAV-associated disease. Other tissue targets included oral mucosal epithelium, which was originally reported in the index case and in this study was detected in numerous additional cases. Viral infection of epithelium ranged from segmental, histologically subtle, to vast tracts of infection with cell degeneration/apoptosis and attendant subepithelial inflammation. In concert with evidence of intestinal infection and demonstration of virions in lingual epithelium and feces by electron microscopy, we suggest that the gastrointestinal system is a site of viral persistence and shedding.[3] Intestinal disease was not seen in this cohort, but oral ulceration was present in a few (two cases) animals. Lastly, RPAV was present within the arterial wall and surrounding affected vessels in cases of arteritis. This lesion has been reported for AMDV infected mink where, like

the kidney lesions, it is considered to be from immune complex deposition. Among affected red pandas, we demonstrate the presence of virus in cells within the inflamed arterial wall or region of the vasa vasorum.[27]

Establishing a causal relationship of RPAV infection with disease is a significant challenge due to the high prevalence of infection, clinically silent infections, and low overall case numbers. We recognize limitations of this study, including a small sample size and the largely descriptive nature of lesion association by ISH. Statistical significance in the association of RPAV detection was not reached for either nephritis or interstitial pneumonia, but the demonstrable presence of virus in a subset of these lesions suggests that, as a cause of infection, a subset of these cases could be attributed to RPAV associated damage. We recognize that the confounding nature of a retrospective study on natural disease in an endangered population further complicates interpretation, and recognize that potential factors, such as host immunity, viral genetics, or co-infections can influence distribution and effects of any pathogen.

Amdoparvoviruses have remarkable genetic diversity, and strains of RPAV among red pandas can vary by up to ~15% (nucleotide identity) across their 5kb genomes.[9] We have reported a 12% divergence even among animals in a single enclosure.[3] We used techniques (PCR, ISH) that depend on sequence stability, so it is plausible that divergent sequences were missed. Additionally, these tissues are archived, and fixation times were variable among institutions, possibly affecting the sensitivity of our molecular techniques.

Where it is associated with tissue damage and inflammation, RPAV is implicated in significant diseases in red pandas. Recognizing the wide tissue distribution and the spectrum of associated lesions is critical for diagnosis of RPAV-associated disease.

Acknowledgements:

We thank the keepers and veterinary staff from Sacramento Zoo for assistance with fecal sampling. We acknowledge the pathology and histopathology technical staff from UC Davis VMTH, SDZWA, Bronx Zoo/WCS, and Aalborg Zoo, and Vet Med Labor/ Div. of IDEXX for assistance with tissue samples and sectioning.

Declaration of conflicting Interests:

The authors report no conflicts of interests.

Funding:

This work was supported in part by a philanthropic grant from the McBeth Foundation via San Diego Zoo Wildlife Alliance. CEA is supported in part by NIH T32 training grant 1T32CA251007.

Tables and figures:

Table S4.1. Detection of RPAV in fecal samples by qPCR. Samples were assayed in triplicate, and mean target copy number per sample (5 μL extracted DNA) is shown. Mean values below the lower limit of detection are considered negative.

Year	Date	Case 1	Case 2
2016	21-Jan-16	185	638
	27-Jan-16	63	28829
	3-Feb-16	26	28829
	12-Feb-16	65	36995
	18-Feb-16	76	2830
	25-Feb-16	92	6425
2017	27-Oct-17	7	51
	31-Oct-17	nt	1410
	1-Nov-17	3	nt
	4-Nov-17	4	124
	8-Nov-17	3	nt
	9-Nov-17	nt	27
	12-Nov-17	neg	25
	15-Nov-17	7	1201
	19-Nov-17	neg	3674
2018	3-Oct-18	229	88
	17-Oct-18	7	511
	31-Oct-18	183	1432
	14-Nov-18	43	1319
	28-Nov-18	556	830
	12-Dec-18	1109	335
	26-Dec-18	71	386

2019	10-Jan-19	neg	nt
	23-Jan-19	4	214
	6-Feb-19	3	168
	20-Feb-19	203	84
	5-Mar-19	13	178
	20-Mar-19	25	351
	3-Apr-19	52	402
	16-Apr-19	12	76
	1-May-19	7	13
	14-May-19	14	33
	30-May-19	nt	432
	31-May-19	15	nt
2020	27-Jun-20	89	242
	13-Jul-20	395	25
2021	3-Jul-21	356	802
	4-Jul-21	nt	385
	5-Jul-21	674	nt
	6-Jul-21	487	3166
	8-Jul-21	4945	5881
	9-Jul-21	2279	3453

nt=not tested

Table S4.2. Summary of necropsy cases from four zoological collections evaluated for RPAV by PCR and ISH.

Cohort	Case#	Sex	Species	Age (days)	Age (yrs)	Date of death	RPAV PCR	Euthanized?	Cause of death or euthanasia
1	1	M	Western	0	0.0	Jun-97	Positive	no	Neonatal death; possible sepsis
	2	F	Western	1839	5.0	Jun-98	Positive	no	Poor body condition, ulcerative esophagitis
	3	M	Western	2509	6.9	May-01	Positive	no	Hyperthermia, meningoencephalitis
	4	F	Western	0	0.0	Jun-02	Positive	no	Stillbirth/perinatal death
	5	F	Western	2	0.0	Jun-03	Positive	no	Neonatal death; undetermined
	6	M	Western	2	0.0	Jun-03	Negative	no	Neonatal death; undetermined
	7	M	Western	26	0.1	Jul-03	Positive	no	Neonatal death; trauma
	8	M	Western	3	0.0	Jul-04	Positive	no	Neonatal death; pneumonia
	9	F	Western	3851	10.5	Dec-07	Positive	no	Pneumothorax; possible anaphylaxis (vaccine)
	10	F	Western	5275	14.4	Dec-08	Positive	no	Enteritis (E coli)
	11	M	Western	6240	17.1	Jul-10	Positive	yes	Esophagitis

	12	M	Western	4469	12.2	Sep-10	Positive	yes	Multifactorial (heart disease, pancreatitis, liver disease)
	13	F	Western	4888	13.4	Nov-11	Negative	yes	Multifactorial (fungal rhinitis, hippocampal necrosis)
	14	F	Western	1474	4.0	Jun-15	Negative	no	Undetermined; esophagitis, glossitis
	15	M	Western	2040	5.6	Jan-16	Positive	no	Undetermined
	16	F	Chinese	5775	15.8	Apr-19	Positive	yes	Systemic granulomatous disease
	17	F	Western	24	0.1	Jul-01	Negative	no	Neonatal death; aspiration pneumonia
	18	F	Western	2718	7.4	Dec-03	Positive	no	Enterocolitis
	19	M	Western	3	0.0	Jun-04	Positive	no	Neonatal death; omphaloarteritis, sepsis
2	20	M	Western	6200	17.0	Jun-07	Positive	no	Multisystemic pyogranulomatous disease
	21	F	Western	2	0.0	Jun-14	Positive	no	Neonatal death: drowned
	22	M	Western	7242	19.8	May-15	Positive	no	Systemic pyogranulomatous disease

	23	F	Western	6190	16.9	May-16	Positive	no	Neoplasia (cholangiocarcinoma, jejunal carcinoma)
	24	F	Western	7016	19.2	Aug-16	Positive	no	Undetermined
	25	F	Western	3	0.0	Jun-18	Negative	no	Neonatal death; undetermined
	26	F	Western	21	0.1	Jul-18	Positive	no	Neonatal death; maternal trauma
	27	M	Western	0	0.0	Jun-20	Negative	no	Neonatal death; maternal trauma
	28	M	Western	212	0.6	Jan-21	Positive	yes	Dermatitis
	29	F	Western	220	0.6	Feb-21	Positive	yes	Nephritis, dermatitis
	30	F	Western	1722	4.7	Mar-21	NT*	yes	Enteritis, pharyngitis
3	31	F	Western	252	0.7	Mar-21	NT*	yes	Onychitis, nephritis
	32	F	Western	559	1.5	Mar-20	Positive**	yes	Dermatitis, suspected genetic disease
	33	M	Western	2819	7.7	Jan-22	NT*	yes	Suspected genetic disease - mandibular brachygnathism
	34	F	Western	6725	18.4	Dec-03	Positive	yes	Dermatitis (foot)
4	35	F	Western	5128	14.0	Jul-04	Positive	yes	Dermatitis, cellulitis

	36	F	Western	1303	3.6	Jan-05	Positive	no	Undetermined
	37	F	Western	844	2.3	Nov-06	Negative	no	Bronchopneumonia
	38	M	Western	6066	16.6	Feb-10	Positive	yes	Intestinal perforation, septic peritonitis
	39	M	Western	2569	7.0	Jul-13	Negative	no	Dermatitis/eschar (dorsum)
	40	M	Western	2	0.0	Jul-15	Negative	no	Neonatal death; undetermined
	41	F	Western	508	1.4	Nov-17	Negative	no	Myocardial degeneration and necrosis
	42	M	Western	716	2.0	Jun-18	Negative	no	Adrenal disease
	43	M	Chinese	5046	13.8	Apr-19	Positive	no	Post-anesthetic death; cardiomyopathy, adrenal disease
External	44	F	Western	2696	7.4	Nov-18	Positive**	no	Myocarditis; interstitial pneumonia
External	45	F	Western	2587	7.1	Jul-20	NT*	no	Myocarditis

*Not tested by PCR. RPAV infection confirmed by ISH in each of these cases.
**PCR test used fresh tissue, not FFPE.

Table S4.3. Detection of RPAV by ISH in kidneys.

Case #	Significant histologic diagnoses	ISH result	ISH distribution
2	No significant findings	Positive	Scattered, individual cells of the interstitium (presumed endothelium, circulating leukocytes, and/or individual infiltrating inflammatory cells)
9	No significant findings	Positive	Interstitial cells; tubular epithelium
21	No significant findings	Negative	n/a
23	No significant findings	Negative	n/a
34	Mild interstitial fibrosis	Negative	n/a
35	No significant findings	Negative	n/a
43	No significant findings	Negative	n/a
3	Mild chronic interstitial nephritis	Positive	Scattered interstitial cells and interstitial inflammatory aggregates
10	Minimal chronic interstitial nephritis with fibrosis	Positive	Interstitial inflammatory cells
11	Mild chronic interstitial nephritis with fibrosis, rare glomerulosclerosis	Positive	Scattered interstitial cells and interstitial inflammatory aggregates
22	Mild chronic interstitial nephritis with fibrosis	Positive	Interstitial inflammatory cells; tubular epithelium
24	Mild chronic interstitial nephritis	Negative	n/a
28	Mild chronic interstitial nephritis, mild lymphocytic periartieral/arterial inflammation	Positive	Interstitial inflammatory cells; periarterial/arterial leukocytes
29	Mild chronic interstitial nephritis	Positive	Interstitial inflammatory cells; tubular epithelium
32	Mild chronic interstitial nephritis with fibrosis	Positive	Interstitial cells; tubular epithelium
33	Mild chronic interstitial nephritis with fibrosis	Positive	Interstitial cells
20	Moderate chronic interstitial nephritis with severe fibrosis and tubular degeneration	Positive	Interstitial inflammatory cells

38	Moderate chronic interstitial nephritis with fibrosis; mild membranoproliferative glomerulonephritis	Positive	Scattered interstitial cells and interstitial inflammatory aggregates
18	Lymphocytic arterial/periarterial inflammation	Positive	Interstitial cells; periarterial/arterial leukocytes
30	Mild membranoproliferative glomerulonephritis	Positive	Interstitial cells; pelvic urothelium

Table 4.1. Frequent detection of RPAV in fecal samples from two apparently persistently infected red pandas.

In opportunistically obtained samples spanning a six-year period, RPAV was detected by qPCR in 35/38 and 37/37 fecal samples from two unrelated, co-housed red pandas.

	Case A		Case B	
Year	**Tested**	**Positive**	**Tested**	**Positive**
2016	6	6	6	6
2017	7	5	7	7
2018	7	7	7	7
2019	11	10	10	10
2020	2	2	2	2
2021	5	5	5	5
Total	38	35	37	37

Table 4.2. Detection of RPAV by ISH in cases of myocarditis.

Case #	Significant histologic diagnosis	Fibrosis	ISH result
16	No significant findings	No	Negative
19	No significant findings	No	Negative
21	No significant findings	No	Negative
26	No significant findings	No	Negative
35	No significant findings	No	Negative
34	Fibrosis, mild to moderate, endocardial	Yes	Negative
43	Multifocal cardiomyocyte degeneration, moderate multifocal myocardial fibrosis, minimal lymphoplasmacytic myocarditis	Yes	Negative
22	Myocarditis, pyogranulomatous and lymphoplasmacytic, perivascular to regionally extensive	Yes	Positive
44	Myocarditis, histiocytic and lymphoplasmacytic, regionally extensive	No	Positive
45	Myocarditis, pyogranulomatous and eosinophilic, regionally extensive	Yes	Positive

Table 4.3. Detection of RPAV by ISH in chronic interstitial nephritis.

Histologic diagnosis	Total tested	Total positive
No interstitial inflammation	10	5
Mild chronic interstitial nephritis	8	7
Moderate chronic interstitial nephritis	2	2
Total	20	14

Table 4.4. Detection of RPAV by ISH in lungs.

Case #	Age group	Significant histologic diagnosis	ISH result	ISH distribution
8	Neonate	Interstitial pneumonia	Negative	n/a
21	Neonate	Intra-alveolar hemorrhage and pulmonary edema	Negative	n/a
19	Neonate	No significant findings	Negative	n/a
26	Neonate	Interstitial pneumonia	Negative	n/a
28	Juvenile	No significant findings	Positive	Alveolar wall - presumed endothelium or circulating leukocytes
29	Juvenile	Focally extensive interstitial pneumonia	Positive	Type 2 pneumocytes in region of interstitial pneumonia; intra-alveolar cells (presumed macrophages and sloughed epithelium);
30	Adult	No significant findings	Positive	Alveolar wall - presumed endothelium or circulating leukocytes
32	Adult	No significant findings	Positive	Alveolar wall - presumed endothelium or circulating leukocytes
44	Adult	Interstitial pneumonia	Positive	Intra-alveolar cells (presumed macrophages and sloughed epithelium); infiltrating inflammatory cells (presumed macrophages)
9	Geriatric	Mild interstitial fibrosis, smooth muscle hyperplasia, and alveolar histiocytosis	Negative	n/a
20	Geriatric	Multifocal granulomatous/pyogranulomatous pneumonia	Positive	Granulomatous/pyogranulomatous foci - presumed macrophages
23	Geriatric	Alveolar histiocytosis, peribronchiolar lymphocytic aggregates	Positive	Bronchiolar epithelium, peribronchiolar lymphocytic aggregates
24	Geriatric	Bronchiolitis and atelectasis with fibrosis	Negative	n/a

Figure 4.1. Specific detection of RPAV in cases from multiple zoo collections.

Maximum likelihood phylogeny of amplicons from each of four included cohorts belong to a single viral species within genus Amdoparvovirus. In this short (113nt) segment of the nonstructural gene, sequences from disparate cohorts are sometimes more closely related than sequences within cohorts. The resulting 113-nt-long sequences were aligned using the MUSCLE[14] algorithm in Geneious[18]. The optimal substitution model was determined using a model test in MEGA-X[20] prior to generating a phylogenetic tree. The tree was generated using a Kimura 2-parameter model with discrete gamma distribution.[19,20,32] Reference sequences obtained from GenBank for this analysis are: for AMDV, JN040434 and KU856562; and for SKAV, KX981924 and OL889869.1.

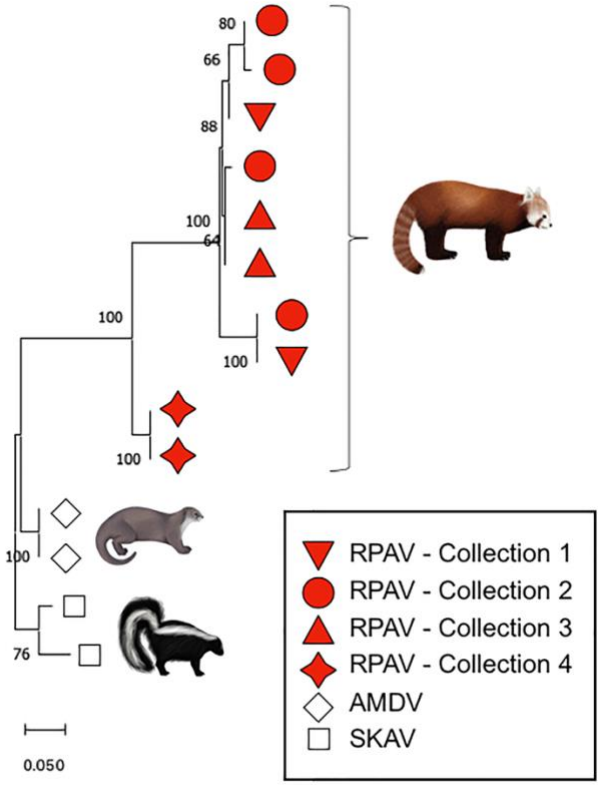

Figure 4.2. RPAV is associated with major causes of red panda mortality. ISH demonstrates viral co-localization with inflammation in cases of myocarditis, chronic interstitial nephritis, and pneumonia. **(a-e)** Myocarditis, 6-year-old red panda. **(a)** H&E, heart (interventricular septum). Dense infiltrates of mixed inflammatory cells multifocally disrupt or replace regions of the myocardium. **(b)** No ISH signal detected with negative control (DapB) probes. **(c)** RPAV ISH demonstrates abundant signal co-localizing to areas of inflammation and necrosis. **(d)** H&E, higher magnification. The inflammatory infiltrate consists primarily of histiocytes, plasma cells, and lymphocytes. **(e)** RPAV ISH, higher magnification. Stippled or punctate ISH signal is present throughout inflammatory infiltrates, and is especially abundant in larger, polygonal cells (presumed macrophages). **(f-j)** Chronic tubulointerstitial nephritis and pyelitis, 6-year-old red panda. **(f)** H&E, kidney. Multifocal infiltrates of lymphocytes and plasma cells in the renal cortex are associated with foci of tubular ectasia and epithelial degeneration, attenuation, or regeneration. Virus is detected in tubular epithelium and intratubular protein casts **(g, h)** and frequently in interstitial inflammatory infiltrates **(I, j)**. **(k-n)** Interstitial pneumonia, 7-year-old red panda. **(k)** H&E, lung. Regionally, alveolar septa are thickened by edema, inflammatory cells, and multifocal type 2 pneumocyte hyperplasia. Alveolar lumina contain an admixture of sloughed epithelial cells, fibrin, and mixed inflammatory cells. **(l)** RPAV ISH demonstrates virus in a segment of the affected tissue. **(m, n)** Higher magnification of k, l. ISH signal is detected in polygonal and spindloid cells in the expanded interstitium.

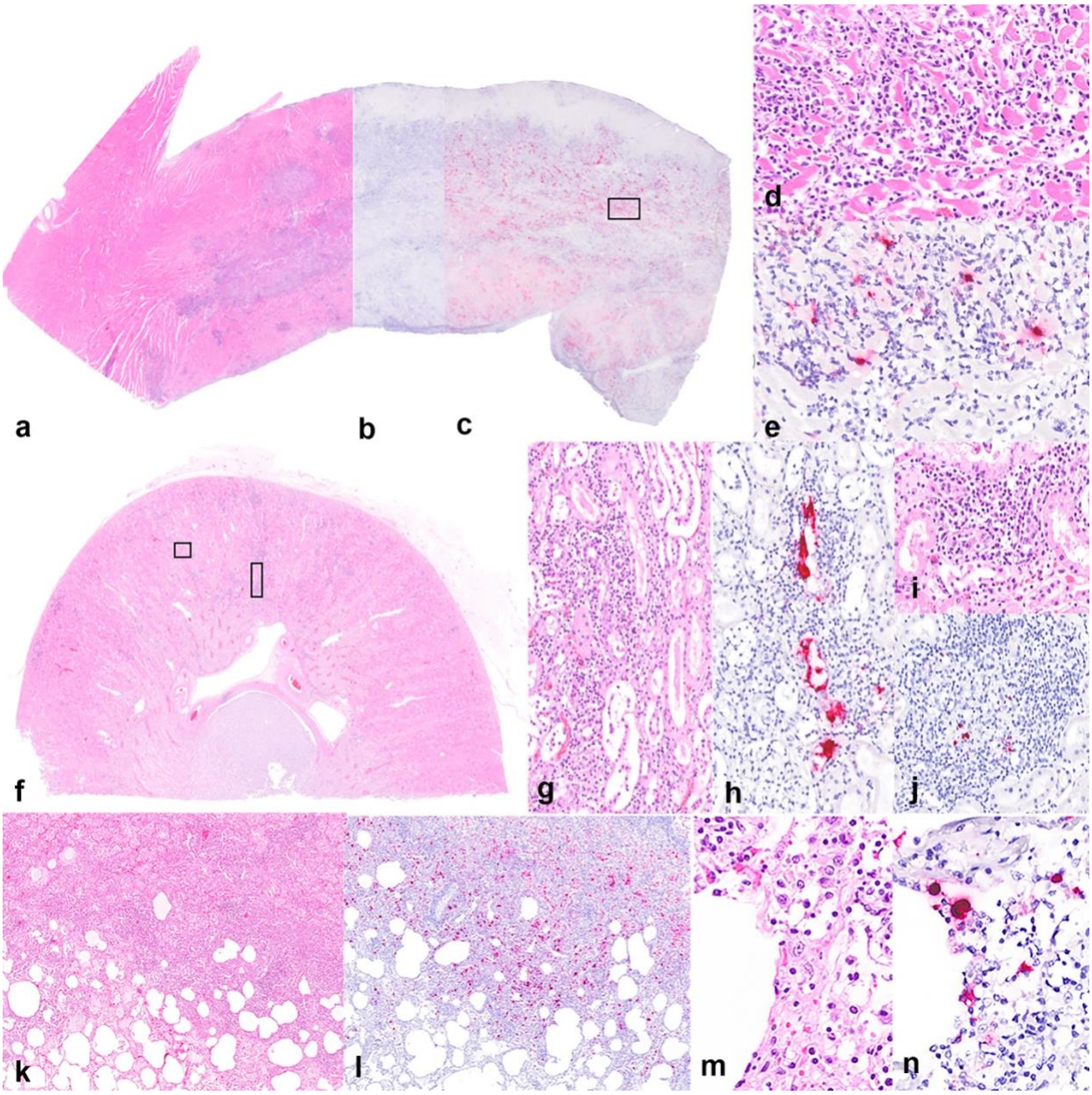
a
b
c
d
e
f
g
h
i
j
k
l
m
n

Figure 4.3. Novel manifestations of Amdoparvovirus disease. RPAV is associated with multisystemic pyogranulomatous lesions and oropharyngeal mucosal inflammation. **(a-b)** Multifocal, random, pyogranulomatous hepatitis with necrosis, 17-year-old male red panda. **(a)** H&E. **(b)** RPAV ISH. Probe hybridization demonstrates viral nucleic acid in infiltrating inflammatory cells. **(c-f).** Oropharyngeal infection, 6-month-old red panda. **(c)** H&E, laryngopharynx. **(d)** RPAV ISH. Intense probe hybridization throughout the epithelial lining. **(e)** H&E, tongue. Mild submucosal inflammation is present, and scattered individual epithelial cells are swollen and pale. **(f)** RPAV ISH demonstrates virus primarily in the basal (replicating) epithelium, with scattered signal present at higher levels. **(g-j)** RPAV infection in the skin. **(g)** Histologically unremarkable skin from a 1-year-old female red panda; H&E. **(h)** RPAV ISH demonstrates individual infected cells in the basal epidermis, basal sebocytes, and a follicular epithelial cell. **(i)** Skin (foot) from a 6-month-old male red panda. Individualized, pale eosinophilic or pyknotic (apoptotic) cells are present. Pigment-laden macrophages are scattered in the superficial stroma, admixed with lymphocytes and plasma cells. H&E. **(j)** RPAV ISH. Abundant signal is detected diffusely in the basal epithelium and in individual cells throughout the upper layers of the epidermis, as well as in infiltrating subepithelial inflammatory cells.

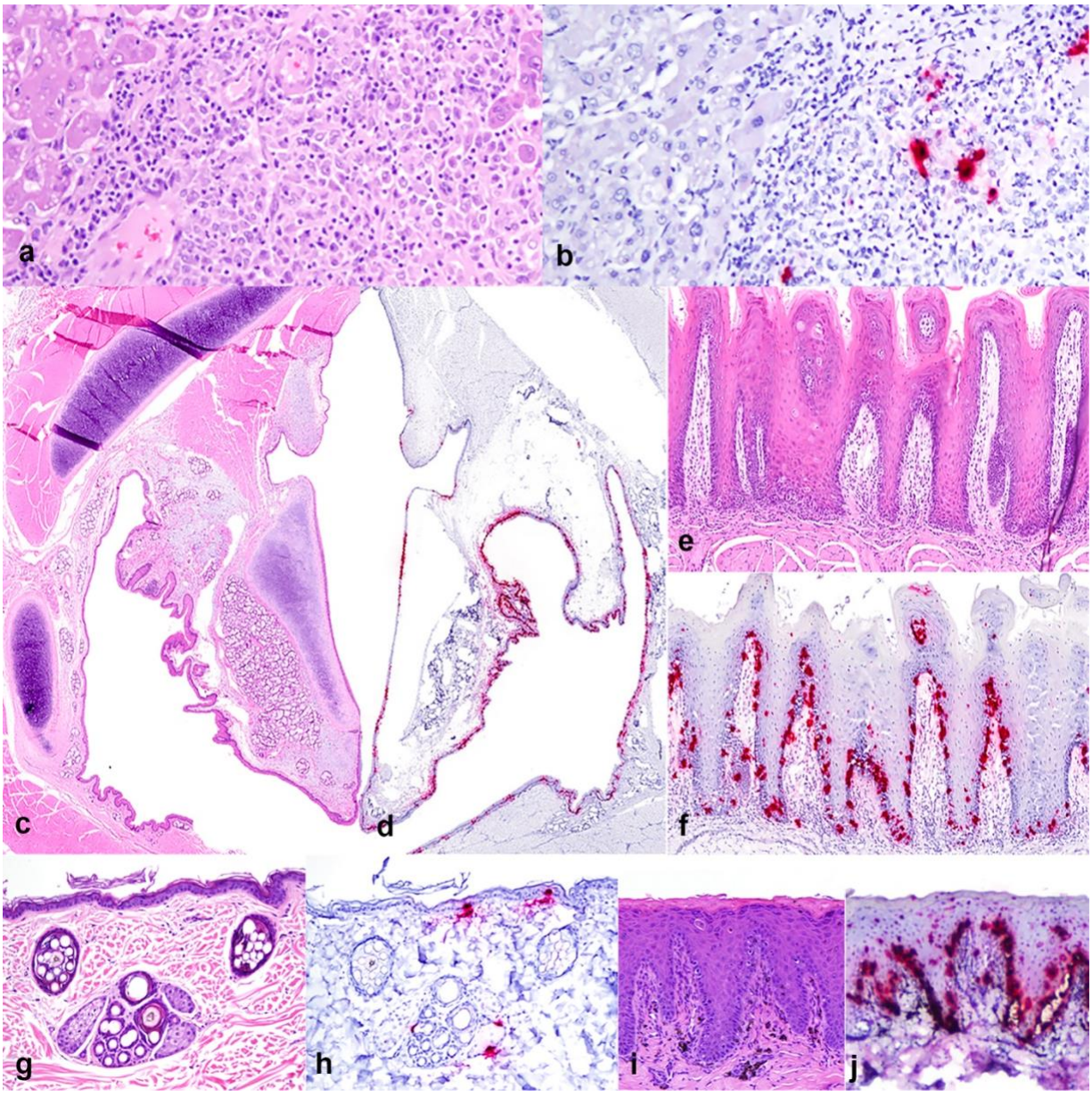
a
b
c
d
e
f
g
h
i
j

References:

1. Alex CE, Canuti M, Schlesinger MS, et al. Natural disease and evolution of an Amdoparvovirus endemic in striped skunks (Mephitis mephitis). *Transbound Emerg Dis*. 2022.

2. Alex CE, Kubiski SV, Jackson KA, Wack RF, Pesavento PA. Amdoparvovirus infections are prevalent, persistent, and genetically diverse in zoo-housed red pandas (Ailurus fulgens). *J Zoo Wildl Med*. 2022;**53**(1):83–91.

3. Alex CE, Kubiski SV, Li L, et al. Amdoparvovirus Infection in Red Pandas (Ailurus fulgens). *Vet Pathol*. 2018;**55**(4):552–561.

4. Alexandersen S, Bloom ME. Studies on the sequential development of acute interstitial pneumonia caused by Aleutian disease virus in mink kits. *J Virol*. 1987;**61**(1):81–86.

5. Alexandersen S, Bloom ME, Wolfinbarger J. Evidence of restricted viral replication in adult mink infected with Aleutian disease of mink parvovirus. *J Virol*. 1988;**62**(5):1495–1507.

6. Canuti M, Doyle HE, P Britton A, Lang AS. Full genetic characterization and epidemiology of a novel amdoparvovirus in striped skunk (Mephitis mephitis). *Emerg Microbes Infect*. 2017;**6**(5):e30.

7. Canuti M, O'Leary KE, Hunter BD, et al. Driving forces behind the evolution of the Aleutian mink disease parvovirus in the context of intensive farming. *Virus Evol*. 2016;**2**(1):vew004.

8. Canuti M, Whitney HG, Lang AS. Amdoparvoviruses in small mammals: expanding our understanding of parvovirus diversity, distribution, and pathology. *Front Microbiol*. 2015;**6**:1119.

9. Cotmore SF, Agbandje-McKenna M, Canuti M, et al. ICTV Virus Taxonomy Profile: Parvoviridae. *J Gen Virol*. 2019;**100**(3):367–368.

10. Cotmore SF, Agbandje-McKenna M, Chiorini JA, et al. The family Parvoviridae. *Arch Virol*. 2014;**159**(5):1239–1247.

11. Cotmore SF, Tattersall P. Parvoviruses: Small Does Not Mean Simple. *Annu Rev Virol*. 2014;**1**(1):517–537.

12. Delaski KM, Ramsay E, Gamble KC. Retrospective analysis of mortality in the North American captive red panda (Ailurus fulgens) population, 1992-2012. *J Zoo Wildl Med*. 2015;**46**(4):779–788.

13. Dyer NW, Ching B, Bloom ME. Nonsuppurative meningoencephalitis associated with Aleutian mink disease parvovirus infection in ranch mink. *J Vet Diagn Invest*. 2000;**12**(2):159–162.

14. Edgar RC. MUSCLE: a multiple sequence alignment method with reduced time and space complexity. *BMC Bioinformatics*. 2004;**5**:113.

15. Glatston A, Wei F, Than Zaw (IUCN SSC Cat SG / Wildlife Conservation Society (WCS), Myanmar Program, Yangon, Myanmar), Sherpa AP. IUCN Red List of Threatened Species: Ailurus fulgens. *IUCN Red List of Threatened Species*. 2015.

16. Heegaard ED, Brown KE. Human parvovirus B19. *Clin Microbiol Rev*. 2002;**15**(3):485–505.

17. Jager MC, Tomlinson JE, Lopez-Astacio RA, Parrish CR, Van de Walle GR. Small but mighty: old and new parvoviruses of veterinary significance. *Virol J*. 2021;**18**(1):210.

18. Kearse M, Moir R, Wilson A, et al. Geneious Basic: an integrated and extendable desktop software platform for the organization and analysis of sequence data. *Bioinformatics*. 2012;**28**(12):1647–1649.

19. Kimura M. A simple method for estimating evolutionary rates of base substitutions through comparative studies of nucleotide sequences. *J Mol Evol*. 1980;**16**(2):111–120.

20. Kumar S, Stecher G, Li M, Knyaz C, Tamura K. MEGA X: Molecular Evolutionary Genetics Analysis across Computing Platforms. *Mol Biol Evol*. 2018;**35**(6):1547–1549.

21. LaDouceur EEB, Anderson M, Ritchie BW, et al. Aleutian Disease: An Emerging Disease in Free-Ranging Striped Skunks (Mephitis mephitis) From California. *Vet Pathol*. 2015;**52**(6):1250–1253.

22. Larsen S, Alexandersen S, Lund E, Have P, Hansen M. Acute interstitial pneumonitis caused by Aleutian disease virus in mink kits. *Acta Pathol Microbiol Immunol Scand A*. 2009;**92A**(1–6):391–393.

23. Markarian NM, Abrahamyan L. AMDV Vaccine: Challenges and Perspectives. *Viruses*. 2021;**13**(9).

24. Pan IC, Tsai KS, Grinyer I, Karstad L. Glomerulonephritis in Aleutian disease of mink: ultrastructural studies. *J Pathol*. 1970;**102**(1):33–40.

25. Pan IC, Tsai KS, Karstad L. Glomerulonephritis in Aleutian disease of mink: histological and immunofluorescence studies. *J Pathol*. 1970;**101**(2):119–127.

26. Pénzes JJ, Söderlund-Venermo M, Canuti M, et al. Reorganizing the family Parvoviridae: a revised taxonomy independent of the canonical approach based on host association. *Arch Virol*. 2020;**165**(9):2133–2146.

27. Porter DD, Larsen AE, Porter HG. The pathogenesis of Aleutian disease of mink. 3. Immune complex arteritis. *Am J Pathol*. 1973;**71**(2):331–344.

28. Porter DD, Larsen AE, Porter HG. Aleutian disease of mink. *Adv Immunol*. 1980;**29**:261–286.

29. Roediger B, Lee Q, Tikoo S, et al. An Atypical Parvovirus Drives Chronic Tubulointerstitial Nephropathy and Kidney Fibrosis. *Cell*. 2018;**175**(2):530-543.e24.

30. Shao X-Q, Wen Y-J, Ba H-X, et al. Novel amdoparvovirus infecting farmed raccoon dogs and arctic foxes. *Emerg Infect Dis*. 2014;**20**(12):2085–2088.

31. Stecher G, Tamura K, Kumar S. Molecular Evolutionary Genetics Analysis (MEGA) for macOS. *Mol Biol Evol*. 2020;**37**(4):1237–1239.

32. Wu Y-H, Wei T, Zhang X-T, et al. Development and evaluation of a direct TaqMan qPCR assay for the rapid detection of diverse carnivore amdoparvoviruses. *Mol Cell Probes*. 2019:101448.

33. ZIMS. Species360 Zoological Information Management System, ZIMS. 2021:

CHAPTER 5:

Amdoparvovirus-associated disease in striped skunks (*Mephitis mephitis*)

Charles E. Alex DVM, DACVP, Katherine Watson DVM, PhD, DACVP, Maya Schlesinger DVM, Kenneth A. Jackson MS, Asli Mete DVM, PhD, DACVP, Peter Chu DVM, DACVP, Patricia A. Pesavento DVM, PhD, DACVP

Submitted for publication in Veterinary Pathology. (Pending review.)

Abstract:

Disease caused by the archetypical Amdoparvovirus (APV), Aleutian Mink Disease Virus (AMDV), has been well studied, but APV infections in other carnivores are poorly understood. Skunk Amdoparvovirus (SKAV), one of a handful of newly discovered APVs, is species-specific in striped skunks (*Mephitis mephitis*) and has a very high prevalence across North America. We have evaluated infection status and viral tissue distribution in a cohort of 26 free-ranging California skunks from a single rehabilitation facility who were euthanized due to poor prognosis for recovery from neurologic disease. SKAV was detected in the majority of this cohort, and virus was associated with a spectrum of lesions including tubulointerstitial nephritis, meningoencephalitis, myocarditis, and arteritis. Tissue targets and patterns of inflammation were only partially overlapping with those of AMDV infection, and were notably distinct in the kidney.

Amdoparvovirus (APV) is a rapidly growing genus within the viral family *Parvoviridae* comprising several important pathogens of carnivores.[6,10] The prototype and archetype Aleutian Mink Disease Virus (AMDV, species *Carnivore amdoparvovirus 1*) has a high prevalence and causes significant losses of farmed mink but no effective vaccine is available.[6,13] The fur industry has struggled for decades to eliminate AMDV. Farmed or experimentally infected mink can be clinically normal but, depending on viral strain and host genetics, infected animals can develop fatal disease, with common sequelae including chronic, slowly progressive dysregulation of the immune system and immune complex–mediated vasculitis and glomerulopathy.[9,15–17] APVs have been identified in many other carnivores including skunks, foxes, raccoon dogs, and red pandas, but clinical outcomes and genetic determinants of host tropism are not characterized.[2,4,12,18]

Our interpretation of the impact of any APV infection requires recognition of potential disease sequelae in the growing number of species known to harbor infections. Striped skunks (*Mephitis mephitis*) are ubiquitous in North America and share dens, food, and water sources with other animals, thereby serving as a reservoir of viruses that infect wildlife and domestic animals. Recent data demonstrates that this species harbors a phylogenetically distinct species called Skunk Amdoparvovirus (SKAV).[2,5] SKAV prevalence, estimated by detection in blood is remarkably high wherever so far tested (Canada, 86%, US 82%), but estimations of potential disease association, including the type and impact of disease, is unknown.[1,3,8,11] Most APVs, including SKAV, were discovered in the last decade, so disease association is further complicated by any literature prior to 2011 which could not distinguish among multiple potential viral species. Specific PCR detection for SKAV species has been performed in a few studies, but given that we have only recently uncovered the high prevalence of SKAV, any unchallenged declaration of disease association based on PCR alone is precarious.[2,5] Molecular detection of

SKAV from diseased tissue coupled with viral distribution by in situ hybridization (ISH) both establishes disease association and reveals mechanisms of pathogenesis such as tissue targets of infection and pathways for SKAV shedding and transmission.

Previously documented SKAV tissue targets reported in 3 animals included cells of the kidney, gastrointestinal tract epithelium, and skin, with the conclusion that transmission was possible by any of these sources.[2] However, viral distribution in other tissues and direct association with lesions have not been evaluated. In this study, we used a retrospective cohort of 26 skunks and a combination of PCR and ISH to analyze the distribution of SKAV and its association with lesions in multiple tissues. All 26 cases were submitted for routine necropsy to one of two University of California laboratories (the UC Davis Veterinary Medical Teaching Hospital (3 cases) or the California Animal Health and Food Safety Laboratories (23 cases)). Cases were included in this study if complete necropsies were performed and adequate formalin-fixed, paraffin-embedded (FFPE) tissues were available. Three cases included in this study were also described in a previous report.[2] All animals (26/26) came directly from a single rehabilitation facility and were euthanized based on decisions by veterinary or rehabilitation center personnel that the animal had neurologic disease and a poor prognosis for recovery. This common clinical presentation was not an inclusion criterion per se, but rather a consequence of the reality that neurologic skunks are more likely to be captured and potentially harbor zoonotic disease (rabies). As a result, this tested cohort is heavily biased, both clinically and geographically.

The spectrum of neurologic signs from subtle (unafraid) to overt (obtunded) are listed in Supplemental Table S5.1. Antemortem trauma occurred in one case (vehicular trauma, spinal

fracture). The cohort included 14 males, 10 females, and 2 skunks of undetermined sex. Seven skunks were juveniles, and 19 were adults. Rabies was ruled out in all cases by ancillary testing (19/26) or by histology alone (7/26). Additionally, 16/26 were tested by IHC for the presence of Canine distemper virus (CDV), and 15/16 were negative. The cohort was variably tested for other pathogens, and trace or high levels of anticoagulants (brodifacoum, bromethelin) were detected in 10 animals, including cases that were both SKAV positive and negative. Postmortem examination findings are summarized in Supplemental Table S5.1.

Splenic tissue is recognized as a sensitive sample for determining APV infection status.[6] Identification of SKAV-positive cases was based on PCR targeting a 365-nucleotide segment of the capsid gene from formalin-fixed, paraffin-embedded (FFPE) scrolls of splenic tissue or tissue pools (Table S5.1). In six cases, PCR detection of Amdoparvovirus infection was performed by outside laboratories using assays designed to detect AMDV, but specific primer strategies were not disclosed by the laboratories. Selected primers in our laboratory, and those of the outside laboratories, could potentially amplify other APVs, but in a separate study all amplicons sequenced (30/100) from skunk spleens were SKAV.[2] In this cohort, Amdoparvovirus infections (presumed SKAV) were detected in 20/26 (76.9%) skunks tested, including all four tested with assays for "AMDV." This is similar to the prevalence previously reported in a collection of 101 skunks (82%), among which 23 were sourced from California.[2]

SKAV ISH was performed as previously described.[2] Based on tissue targeting of the related Aleutian Mink Disease Virus (AMDV), and the frequency of renal lesions in this cohort (21/26), we performed ISH on kidneys of all animals. Correlation of PCR amplification and ISH

probe hybridization (kidney) was high. Of the 20 PCR-positive cases, 19 had detectable probe hybridization in the kidney. Of the 6 PCR-negative cases, 5 were ISH-negative in the kidney. The remaining PCR-negative case, for which FFPE spleen was not available, was PCR-negative in FFPE tissue pools containing kidney, GI tract, and lymph nodes, but nonetheless exhibited scant, multifocal positive probe hybridization in the kidney.

The predominant renal lesion in SKAV-infected skunks was a mononuclear interstitial infiltrate, often surrounding degenerate or necrotic tubules in the renal cortex with variable extension into the medulla (19/20 PCR-positive cases, 95%). The proportion of plasma cells in inflammatory infiltrates varied widely between cases. While similar inflammation is described in spontaneous Aleutian disease of mink, the "classical" observation of AMDV in the mink kidney is a glomerulopathy/glomerulonephritis, which was an uncommon finding in skunks (4/21; 19.1%).[9] In skunks, cortical and/or medullary segments of renal tubules were variably to widely separated by interstitial inflammation (Figure 5.1). In affected areas, renal tubular epithelium exhibited one or more of the following changes: swelling with cytoplasmic microvacuolation (degeneration); cytoplasmic hypereosinophilia; or shrinking with nuclear pyknotic, karyorrhexis, and/or karyolysis (necrosis). Tubules were variably ectatic and contained hyaline, granular, or cellular casts. SKAV ISH probe hybridization was detectable in the kidneys of 19 cases. Viral nucleic acid was present in the tubular epithelium of cases that were minimally affected to severely affected, with probe hybridization present at all levels of the tubular nephron, as well within glomerular parietal epithelium. Virus was predictably detected in the most severely affected tubules in the section, including in necrotic, degenerate, remnant, or sloughed epithelial cells, establishing a convincing causative role in inducing tubular degeneration and necrosis.

However, signal was also present in some cases in tubules with minimal histologic changes, so it is additionally possible that renal tubular epithelium is a site of persistence. Viral nucleic acid was also detected in infiltrating inflammatory cells – presumed macrophages – as well as in scattered individual cells morphologically resembling endothelial cells.

Additional histologic lesions identified frequently in this cohort included meningoencephalitis (n=17), myocarditis (n=15), and arteritis (n=8). Because similar lesions have been associated with APV infections in other species, we tested representative cases by ISH to evaluate the possible association of SKAV in skunks.[2,7,17]

Meningitis, encephalitis, or meningoencephalitis were present in 17 PCR-positive skunks and 1 PCR-negative skunk. The lesions ranged from scant lymphoplasmacytic infiltrates to marked pleocellular inflammation and gliosis with regions of necrosis. In cases with meningitis, meningeal blood vessels were eccentrically or concentrically surrounded by mononuclear cells, and peripheral (penetrating) vessels within the neuropil were cuffed. By ISH, SKAV probe hybridized within scattered cells in the adventitia of affected vessels in the neuropil or meninges (Figure 5.2, a-b).

Myocarditis was observed in 15/20 PCR-positive skunks. This was primarily lymphoplasmacytic, multifocal, and in 5 cases was detected in combination with arteritis of the coronary arteries or their branches. Severe cases had dense infiltrates of plasma cells and lymphocytes disrupting the myocardium, admixed with neutrophils and macrophages and regions of necrosis that were attributed to infarction. Three cases were analyzed by ISH, and

viral nucleic acid was detected in myocardial inflammatory infiltrates in 3/3 cases tested (Figure 5.2, c-d). Virus was not convincingly detected in cardiomyocytes.

Arteritis was present in 8 PCR-positive animals, most often involving muscular arteries including coronary arteries and their branches (5/8) or renal or arcuate arteries in the kidney (5/8). In affected arteries, the adventitia concentrically to eccentrically was surrounded with lymphocytes and fewer plasma cells that expanded and sometimes obscured the vasa vasorum. In segmental regions lymphocytes disrupted and separated layers of the muscular wall. Fibrinoid necrosis, characterized by intramural karyorrhectic lymphocytes and fibrin fibrinoid necrosis, was present segmentally to circumferentially in three cases. SKAV probe hybridization was detected in inflammatory cells surrounding and infiltrating affected arteries (Figure 5.2, e-h).

Splenitis has rarely been associated with APV infections in red pandas, and although spleen is the tissue of choice for diagnosis of infection in FFPE tissues, splenitis was only observed in one skunk in this study (Pesavento lab, unpublished). This finding suggests that the spleen provides a sensitive representation of viremia. This is further suggested by the distribution of SKAV in normal spleens, where viral nucleic acid was detected both in scattered round to polygonal cells – presumably circulating macrophages – in the red pulp and in a patchy distribution in the centers of white pulp germinal centers. The latter, by morphology, is presumed to reflect infection of dendritic cells, similar to what has been proposed for RPAV.[3]

In 2/3 available samples of skin from PCR-positive cases, SKAV was detected in basilar cells of surface and follicular epithelium. In these cases, histopathologic findings were

lymphoplasmacytic dermatitis underlying and occasionally extending into the epithelium, with apoptosis or necrosis of individual epithelial cells.

The archetype *Amdoparvovirus*, AMDV, is well-studied in the narrow genetic context of farm-raised mink, where the most common reason for renal failure is persistent infection leading to a hypergammopathy and immune-complex deposition within glomeruli.[6] In skunks, SKAV infection in a subset of infected skunks causes multi-systemic disease that only partially overlaps with the related mink virus. The predominant lesion within the kidney of skunks was necrotizing tubulointerstitial nephritis, usually with regions acutely affected embedded in a background of fibrosis and nephron loss. The pattern suggests a multiphasic destruction that we propose is sequela of persistent SKAV infection. Meningitis, or meningoencephalitis, while common in this cohort, carries the important caveat that animals were submitted for necropsy because of neurologic disease. Alternate etiologies for central nervous system inflammation were not specifically identified in most cases, however, and the demonstration of SKAV nucleic acid in inflammatory brain lesions supports the possibility of causality in at least a subset of cases. More sporadic findings like pneumonia, dermatitis, glossitis, enteritis, and hepatitis with associated virus – encountered in individual cases – demonstrate that SKAV can target multiple tissues.

Small carnivores are increasingly crowded in suburban settings. While most APV infections to-date appear to be species-specific, cross-species infections have been demonstrated in some cases.[4,14] SKAV was first recognized as distinct viral species in 2017, and since then has been demonstrated to have both a remarkably high prevalence – even among APVs – and remarkable genetic diversity – with up to ~15% sequence variation among individual isolates from infected skunks.[1,3,8] This genetic plasticity may have implications for virulence or host

tropism, as it remains plausible that striped skunks could share infections – and disease – with related, in-contact species.

Diagnostic recognition of the unique spectrum of both acute and chronic SKAV-associated lesions is prerequisite to estimating the potential impact of SKAV on the greater population of free-ranging skunks. SKAV infection should be a differential diagnosis for a variety of inflammatory lesions including nephritis, arteritis, meningoencephalitis, and myocarditis. Unique APV species have been identified from 5 carnivore species in the past 12 years, and among those studied, infection is highly prevalent and is associated with disease in a subset of animals.[2,4,5,12,18] AMDV has been detected in hosts other than mink, but we have no idea whether or how co-infections and/or host-switching influence clinical outcome. Comparisons of disease expression among hosts would benefit from pathogenesis studies that consider viral evolution and potential for viral spillover.

Acknowledgements:

Many cases in this study were originally evaluated by Drs. Anderson, Woods, Diab, Giannitti, Rimoldi, and Montiel (CAHFS), and we are grateful for their thorough and thoughtful examinations. We thank the clinicians and staff of WildCare and Dr. Deanna Clifford of the California Department of Fish and Wildlife for their assistance and support. This project was supported in part by the Karen C. Drayer Wildlife Health Center, School of Veterinary Medicine, University of California, Davis. M.S.S. was supported by funding from the NIH Student Advanced training in Research grant 2T35 OD010956.

Tables and Figures:

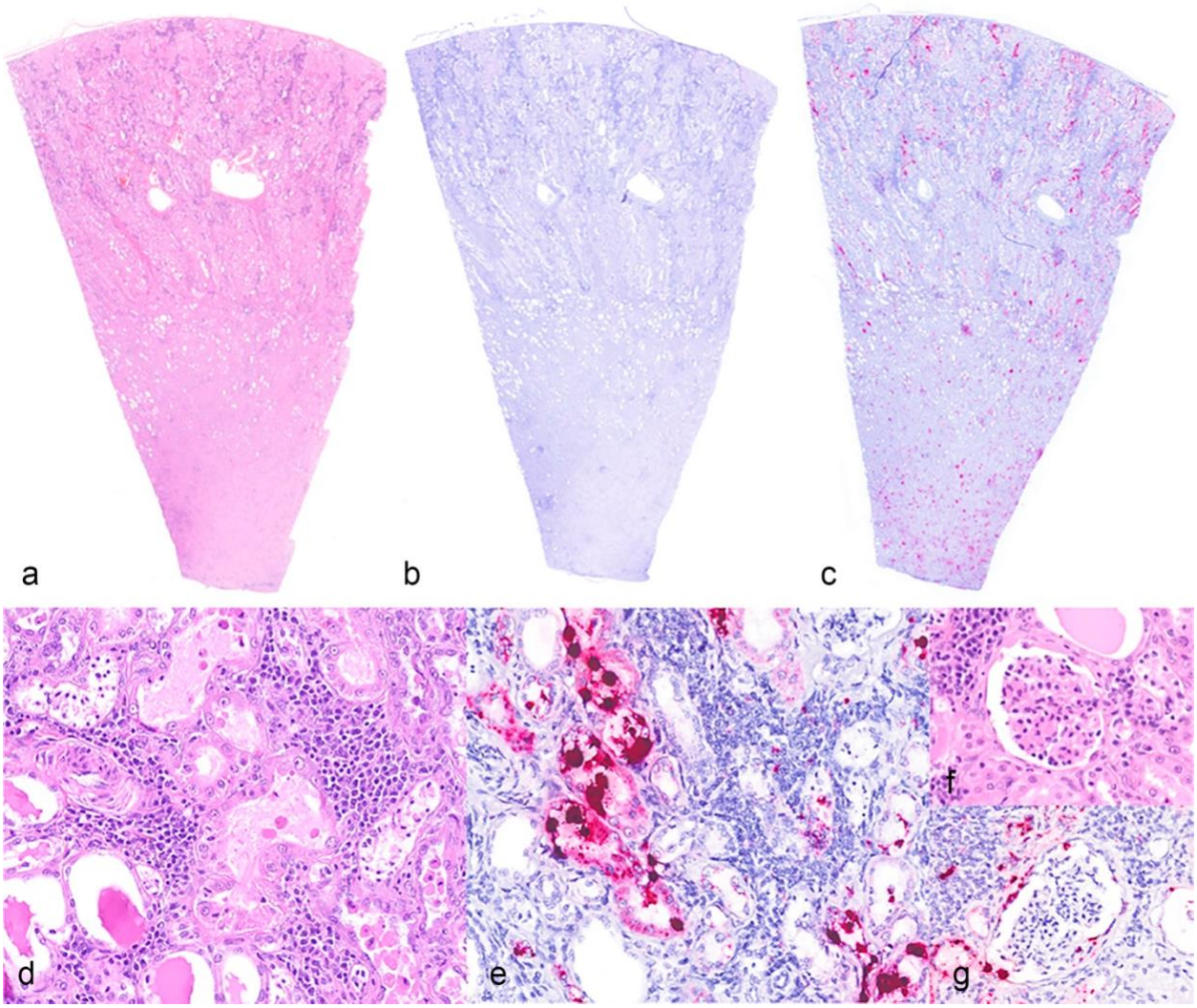

Figure 5.1. Chronic tubulointerstitial nephritis, striped skunk, case 3. (a) Zones of dense hypercellularity separate or replace renal tubules. Hematoxylin and eosin (HE). (b) No hybridization observed with negative control (DapB) ISH probe. (c) ISH with SKAV-specific probes demonstrates abundant viral nucleic acid (red) at all levels of the kidney. (d) Tubules are separated by dense aggregates of lymphocytes and plasma cells. Tubules are multifocally ectatic and often contain brightly eosinophilic luminal proteinaceous fluid. (HE) (e) ISH Signal is detected in renal tubule epithelial cell, in tubular protein casts, and scattered in inflammatory infiltrates. (SKAV ISH) (f) Except where abutted by inflammatory lesions, glomeruli are

essentially within normal limits. (HE) (g) ISH signal is detectable in glomerular parietal epithelium without evidence of membranous glomerulopathy. (SKAV ISH)

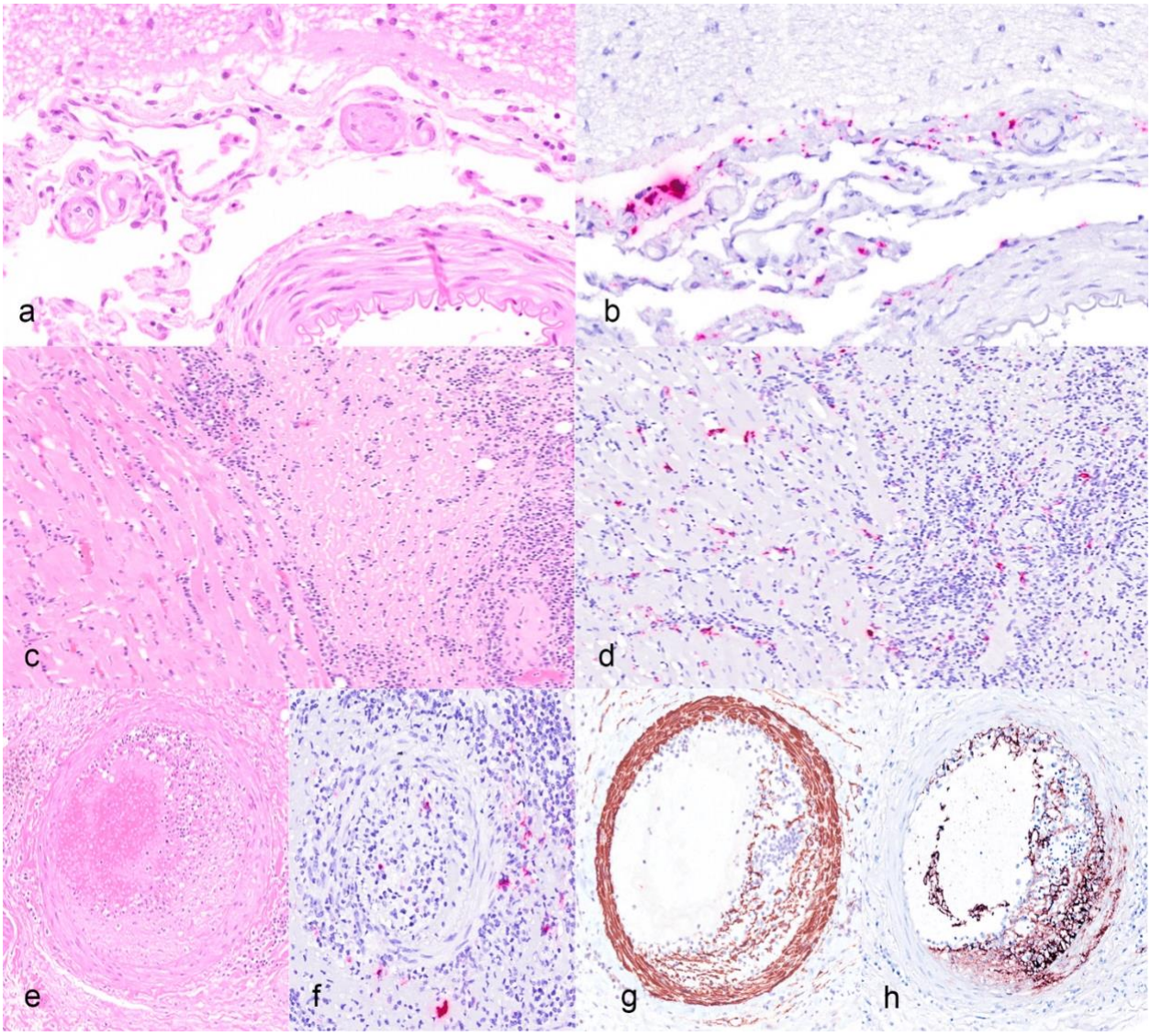

Figure 5.2. Non-kidney targets of SKAV. (a-b) Meningitis, striped skunk, case 3. (a) Scant lymphocytic and plasmacytic inflammation is present in the meninges, particularly around small blood vessels. (HE) (b) SKAV nucleic acid is detected in infiltrating inflammatory cells. (SKAV ISH). (c-d) Myocarditis, striped skunk, case 17. (c) Lymphocytes and plasma cells multifocally expand the interstitium, admixed with fibrin. (HE) (d) Viral nucleic acid is evident in inflamed regions, including in elongate cells between cardiomyocytes (suspect endothelial cells). (SKAV ISH). (e-h) Arteritis, striped skunk, case 17. (e) Adventitial inflammation and segmental disruption of the muscular wall are evident, with infiltrating mixed inflammatory cells, fibrin,

and eccentric expansion of the intima. (HE) (f) SKAV nucleic acid is present amid periarterial and mural inflammatory cells. (SKAV ISH) (g) Immunohistochemistry for smooth muscle actin (SMA) demonstrates partial disruption of the muscular wall. (h) Immunohistochemistry for Factor VIII demonstrates immunoreactivity within the disrupted arterial wall, presumably indicating platelet extravasation due to loss of endothelial integrity.

Table S5.1.

Case	Age	Sex	Clinical presentation	Histopathologic diagnoses				SKAV PCR[a]	SKAV ISH (Kidney)	Ancillary testing within normal limits	Significant ancillary test results
				Nephritis	CNS inflammation	Myocarditis	Arteritis				
1	Adult	F	Unafraid	+	+	+	+	Positive (kidney, liver, lung, spleen)[b]	Positive	RV, WNV, CPV-2, Lepto, Heavy metals	
2	Adult	M	Quiet, seizure-like episodes	+	+	+	+	Positive (kidney, liver, lung, brain)[b]	Positive	RV, CDV, CPV-2, Lepto, Heavy metals	
3	Adult	F	"Neurologic"	+	+	-	-	Positive	Positive	RV, CDV, Lepto	Brodifacoum
4	Juvenile	F	Out in daytime, unafraid	+	+	+	-	Positive[c]	Positive	RV, WNV, CDV, Lepto, Virus isolation, Brodifacoum (trace)	
5	Adult	M	Obtunded, sensitive to sound, weak	+	+	+	+	Positive[c]	Positive	RV, CDV, Toxoplasma, Neospora, Sarcocystis	Brodifacoum
6	Adult	M	Abnormal vocalization, poor mentation, hypersensitive to touch and noise	+	+	+	-	Positive	Positive	RV, CDV, Toxoplasma, Neospora, Sarcocystis, Heavy metals	Brodifacoum
7	Adult	F	Poor mentation	+	+	+	-	Positive[c]	Positive	RV, CDV, Sarcocystis, Anticoagulants (trace)	
8	Adult	M	Shaky, sensitive to touch	+	-	-	-	Positive	Positive	RV, Virus isolation, Brodifacoum (trace)	
9	Juvenile	F	Lethargic	+	+	+	-	Positive	Positive	WNV, CDV, Toxoplasma, Neospora, Sarcocystis, Anticoagulants, Heavy metals	
10	Juvenile	F	Lethargic	+	+	+	+	Positive	Positive	CDV, WNV, Toxoplasma, Sarcocystis	
11	Juvenile	F	Circling, twitching, shaky, drooling	+	+	-	-	Positive	Positive	RV, WNV, CDV, Brodifacoum (trace)	
12	Adult	M	Twitching, sensitive	+	+	+	+	Positive	Positive	RV, Heavy metals, Anticoagulants (trace)	Bromethalin detected
13	Adult	F	Weak	+	+	-	+	Positive	Positive	RV, WNV, CDV, Lepto, Anticoagulants	
14	Adult	F	Lethargy, obtundation, ulcerative lesions	+	+	+	-	Negative (lymph node, kidney, GI)	Positive	RV, CDV	Brodifacoum
15	Adult	F	Ataxia	+	+	+	-	Positive	Positive	RV, CDV, Toxoplasma, Sarcocystis	Aerobic culture (liver, intestine, spleen, lung) - Pseudomonas (secondary)
16	Adult	M	"Behaving abnormally"	+	+	-	-	Positive	Positive	RV, CDV	Leptospira IHC positive (kidney)
17	Adult	U	"Neurologic"	+	+	+	+	Positive	Positive	CDV	
18	Juvenile	F	Seizures	+	-	-	-	Positive	Positive	Anticoagulants, Heavy metals	
19	Adult	M	Unafraid, paresis, seizures	+	+	+	-	Positive	Positive	RV, CDV, Anticoagulants	
20	Adult	F	Lethargy, paresis	+	+	+	-	Positive	Positive	RV, CDV, Anticoagulants, Heavy metals,	
21	Adult	F	Hit by car, spinal fracture	-	-	+	+	Positive[c]	Negative	RV, Anticoagulants	
22	Adult	F	Aggression	-	+	-	-	Negative	Negative	RV, Bromethalin	CDV positive (multiple tissues)
23	Juvenile	M	Unafraid, nuisance	-	-	-	-	Negative	Negative	None	
24	Juvenile	M	Unafraid, nuisance	-	-	-	-	Negative	Negative	None	
25	Adult	U	"Neurologic"	+	-	-	-	Negative	Negative	None	Bromethalin detected
26	Adult	M	Twitching, unafraid, pale	-	-	-	-	Negative	Negative	RV, Heavy metals, Anticoagulants (trace)	Bromethalin detected

[a]PCR performed on FFPE spleen unless otherwise indicated. [b]qPCR for Aleutian Disease performed at the Wisconsin Veterinary Diagnostic Laboratory. Specific PCR methods not disclosed. [c]qPCR performed at the University of Georgia Infection Disease Laboratory. specific PCR methods not disclosed.

Abbreviations: RV, Rabies virus; WNV, West Nile Virus; cPV-2, Canine Parvovirus-2; Lepto, Leptospira; CDV, Canine Distemper Virus.

References:

1. Alex CE, Canuti M, Schlesinger MS, et al. Natural disease and evolution of an Amdoparvovirus endemic in striped skunks (Mephitis mephitis). *Transbound Emerg Dis*. 2022.

2. Alex CE, Kubiski SV, Li L, et al. Amdoparvovirus Infection in Red Pandas (Ailurus fulgens). *Vet Pathol*. 2018;**55**(4):552–561.

3. Britton AP, Redford T, Bidulka JJ, et al. Beyond Rabies: Are Free-Ranging Skunks (Mephitis mephitis) in British Columbia Reservoirs of Emerging Infection? *Transbound Emerg Dis*. 2017;**64**(2):603–612.

4. Canuti M, Doyle HE, P Britton A, Lang AS. Full genetic characterization and epidemiology of a novel amdoparvovirus in striped skunk (Mephitis mephitis). *Emerg Microbes Infect*. 2017;**6**(5):e30.

5. Canuti M, Pénzes JJ, Lang AS. A new perspective on the evolution and diversity of the genus Amdoparvovirus (family Parvoviridae) through genetic characterization, structural homology modeling, and phylogenetics. *Virus Evol*. 2022;**8**(1):veac056.

6. Canuti M, Whitney HG, Lang AS. Amdoparvoviruses in small mammals: expanding our understanding of parvovirus diversity, distribution, and pathology. *Front Microbiol*. 2015;**6**:1119.

7. Dyer NW, Ching B, Bloom ME. Nonsuppurative meningoencephalitis associated with Aleutian mink disease parvovirus infection in ranch mink. *J Vet Diagn Invest*. 2000;**12**(2):159–162.

8. Glueckert E, Clifford DL, Brenn-White M, et al. Endemic Skunk amdoparvovirus in free-ranging striped skunks (Mephitis mephitis) in California. *Transbound Emerg Dis*. 2019.

9. Henson JB, Leader RW, Gorham JR, Padgett GA. The sequential development of lesions in spontaneous Aleutian disease of mink. *Pathol Vet*. 1966;**3**(4):289–314.

10. Jager MC, Tomlinson JE, Lopez-Astacio RA, Parrish CR, Van de Walle GR. Small but mighty: old and new parvoviruses of veterinary significance. *Virol J*. 2021;**18**(1):210.

11. LaDouceur EEB, Anderson M, Ritchie BW, et al. Aleutian Disease: An Emerging Disease in Free-Ranging Striped Skunks (Mephitis mephitis) From California. *Vet Pathol*. 2015;**52**(6):1250–1253.

12. Li L, Pesavento PA, Woods L, et al. Novel amdovirus in gray foxes. *Emerg Infect Dis*. 2011;**17**(10):1876–1878.

13. Markarian NM, Abrahamyan L. AMDV Vaccine: Challenges and Perspectives. *Viruses*. 2021;**13**(9).

14. Oie KL, Durrant G, Wolfinbarger JB, et al. The relationship between capsid protein (VP2) sequence and pathogenicity of Aleutian mink disease parvovirus (ADV): a possible role for raccoons in the transmission of ADV infections. *J Virol*. 1996;**70**(2):852–861.

15. Pan IC, Tsai KS, Grinyer I, Karstad L. Glomerulonephritis in Aleutian disease of mink: ultrastructural studies. *J Pathol*. 1970;**102**(1):33–40.

16. Pan IC, Tsai KS, Karstad L. Glomerulonephritis in Aleutian disease of mink: histological and immunofluorescence studies. *J Pathol*. 1970;**101**(2):119–127.

17. Porter DD, Larsen AE, Porter HG. The pathogenesis of Aleutian disease of mink. 3. Immune complex arteritis. *Am J Pathol*. 1973;**71**(2):331–344.

18. Shao X-Q, Wen Y-J, Ba H-X, et al. Novel amdoparvovirus infecting farmed raccoon dogs and arctic foxes. *Emerg Infect Dis*. 2014;**20**(12):2085–2088.

CHAPTER 6:

Viruses in unexplained encephalitis cases in American black bears (*Ursus americanus*)

Charles Alex DVM, DACVP, Elizabeth Fahsbender PhD, Eda Altan PhD, Robert Bildfell DVM, PhD, DACVP, Peregrine Wolff DVM, Ling Jin DVM, MS, PhD, Wendy Black, Kenneth Jackson MS, Leslie Woods DVM, PhD, DACVP, Brandon Munk DVM, Tiffany Tse, Eric Delwart PhD, Patricia Pesavento DVM, PhD, DACVP

Published in PLoS One (2020) 15(12):e0244056. https://doi.org/10.1371/journal.pone.0244056

Abstract:

Viral infections were investigated in American black bears (*Ursus americanus*) from Nevada and northern California with and without idiopathic encephalitis. Metagenomics analyses of tissue pools revealed novel viruses in the genera *Circoviridae*, *Parvoviridae*, *Anelloviridae*, *Polyomaviridae*, and *Papillomaviridae*. The circovirus and parvovirus were of particular interest due to their potential importance as pathogens. We characterized the genomes of these viruses and subsequently screened bears by PCR to determine their prevalence. The circovirus *(Ursus americanus* circovirus, UaCV) was detected at a high prevalence (10/16, 67%), and the chaphamaparvovirus (*Ursus americanus* parvovirus, UaPV) was found in a single bear. We showed that UaCV is present in liver, spleen/lymph node, and brain tissue of selected cases by *in situ* hybridization (ISH) and PCR. Infections were detected in cases of idiopathic encephalitis and in cases without inflammatory brain lesions. Infection status was not clearly correlated with disease, and the significance of these infections remains unclear. Given the known pathogenicity of a closely related mammalian circovirus, and the complex manifestations of circovirus-associated diseases, we suggest that UaCV warrants further study as a possible cause or contributor to disease in American black bears.

Introduction:

American black bears (*Ursus americanus*) are the most common and widely distributed bear species in North America. Categorized as a species of "Least Concern" by the International Union for Conservation of Nature, their total population in North America is estimated at approximately 850,000-950,000 and growing [1]. Their adaptability to suburban and urban environments—and the expansion of those environments—brings them into relatively frequent contact and conflict with human and domestic animal populations. A clear understanding of the diseases affecting black bears is critical to the management of these populations, including mitigation of outbreaks and potential pathogen spillovers. Black bears may be susceptible to various pathogens infecting domestic animals, including several important viruses such as Canine distemper virus, Canine adenovirus 1, and Canine parvovirus. Serology-based surveillance has established that these exposures are not infrequent [2–6]. However, efforts to correlate infection status with clinical disease have been much more limited. Sporadic case reports have described encephalitis in ursid species due to viral etiologies including Canine adenovirus 1, Canine distemper virus, or cross-species transmission of Equine herpesvirus 1 and 9 [7–10]. Cases of clinical disease from Rabies infection appear to be exceedingly rare in bears. In general, disease threats in this species are not well characterized, and the full range of viruses infecting black bears has yet to be thoroughly explored.

A series of cases of idiopathic encephalitis was observed in American black bears from Nevada (2014-2019). Lesions were suggestive of viral etiologies, but diagnostic efforts ruled out known etiologic agents based on histopathology and molecular techniques. Because viral disease was still considered most likely based on histopathologic lesions, we investigated potential viral etiologies by metagenomics analyses. We identified novel viruses in the families *Circoviridae*,

Parvoviridae, *Anelloviridae*, *Polyomaviridae*, and *Papillomaviridae*. Of these, the circovirus and parvovirus were considered plausible causes of the observed neurologic lesions based on patterns of disease recognized in other species. Encephalitis and cerebellar vasculitis have been associated with Porcine Circovirus infections in pigs, and the human Parvovirus B19 has been associated with a spectrum of neurologic inflammatory lesions in human patients [11–13]. Anelloviruses are highly prevalent, but their association with disease has not been well-established and they are commonly considered to be commensal, asymptomatic infections. Viruses in the *Polyomaviridae* and *Papillomaviridae* families were considered unlikely causes of the observed lesions, and were not pursued. Given their potential pathogenicity, the novel circovirus and parvovirus were further investigated for prevalence by PCR. The novel circovirus was detected at high prevalence, and was further evaluated for tissue distribution and possible lesion association by *in situ* hybridization (ISH).

Materials and methods:

Animals:

The investigation included 17 yearling to adult black bears. Cases 1-8 were free-ranging animals from the Reno and Lake Tahoe areas of Nevada. Case 1 was euthanized because severe clinical disease was observed, and cases 2-7 were euthanized due to behavioral problems (human-bear conflict). Case 8 was killed by a car. For these cases, postmortem examinations took place at the Nevada Department of Agriculture, Animal Disease Lab in Sparks, Nevada. Collected tissues were submitted to the Oregon Veterinary Diagnostic Laboratory in Corvallis, Oregon as part of an investigation of a cluster of cases of non-suppurative encephalitis. That investigation identified a novel gammaherpesvirus, but a specific cause for neurologic disease was not identified [14].

Cases 9-12 were free-ranging bears either found dead or euthanized due to severe disease or human-wildlife conflict from El Dorado, Mendocino, and Santa Barbara counties in California. These cases were necropsied at the California Department of Fish and Wildlife's Wildlife Investigations Laboratory, and tissues were submitted to the California Animal Health and Food Safety laboratory in Davis, CA for histopathology and ancillary testing.

Cases 13-16 had been housed in a wildlife sanctuary in northern California for 10-15 years prior to their deaths. Cases 13-15 were geriatric animals euthanized for progressive mobility difficulties associated with degenerative joint disease, and case 16 died spontaneously with non-suppurative encephalitis. These cases were necropsied at the UC Davis School of Veterinary Medicine. Case information and significant postmortem findings are summarized in Table 6.1.

Metagenomic analyses:

Frozen tissues were mechanically homogenized with a handheld rotor in 1 mL of PBS buffer and the homogenate was centrifuged at 9,000 *rpm* for 5 min. Supernatant (500 µl) was placed in a microcentrifuge tube with 100 µl of zirconia beads and quickly frozen on dry ice, thawed, and vortexed five times, then centrifuged for 5 minutes at 9,000 *rpm*. Tissue samples were pooled according to animal and not by tissue type. The supernatants were then passed through a 0.45 µm filter (Millipore, Burlington, MA, USA) and digested for 1.5 hours at 37°C with a mixture of nuclease enzymes consisting of 14U of Turbo DNase (Ambion, Life Technologies, USA), 3U of Baseline-ZERO (Epicentre, USA), 30U of Benzonase (Novagen, Germany) and 30U of RNase One (Promega, USA) in DNase buffer (Ambion, Life Technologies, USA) to enrich for viral particles. Nucleic acids were extracted immediately afterwards using the MagMAX™ Viral RNA Isolation kit (Applied Biosystems, Life

Technologies, USA) according to the manufacturer's instructions. Nucleic acids were incubated for 2 min with 100 pmol of random primer A (5'GTTTCCCACTGGANNNNNNNN3') followed by a reverse transcription step using Superscript III (Invitrogen) with a subsequent Klenow DNA polymerase step (New England Biolabs). cDNA was then further amplified by a PCR step using AmpliTaq Gold™ (ThermoFisher Scientific) DNA polymerase LD with primer B (similar to primer A but minus the randomized 3' end, or 5'GTTTCCCACTGGATA3'). The reaction (25 µL) contained with 2 µM of primer B, 1.85U of AmpliTaq Gold® DNA Polymerase (Applied Biosystems, Thermo Fisher, Waltham, MA, USA), 0.25 of mM dNTPs, 4 mM of MgCl2, 1× PCR Buffer, and 5 µL of cDNA template. The thermal profile for amplification was composed of 95 °C for 5 min, 5 cycles of 95 °C for 30 s, 59 °C for 60 s, and 72 °C for 90 s, 35 cycles of 95 °C for 30 s, 59 °C for 30 s, and 72 °C for 90 s (+2 s per cycle) followed by 72 °C for 10 min and hold at 4 °C. The amplified product was checked by gel electrophoresis (approximately expected size 300–1000 bp), and one ng was used as target for Illumina library generation. The randomly amplified DNA products were quantified by Quant-iT™ DNA HS Assay Kit (Invitrogen, USA) using Qubit fluorometer (Invitrogen, USA). The library was generated using the transposon-based Nextera™ XT Sample Preparation Kit (Illumina, San Diego, CA, USA) and the concentration of DNA libraries was measured by Quant-iT™ DNA HS Assay Kit. The libraries were pooled at equal concentration and size-selected for a range of 300-1,000 bp using the Pippin Prep (Sage Science, Beverly, MA, USA). The library was quantified using the KAPA library quantification kit for Illumina platforms (Kapa Biosystems, USA) and a 10 pM concentration was loaded on the MiSeq sequencing platform for 2x250 cycles pair-end sequencing with dual barcoding. Human and bacterial reads were identified and removed by comparing the raw reads with human reference genome hg38 and bacterial genomes release 66

(collected from ftp://ftp.ncbi.nlm.nih.gov/blast/db/FASTA/, Oct. 20, 2017) using local search mode. The filtered sequences were de-duplicated if base positions 5 to 55 were identical. One random copy of duplicates was kept. The sequences were then trimmed for quality and adaptor and primer sequences by using VecScreen [15]. After that, the reads were de novo assembled by EnsembleAssembler [16]. Assembled contigs and all singlet reads were aligned to an in-house viral protein database (collected from ftp://ftp.ncbi.nih.gov/refseq/release/viral/, Oct. 20, 2017) using BLASTx (version 2.2.7) with E-value cutoff of 0.01. The significant viral hits were then aligned to an in-house non-virus-non-redundant (NVNR) universal proteome database using DIAMOND [17] to eliminate false positive viral hits. Hits with more significant E-value to NVNR than to viral database were removed. Remaining singlets and contigs were compared to all eukaryotic viral protein sequences in GenBank's non-redundant database using BLASTx. The genome coverage of the target viruses was further analyzed by Geneious R11.1.4 software (Biomatters, New Zealand). Genome features were identified by visualization of expected protein sequences of canonical domains, and splice sites were predicted based on expected RNA transcripts.

PCR detection:

For UaCV DNA detection in fresh tissue, DNA was extracted from tissue samples that were collected at necropsies and stored frozen (-80 °C) until use, using the DNEasy Blood and Tissue Kit (Qiagen) according to the manufacturer's instructions. A nested PCR ("Assay 1") was used, consisting of two separate PCR reactions wherein the PCR product from the first round was used as template for the second reaction. The assay targeted part of the Rep gene, based on the contig discovered through metagenomic analysis, with the first-round primers S6_circo_322F (5'-

GGCGGGGATTCAAGTGCTAT-3') and S6_circo_651R (5'-TGGGTTCCCACAGGTAAAGC-3') to amplify a 329-nt first round product, and second round primers S6_circo_356FN (5'-GGGGTAATTGGTGGGATGGG-3') and S6_circo_625RN (5'-GCCCTTCATCCCAGGTAAGG-3') to amplify a 269-nt second-round product. The PCR [containing a final concentration of 0.2 µm of each primer, 0.2 mM of dNTPs, 0.625 U of Amplitaq Gold® DNA polymerase (Applied Biosystems, Waltham, MA, USA), 1× PCR Gold buffer II, 1.5 mM of $MgCl_2$ and 1 µL of DNA template in a 25 µl reaction] proceeded as follows: 95 °C for 5 min, 40 cycles of (95 °C for 30 s, (52 °C for the first round and 54 °C for the second round of primers) for 30 s, and 72 °C for 30 s), followed by a final extension at 72 °C for 7 min. PCR products of the correct size were verified by gel electrophoresis and Sanger sequencing.

For formalin-fixed, paraffin-embedded (FFPE) tissues, a separate, single-amplification assay ("Assay 2") was used to amplify a 276-nt segment of the Rep gene using primers BearCV.92F (5'-CTGACCTTGAAGATGCCTGTAG-3') and BearCV.368R (5'-CATACCCATCCCACCAATTACC-3'). This one-step assay amplifies a slightly smaller product than the first round of Assay 1, and was utilized to circumvent problems of viral genomic degradation due to formalin fixation. Multiple serial sections (scrolls) or single 5-µm-thick unstained sections scraped from slides of FFPE liver tissue were deparaffinized in xylene and graded alcohol washes, and DNA was extracted using the DNEasy Blood and Tissue Kit (Qiagen) according to manufacturer instructions. PCR targeting a housekeeping gene (GAPDH) was used to confirm successful DNA extractions. For UaCV "Assay 2," reactions consisted of HotStarTaq Plus Master Mix (Qiagen), 5 pmol of each primer, 2.5 µL of dye, and approximately 25-50 ng of template DNA, diluted to a final volume of 25 µL. Cycling conditions were: 95 °C for 5 minutes, followed by 40 cycles of 94 °C (30s), 52 °C (30s), 72 °C (30s), and a final 72 °C elongation step

for 10 minutes. For visualization, products were run on 1.4% agarose gels containing Gel Red (Biotium).

In situ hybridization:

To demonstrate viral genome in tissue sections, colorimetric *in situ* hybridization (ISH) was performed on 5-μm-thick sections of formalin-fixed, paraffin-embedded tissues on Superfrost Plus slides (Fisher Scientific, Pittsburgh, PA) using the RNAscope 2.5 Red assay kit (Cat #322360, Advanced Cell Diagnostics, Inc., Hayward, CA). We designed V-UaCirV, (ACD Cat #555001) as 26 ZZ-paired probe sets targeting a 1409 nt segment of the viral genome corresponding to nucleotide positions 478-1887 of the reference sequence (GenBank accession MN371255). Selected tissues included livers and spleens, as these are established sites of circoviral distribution in related species, as well as brains in order to evaluate the possible association with neurologic disease in these cases. Each 5-μm-thick tissue section was pretreated with heat and protease prior to probe hybridization for 2 hours at 40°C. Negative controls used for validation of signal included an unrelated (GC-content matched) probe on serial sections. Slides were counterstained with hematoxylin and mounted with EcoMount (Biocare Medical, Concord, CA).

Results:

Metagenomics:

Metagenomics analysis was performed on tissues from seven black bears (cases 1-6, 9). The analyzed tissues and results are summarized in Table 6.2. Metagenomic analysis revealed the presence of a novel circovirus in all but one pool, a polyomavirus in two pools, and a novel papillomavirus and a novel parvovirus each present in one pool. Anellovirus reads were detected

in all sample pools. The 812 bp polyomavirus contig in case 3 showed 95% aa identity to the large T antigen of the giant panda polyomavirus (NC_035181.1), while the polyomavirus in case 9 had 74% identity to the *Leptonychotes wedellii* (Weddell seal) polyomavirus large T antigen (NC_032120). The 887 bp papillomavirus contig present in case 9 had 55% identity to L2 *Canis familliaris* papillomavirus (NC 013237). All raw reads were submitted to the short read archive under PRJNA564639.

New parvovirus:

A novel parvovirus, *Ursus americanus* Parvovirus (UaPV, accession MN166196) in the new genus Chaphamaparvovirus, was identified in the kidney and liver of case 1. The nearly complete genome is 3,787 bp containing three major open reading frames (ORFs), including a 660 aa non-structural protein (NS1), a 165 aa NP, and the 490 aa viral capsid (VP) (Fig. 6.1). The NP was detected in two potential isoforms, including NS2-L (165 aa) and after splicing NS2-P (490 aa). BLASTp of these proteins revealed 73% identity in NS1, 76% identity in VP, 85% identity in NS2-L, and 76% identity in NS2-P to the recently described mouse kidney parvovirus (MKPV) that induces kidney disease in laboratory mice (MH670587) [18]. UaPV is therefore currently the closest relative of MKPV. The *in silico* predicted splicing is similar to that of MKPV based on the putative promotors, predicted splice sites, and polyadenylation signals. There is a conserved acceptor site just before the start of the VP ORF. Two polyadenylation sites were identified based on the conserved nature of these sites in other chaphamaparvoviruses. There are four putative promoter sites reported in this genome, however, the promoter located upstream of the VP start codon is conserved among chaphamaparvoviruses [19]. Putative exons include the NS1, two isoforms of the NS2, and VP.

New circovirus:

The *Ursus americanus* circovirus (UaCV) genome (GenBank accession MN371255) is 2,054 bp with two ambisense open reading frames encoding capsid and replication-associated proteins (Fig. 6.2). Based on full nucleotide sequence, it is most similar to a circovirus identified in a masked palm civet (*Paguma larvata*; Pl-CV8, GenBank accession LC416890.1), with which it shares 75.42% nt sequence identity. A BLASTp showed the Cap (260 aa) had 80% identity to Pl-CV8, and the Rep (287 aa) had a 72% identity to another masked palm civet circovirus sequence, Pl-CV9 (GenBank accession LC416391.1). UaCV contains a stem-loop motif between the intergenic region of the two ORFs consisting of a palindromic 15 bp stem, an 11 bp loop for the initiation of rolling-circle replication, and a 9 bp canonical nonamer (5'-TACTATTAC-3') on the apex of the loop. The Rep contains 3 rolling circle replication motifs at the N-terminus including, motif I [CFTVNN], motif II [PHLQG], and motif III [YCKK]. The superfamily 3 helicase motifs located at the C-terminus of the UaCV replication-associated protein displayed a Walker-A motif [GPPGCGKT], a Walker–B motif [CLDD], and motif C [ITSN]. Similar to the PlCV, two introns were identified in the Rep encoding ORF at locations 47-96 and 363-505. A BLASTx of the Rep showed a 235 aa region that has a 51% identity to porcine circovirus 3 (PCV3-CN-AHB004-2018, accession MK178285.1).

Prevalence:

Having detected UaPV in one case and UaCV in multiple cases by metagenomics, we elected to screen additional black bears for these viruses by PCR. In total, tissues from 16 black bears were tested by PCR for circovirus and parvovirus. For cases 1-6, the same fresh tissue samples used for metagenomics were screened. For cases 7-16, only formalin-fixed, paraffin-

embedded (FFPE) tissues were available. Parvovirus was detected in one case (index case 1). Circovirus was detected in 10/16 cases (62.5%) by one or both PCR assays. Results of PCR detection are summarized in Table 6.3.

Circovirus ISH:

Given the high frequency of UaCV detection, we evaluated possible tissue targets of infection by *in situ* hybridization. Selected tissues from 12 cases were examined for circovirus by ISH. Positive probe hybridization was detected in 6 cases. Tissues examined included liver, spleen, and brain sections (5 cases), brain only (2 cases), liver only (2 cases), liver and spleen (2 cases), or lymph node only (1 case). Individuals and specific tissues tested were limited by availability of tissue blocks with adequate tissue preservation. Sections examined and results are summarized in Table 6.4.

Livers that were positive by ISH (4/10) exhibited punctate to diffuse cytoplasmic hybridization in individual cells in hepatic sinusoids (presumed Kupffer cells and/or endothelial cells). This pattern was seen diffusely throughout liver sections (Fig. 6.3), and is consistent with patterns of circovirus detection in the livers of PCV-infected pigs [20] and in dogs infected with Canine circovirus (Pesavento lab, unpublished data).

In 5/9 cases, lymphoid tissues (spleen or lymph node) exhibited similar but more sparse punctate hybridization in individual cells. In spleens, signal was distributed throughout the tissue in the cytoplasm of scattered individual round cells (presumed lymphocytes and/or macrophages).

Lymph nodes exhibited a similar pattern, with signal appearing most prominently in cells in the medullary sinuses and occasionally in cortices.

Brains were of particular interest due to a series of cases of unexplained encephalitis in black bears in the region. Ten of the cases in this study had postmortem diagnoses of mild to severe cerebral cortical inflammation characterized by multifocal to coalescing zones of mononuclear perivascular cuffing, edema, gliosis, hemorrhage, and necrosis. Sections of cerebrum from 8 cases were examined by ISH. Five of these cases had histologic evidence of encephalitis, and three did not. For animals with encephalitis, sections including inflammatory lesions were selected. Sparse positive hybridization was observed in brains from 3 cases—two with encephalitis and one without—occurring as scattered punctate intracellular or extracellular foci. To confirm positive probe hybridization above spurious background staining, two authors (CA, TT) evaluated ISH slides and negative controls for these sections and tallied individual punctate foci of hybridization, noting their location with respect to blood vessels: vessel-associated (including luminal, endothelial, mural, and Virchow-Robbins space signal) or neuroparenchymal. Counts from the two reviewers were averaged to compare signal from circovirus-specific ISH slides with their corresponding negative controls. Cases were interpreted as positive when the number of puncta of specific probe hybridization far exceeded (>10x) background signal. In all three cases, most hybridization signal was seen in the lumen, endothelium, wall, or Virchow-Robbins spaces of small-caliber blood vessels, suggesting the possibility of endothelial or vascular mural infection. Affected vessels were distributed throughout the examined brain sections, without apparent co-localization to lesions of encephalitis. No clear association between infection and disease was established. No other tissues exhibited similar vessel-associated ISH signal. Counts of ISH signal foci by brain region in these cases are summarized in Supplemental Table S6.1.

Discussion:

A metagenomic investigation of black bears identified novel viruses belonging to five genera: *Circoviridae, Parvoviridae, Anelloviridae, Polyomaviridae,* and *Papillomaviridae.* Of these, circovirus and anellovirus genomes were detected at high prevalence in the study cohort, while parvovirus, polyomavirus, and papillomavirus genomes were identified in 1-2 cases each. Although a definitive association of viral infection with encephalitis lesions was not established, our results expand the known diversity of viruses infecting black bears, and several of the identified viruses warrant further consideration as potential pathogens.

Circovirus infection was detected in 10/16 (62.5%) of cases tested, but the clinical significance of these infections remains to be established. Within Circoviridae, an 80% nucleotide sequence identity threshold is used for species demarcation [21]. Thus UaCV, which shares 75.42% nt sequence identity with its closest known relative (Pl-CV8), warrants classification as a novel viral species. While both UaCV and Pl-CV8 were identified in carnivore hosts (the latter in a masked palm civet), the two host species are not closely related and do not share a geographic range. There is no evidence to suggest a recent viral spillover from palm civet to black bear; rather, we speculate that UaCV has been enzootic but previously undetected in black bears. Retrospective studies of archived black bear cases from across their geographic range would be useful to clarify the evolutionary history and historical prevalence of UaCV in this population, as well as any association with disease.

The presence and distribution of UaCV sequences in spleens and livers, as demonstrated by PCR and ISH, is consistent with the behavior of known circoviruses in other mammalian hosts, including pathogenic circoviruses of pigs. However, the “classic” histologic lesion of circovirus infection derived from PCV2 studies, characterized by lymphoid depletion with histiocytic

replacement and botryoid cytoplasmic inclusions [22], was not evident in these cases. Circoviral nucleic acid was detected by ISH in brains of 3 bears—two with encephalitis and one without—and the distribution in these sections was overwhelmingly vascular or perivascular. It is plausible that the positive ISH signal we observed in these sections indicates a viral tropism for endothelial cells, as has been demonstrated for other circoviruses, but no association could be made between the distribution of ISH signal and histologic brain or vascular lesions. In pigs, PCV2 is known to be endotheliotropic and has been associated with vascular lesions including lymphohistiocytic vasculitis and fibrinoid vascular necrosis, with PCV2 genome demonstrable in endothelium, mural myocytes, and perivascular/infiltrating leukocytes[12]. Although affected vessels may be found anywhere in the body, neurovascular (particularly cerebellar) involvement has been reported in a subset of cases [13]. Similarly, canine circovirus was demonstrated by ISH in (histologically normal) presumed endothelial cells in at least two cases that had evidence of necrotizing vasculitis in other tissues [23]. We speculate that the observed distribution of UaCV in bear brains could be consistent with infection of endothelial cells or vascular mural cells. Alternatively, in encephalitic bears, a compromised blood-brain barrier could allow leakage of virions or virus-infected cells from circulation, accounting for an observed vascular/perivascular distribution. However, the affected blood vessels were often histologically normal by routine staining, and in cases with encephalitis ISH signal was not obviously associated with areas of inflammation.

Several cases exhibited inconsistent circovirus testing results. Disparate results between PCR assays (cases 2, 4, and 5) may be attributable to differences in tissues tested (case 2) and/or degradation of genomic material in formalin-fixed, paraffin-embedded tissues (cases 4 and 5). Several PCR-positive cases were negative by ISH (cases 2, 11, and 13), possibly reflecting low viral load or variation in the tissue distribution of virus. Extended formalin fixation time or

advanced autolysis are also plausible causes for loss of ISH signal in tissue sections. Two cases (8 and 12) were PCR-negative for circovirus but exhibited convincing probe hybridization by ISH. In these cases, tissues used for PCR differed from those examined by ISH, and the PCRs also utilized DNA from FFPE tissues, so tissue distribution, low viral concentration, and genomic degradation from prolonged fixation are also possible causes for these results.

The identification of a circovirus infecting black bears expands the known mammalian host range of the *Circoviridae*, and could provide new insight into the disease threats affecting this species. These infections were not definitively associated with pathologic findings. However, given the complicated manifestations of circovirus-associated diseases, we suggest that UaCV warrants further study as a possible cause or contributor to disease in American black bears, particularly (as with other pathogenic mammalian circoviruses) in the context of viral persistence, immunologic effects, and potentiation of/by co-infections. The pathogenic potential of UaCV and other viruses in this study could be influenced by co-pathogens and the general health and immune status of these bears.

Viruses in the genus *Chaphamaparvovirus* are a recent addition to the family *Parvoviridae*[19,24]. Chaphamaparvovirus infections have been demonstrated to cause chronic kidney disease in laboratory mice, and a chaphamaparvovirus in domestic dogs has been suggested to play a role in diarrhea, but the full spectrum of chaphamaparvovirus-associated disease remains to be elucidated [18,25]. Species demarcation criteria within *Parvoviridae* dictate that members of a given species share >85% amino acid sequence identity in the nonstructural (NS1) protein [24]. UaPV shares ~73% aa sequence identity with its closest phylogenetic neighbors (murine chaphamaparvoviruses), and thus warrants classification as a novel parvoviral species. UaPV was detected in one case in the present study, and its clinical significance is unknown. Given the known

association of murine chaphamaparvoviruses with renal disease, further investigations of UaPV focused on renal tissue may be warranted. Sample availability precluded this possibility in the present study.

Anellovirus genomic material was found in all cases investigated by metagenomic analysis. *Anelloviridae* is a ubiquitous family of small, single-stranded, circular DNA viruses that are highly prevalent in the human population (>90%) and cause persistent, presumably life-long infections [26]. Anelloviruses are also ubiquitous in other mammals and generally considered commensal infections [27]. In pigs, Torque teno sus anellovirus viral loads are increased when co-infected with porcine circovirus 2 [28] and anellovirus loads also increase in immunosuppressed humans [29–36]. The possible contribution to neurologic lesions or other disease in these bears remains unknown, and the high rate of detection could reflect immune compromise in some of these cases.

The papillomavirus and the two distinct polyomaviruses identified in this investigation were also found in 1 and 2 cases, respectively, and were considered unlikely to have been associated with significant apparently clinical disease in this cohort.

In summary, we identified diverse novel viruses infecting black bears from California and Nevada. A clear relationship between infection status and neurologic lesions was not established for any of these viruses. However, this work expands the known diversity of viruses infecting free-ranging black bears in north America, and several of the identified viruses warrant further investigation as potential pathogens.

Acknowledgements:

We thank Vorthon Sawasong for helpful discussions, and Carl Lackey and Drs. Terza Brostoff and Steven Kubiski for reviewing the manuscript. We thank the field and wildlife health staff at CDFW and NDOW for their technical and logistical support in handling these cases. Support to E.F. and E.D. was provided by Vitalant Research Institute. C.A. is supported in part by the McBeth Foundation and San Diego Zoo Global. The Pesavento lab is supported in part by the Bernice Barbour Foundation.

References:

1. Garshelis, D.L., Scheick, B.K., Doan-Crider, D.L., Beecham, J.J. & Obbard, M.E. Ursus americanus (errata version published in 2017). In: The IUCN Red List of Threatened Species [Internet]. 2016 [cited 14 Jan 2020]. Available: https://dx.doi.org/10.2305/IUCN.UK.2016-3.RLTS.T41687A45034604.en.

2. Bard SM, Cain JW 3rd. Pathogen prevalence in American black bears (*Ursus americanus amblyceps*) of the Jemez Mountains, New Mexico, USA. J Wildl Dis. 2019;55: 745–754.

3. Stephenson N, Higley JM, Sajecki JL, Chomel BB, Brown RN, Foley JE. Demographic characteristics and infectious diseases of a population of American black bears in Humboldt County, California. Vector Borne Zoonotic Dis. 2015;15: 116–123.

4. Ramey AM, Cleveland CA, Hilderbrand GV, Joly K, Gustine DD, Mangipane B, et al. Exposure of Alaska brown bears (*Ursus arctos*) to bacterial, viral, and parasitic agents varies spatiotemporally and may be influenced by age. J Wildl Dis. 2019;55: 576–588.

5. Niedringhaus KD, Brown JD, Ternent MA, Cleveland CA, Yabsley MJ. A Serosurvey of Multiple Pathogens in American Black Bears (*Ursus americanus*) in Pennsylvania, USA Indicates a Lack of Association with Sarcoptic Mange. Vet Sci China. 2019;6. doi:10.3390/vetsci6040075

6. Bronson E, Spiker H, Driscoll CP. Serosurvey for selected pathogens in free-ranging American black bears (*Ursus americanus*) in Maryland, USA. J Wildl Dis. 2014;50: 829–836.

7. Knowles S, Bodenstein BL, Hamon T, Saxton MW, Hall JS. Infectious Canine Hepatitis in a Brown Bear (*Ursus arctos horribilis*) from Alaska, USA. J Wildl Dis. 2018;54: 642–645.

8. Cottrell WO, Keel MK, Brooks JW, Mead DG, Phillips JE. First report of clinical disease associated with canine distemper virus infection in a wild black bear (*Ursus americana*). J Wildl Dis. 2013;49: 1024–1027.

9. Wohlsein P, Lehmbecker A, Spitzbarth I, Algermissen D, Baumgärtner W, Böer M, et al. Fatal epizootic equine herpesvirus 1 infections in new and unnatural hosts. Vet Microbiol. 2011;149: 456–460.

10. Schrenzel MD, Tucker TA, Donovan TA, Busch MDM, Wise AG, Maes RK, et al. New hosts for equine herpesvirus 9. Emerg Infect Dis. 2008;14: 1616–1619.

11. Watanabe T, Kawashima H. Acute encephalitis and encephalopathy associated with human parvovirus B19 infection in children. World J Clin Pediatr. 2015;4: 126–134.

12. Resendes AR, Segalés J. Characterization of vascular lesions in pigs affected by porcine circovirus type 2-systemic disease. Vet Pathol. 2015;52: 497–504.

13. Seeliger FA, Brügmann ML, Krüger L, Greiser-Wilke I, Verspohl J, Segalés J, et al. Porcine circovirus type 2-associated cerebellar vasculitis in postweaning multisystemic wasting syndrome (PMWS)-affected pigs. Vet Pathol. 2007;44: 621–634.

14. Black W, Troyer RM, Coutu J, Wong K, Wolff P, et al. Identification of gammaherpesvirus infection in free-ranging black bears (*Ursus americanus*). Virus Res. 2019;259: 46-53.

15. Schäffer AA, Nawrocki EP, Choi Y, Kitts PA, Karsch-Mizrachi I, McVeigh R. VecScreen_plus_taxonomy: imposing a tax(onomy) increase on vector contamination screening. Bioinformatics. 2018;34: 755–759.

16. Deng X, Naccache SN, Ng T, Federman S, Li L, Chiu CY, et al. An ensemble strategy that significantly improves de novo assembly of microbial genomes from metagenomic next-generation sequencing data. Nucleic Acids Res. 2015;43: e46.

17. Buchfink B, Xie C, Huson DH. Fast and sensitive protein alignment using DIAMOND. Nat Methods. 2015;12: 59–60.

18. Roediger B, Lee Q, Tikoo S, Cobbin JCA, Henderson JM, Jormakka M, et al. An Atypical Parvovirus Drives Chronic Tubulointerstitial Nephropathy and Kidney Fibrosis. Cell. 2018;175: 530–543.e24.

19. Pénzes JJ, de Souza WM, Agbandje-McKenna M, Gifford RJ. An Ancient Lineage of Highly Divergent Parvoviruses Infects both Vertebrate and Invertebrate Hosts. Viruses. 2019;11. doi:10.3390/v11060525

20. Rosell C, Segalés J, Domingo M. Hepatitis and staging of hepatic damage in pigs naturally infected with porcine circovirus type 2. Vet Pathol. 2000;37: 687–692.

21. Breitbart M, Delwart E, Rosario K, Segalés J, Varsani A, Ictv Report Consortium. ICTV Virus Taxonomy Profile: Circoviridae. J Gen Virol. 2017;98: 1997–1998.

22. Meng X-J. Porcine circovirus type 2 (PCV2): pathogenesis and interaction with the immune system. Annu Rev Anim Biosci. 2013;1: 43–64.

23. Li L, McGraw S, Zhu K, Leutenegger CM, Marks SL, Kubiski S, et al. Circovirus in tissues of dogs with vasculitis and hemorrhage. Emerg Infect Dis. 2013;19: 534–541.

24. Pénzes JJ, Söderlund-Venermo M, Canuti M, Eis-Hübinger AM, Hughes J, Cotmore SF, et al. Reorganizing the family Parvoviridae: a revised taxonomy independent of the canonical approach based on host association. Arch Virol. 2020;165: 2133–2146.

25. Fahsbender E, Altan E, Seguin MA, Young P, Estrada M, Leutenegger C, et al. Chapparvovirus DNA Found in 4% of Dogs with Diarrhea. Viruses. 2019;11. doi:10.3390/v11050398

26. Spandole S, Cimponeriu D, Berca LM, Mihăescu G. Human anelloviruses: an update of molecular, epidemiological and clinical aspects. Arch Virol. 2015;160: 893–908.

27. Manzin A, Mallus F, Macera L, Maggi F, Blois S. Global impact of Torque teno virus infection in wild and domesticated animals. J Infect Dev Ctries. 2015;9: 562–570.

28. Kekarainen T, Segalés J. Torque teno sus virus in pigs: an emerging pathogen? Transbound Emerg Dis. 2012;59 Suppl 1: 103–108.

29. De Vlaminck I, Khush KK, Strehl C, Kohli B, Luikart H, Neff NF, et al. Temporal response of the human virome to immunosuppression and antiviral therapy. Cell. 2013;155: 1178–1187.

30. Li L, Deng X, Linsuwanon P, Bangsberg D, Bwana MB, Hunt P, et al. AIDS alters the commensal plasma virome. J Virol. 2013;87: 10912–10915.

31. Touinssi M, Gallian P, Biagini P, Attoui H, Vialettes B, Berland Y, et al. TT virus infection: prevalence of elevated viraemia and arguments for the immune control of viral load. J Clin Virol. 2001;21: 135–141.

32. Shibayama T, Masuda G, Ajisawa A, Takahashi M, Nishizawa T, Tsuda F, et al. Inverse relationship between the titre of TT virus DNA and the CD4 cell count in patients infected with HIV. AIDS. 2001;15: 563–570.

33. Thom K, Petrik J. Progression towards AIDS leads to increased Torque teno virus and Torque teno minivirus titers in tissues of HIV infected individuals. J Med Virol. 2007;79: 1–7.

34. Christensen JK, Eugen-Olsen J, SŁrensen M, Ullum H, Gjedde SB, Pedersen BK, et al. Prevalence and prognostic significance of infection with TT virus in patients infected with human immunodeficiency virus. J Infect Dis. 2000;181: 1796–1799.

35. Devalle S, Rua F, Morgado MG, Niel C. Variations in the frequencies of torque teno virus subpopulations during HAART treatment in HIV-1-coinfected patients. Arch Virol. 2009;154: 1285–1291.

36. Madsen CD, Eugen-Olsen J, Kirk O, Parner J, Kaae Christensen J, Brasholt MS, et al. TTV viral load as a marker for immune reconstitution after initiation of HAART in HIV-infected patients. HIV Clin Trials. 2002;3: 287–295.

Tables and Figures;

Table 6.1. American black bear cases included in this investigation

Case	Location (county)	Sex	Age	Significant post-mortem findings	Euthanized	Date of death or euthanasia
1	Washoe, NV	M	1y	Encephalitis	Y	30 Jan 2014
2	Washoe, NV	F	1y	Encephalitis	Y	17 Mar 2014
3	CA, near Reno, NV[#]	M	1y	Encephalitis	Y	7 Apr 2017
4	Washoe, NV	F	1y	Encephalitis, tooth root abscess	Y	21 Feb 2018
5	Douglas, NV	M	3y	Encephalitis	Y	9 Jul 2014
6	Reno/Tahoe, NV[#]	M	1y	Mild dermatitis	Y	24 Apr 2017
7	Douglas, NV	F	1y	Encephalitis	Y	2 Jul 2018
8	Reno/Tahoe, NV[#]	M	1y	Trauma (hit by car)	N	22 Aug 2018
9	Mendocino, CA	M	adult	Meningeal lymphoma	Y	8 Mar 2018
10	El Dorado, CA	M	11m	Hepatic necrosis, encephalitis	N	25 Dec 2018
11	El Dorado, CA	M	11m	Hepatitis, encephalitis (Sarcocystis)	N	15 Dec 2018
12	Santa Barbara, CA	M	adult	Nasal tumor	Y	20 Aug 2017
13	Calaveras, CA*	F	adult	Degenerative joint disease, nasal tumor	N	26 Dec 2017
14	Calaveras, CA*	M	adult	Degenerative joint disease	Y	9 Jul 2018
15	Calaveras, CA*	M	adult	Degenerative joint disease	Y	31 Jul 2017
16	Calaveras, CA*	F	adult	Encephalitis	Y	20 Jan 2011

*Sanctuary-housed
[#]Specific county of origin unknown

Table 6.2. Viruses detected by metagenomics analyses

Case	Tissue pools	Virus family	Reads per million
1	Kidney	*Anelloviridae*	17950
		Circoviridae	149
		Parvoviridae	169
2	Cerebrum	*Anelloviridae*	28
	Lymph node	*Circoviridae*	3
3	Cerebrum	*Anelloviridae*	774
		Circoviridae	39
4	Cerebrum	*Anelloviridae*	507
		Circoviridae	29
5	Cerebrum	*Anelloviridae*	3432
		Circoviridae	4
6	Cerebrum	*Anelloviridae*	243
	Lymph node	*Polyomaviridae*	12
9	Cerebrum	*Anelloviridae*	20827
		Circoviridae	2
		Papillomavirus	27
		Polyomaviridae	1

Table 6.3. PCR detection of circovirus and parvovirus in black bear tissue samples

Case	Encephalitis	Tissue	Fresh/FFPE	Circovirus PCR		Parvovirus PCR
				Result	Assay	
1	Y	Kidney	Fresh	+	1	+
		Liver	Fresh	+	1	+
2	Y	Lymph node	Fresh	+	1	-
		Cerebrum	Fresh	-	1	-
3	Y	Lymph node	Fresh	-	1	-
		Cerebrum	Fresh	-	1	-
		Liver	FFPE	-	2	-
4	Y	Cerebrum	Fresh	+	1	-
		Liver	FFPE	-	2	-
5	Y	Cerebrum	Fresh	+	1	-
		Liver	FFPE	-	2	-
6	N	Cerebrum	Fresh	+	1	-
7	Y	Liver	FFPE	+	2	-
8	N	Liver	FFPE	-	2	-
9	N	Liver	FFPE	+	2	-
10	Y	Liver	FFPE	-	2	-
11	Y	Liver	FFPE	+	2	-
12	N	Liver	FFPE	-	2	-
13	N	Liver	FFPE	+	2	-
14	N	Liver	FFPE	+	2	-
15	N	Liver	FFPE	-	2	-
16	N	Liver	FFPE	-	2	-

Table 6.4. Summary of circovirus *in situ* hybridization testing and results.

Case	PCR result	PCR-positive tissue	*In situ* hybridization		
			Liver	Spleen/Lymphoid[a]	Brain
1	+	Kidney, liver	+	+	+*
2	+	Lymph node	-	-	-*
3	-		-	-	-*
4	+	Cerebrum	+	+	+*
5	+	Cerebrum	+	+	NT*
7	+	Liver	+	+	-*
8	-		-	-	+
9	+	Liver	NT	NT	-
10	-		-	NT	NT*
11	+	Liver	-	NT	NT*
12	-		NT	+ (LN)	NT
13	+	Liver	-	-	-

Positive UaCV ISH probe hybridization was detected in various tissues from a subset of cases. Positive results are highlighted in green.
NT=not tested due to lack of available tissue blocks or lack of adequate tissue preservation.
*Histologic diagnosis of encephalitis.
[a]Spleen tissue was tested whenever possible. In case 12, spleen tissue was unavailable but positive ISH probe hybridization was observed in other lymphoid tissues (lymph nodes).

Table S6.1. Foci of probe hybridization in cases exhibiting ISH signal in sections of brain. Signal was distributed throughout sections, but predominantly identified in/around small-caliber blood vessels (lumen, endothelium, wall, or Virchow-Robbins space). Counts are averages from two reviewers.

Case	ISH Probe	Vessel-associated	Neuroparenchyma	Total
1	UaCV	279	193	472
	Neg. Control	2.5	7.5	10
4	UaCV	119	45	164
	Neg. Control	1	4.5	5.5
8	UaCV	74	19.5	93.5
	Neg. Control	1	4.5	5.5

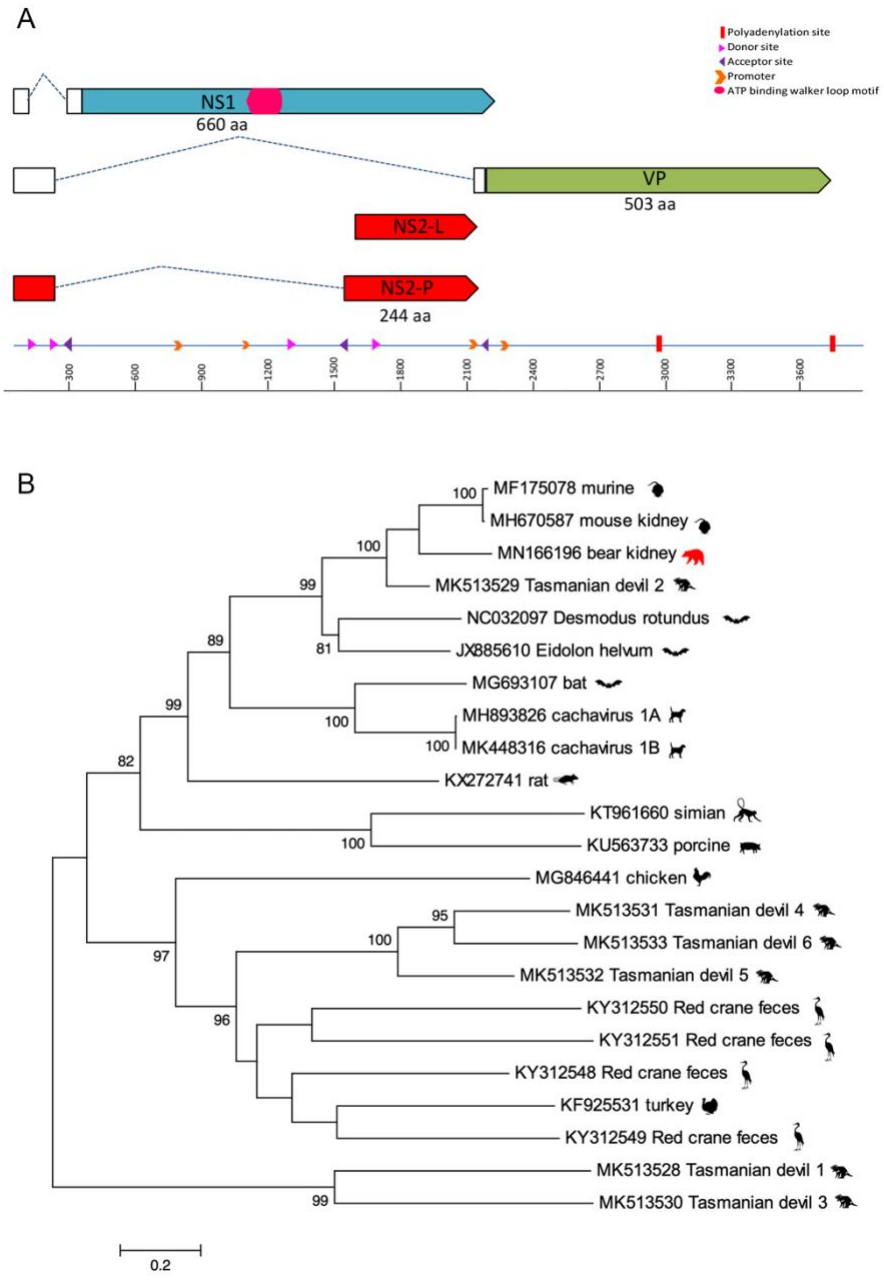

Figure 6.1. A. The genome schematic of UaPV. Clear boxes represent untranslated regions, while the dashed lines represent splicing. The arrows represent ORFs. **B.** Maximum likelihood tree of NS1 aa chaphamaparvovirus sequences. Bar, 0.2 amino acid substitutions per site. Bootstrap values below 60 were removed.

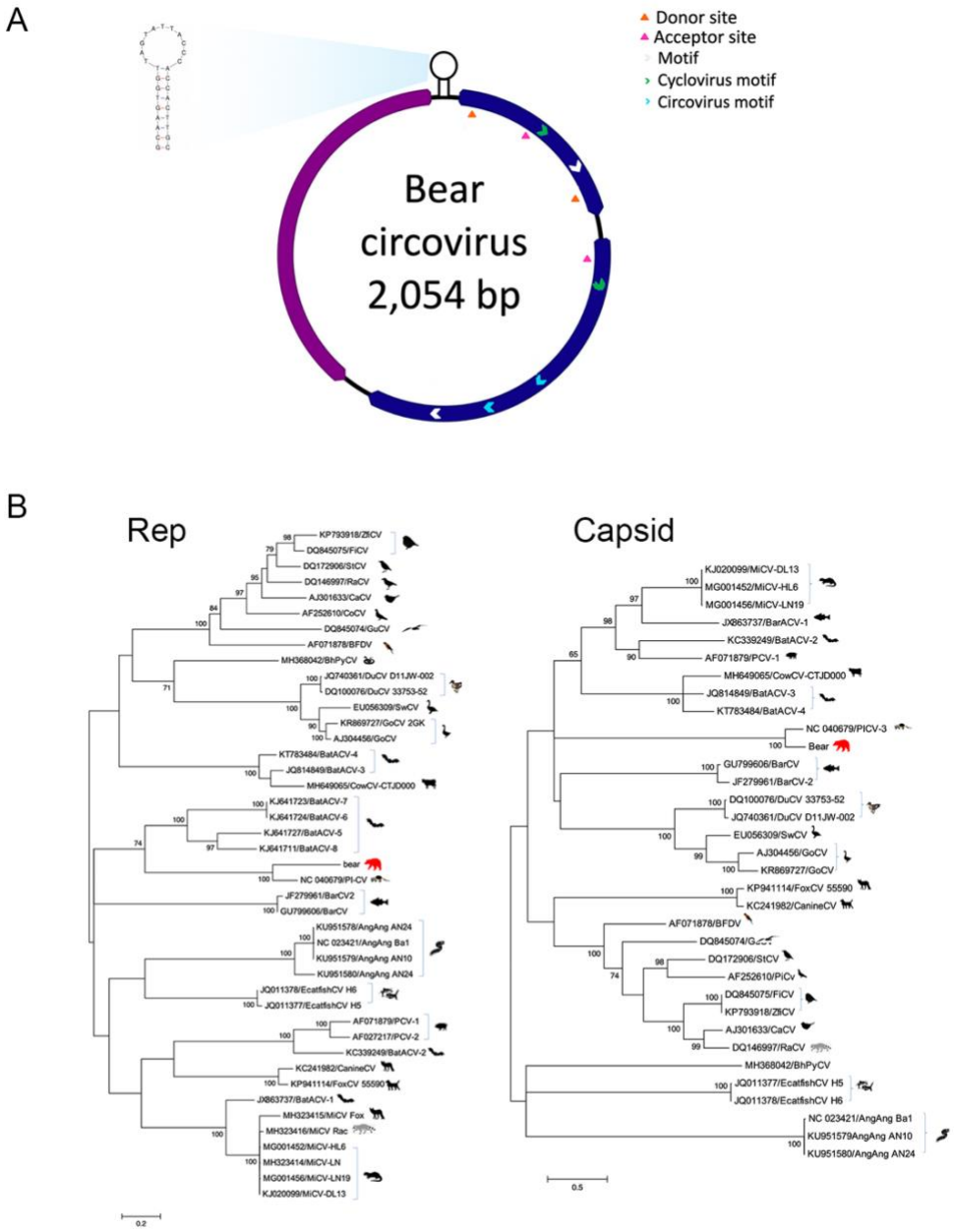

Figure 6.2. A. Genome map of *Ursus americanus* circovirus (UaCV) including Rep (blue) and Capsid (purple) genes. **B.** Maximum likelihood trees of the Rep (left) and Capsid (right) aa circovirus sequences. Bar, 0.2 (Rep) and 0.5 (Capsid) amino acid substitutions per site. Bootstrap values below 60 were removed.

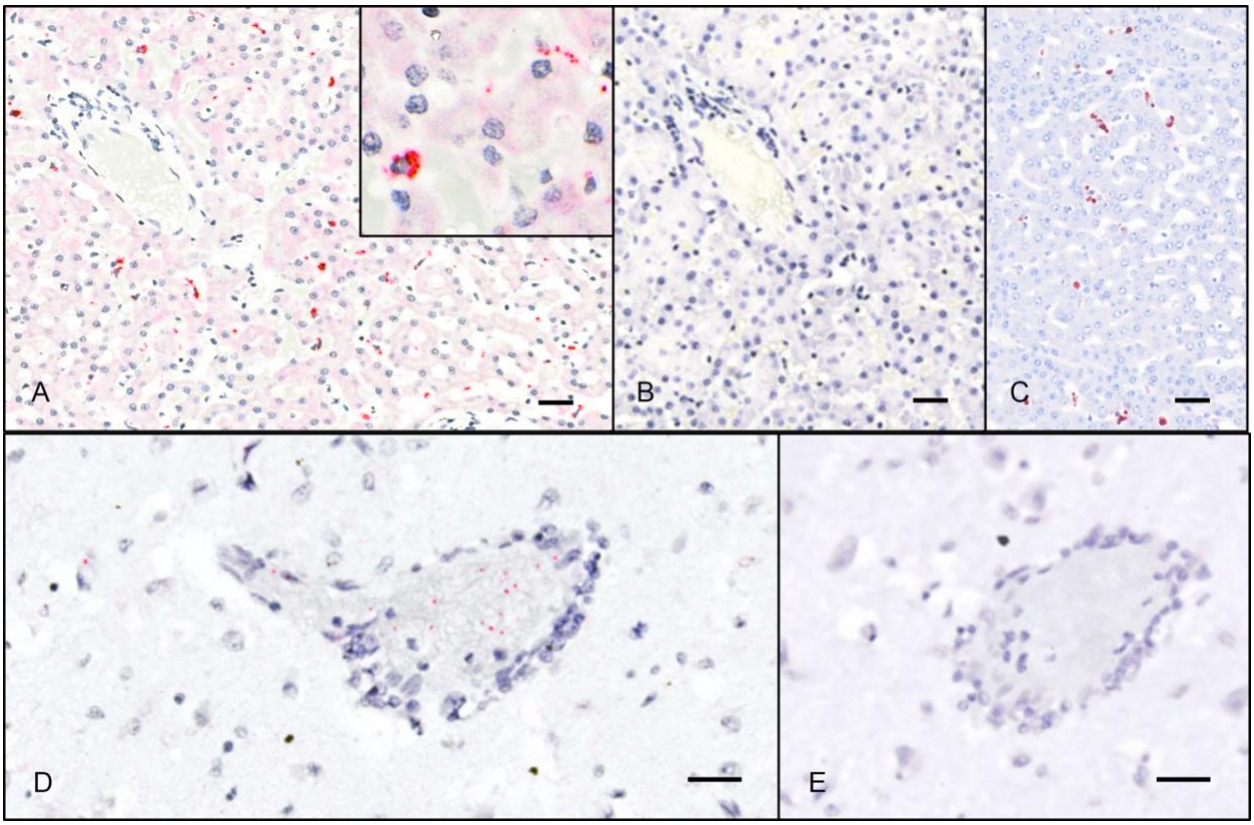

Figure 6.3. ISH detection of UaCV nucleic acid in tissue sections. Case 1. UaCV probes (A, D) and negative control (DapB) probes (B, E); hematoxylin counterstain. **A.** In sections of liver, UaCV ISH signal is detected in scattered polygonal cells (presumed Kupffer cells or endothelial cells) in hepatic sinusoids. Inset: higher magnification of a cell exhibiting positive probe hybridization. **B.** No signal is detected with negative control (DapB) probes. **C.** Immunohistochemistry for PCV2 in the liver of a pig demonstrates a similar pattern of immunoreactivity. (UC Davis SVM archives. IHC performed at California Animal Health and Food Safety Laboratory, Davis CA.) **D.** Sections of brain exhibit punctate UaCV ISH signal in and around small-caliber blood vessels. **E.** No signal is detected with negative control probes. Bars = 25µm.

CHAPTER 7:

Summary and Conclusions

Charles Alex DVM, DACVP

The studies presented in this dissertation interrogate the impact of novel parvoviruses in North American free-ranging and zoo-housed wildlife. The overarching goal was to integrate epidemiological data and examination of natural disease to clarify the population-level significance of these persistent viral infections. The advent of highly sensitive sequencing techniques has given rise to the burgeoning field of virome studies and the identification of myriad novel viral sequences. Our ability to detect viruses now far outpaces our ability to determine their consequences for the host – particularly when the expression of clinical disease is inconsistent. The combination of epidemiology and pathology data can provide meaningful insight into novel potential pathogens in all species, among which new members of the *Parvoviridae* are well represented.

The studies presented here focus on members of two rapidly growing Parvovirus genera:

The Amdoparvoviruses have expanded in just the past decade from a monotypic genus to one that includes five officially recognized members, with a growing roster of species awaiting recognition or ineligible for recognition due to incomplete sequence data. It is highly likely that a rich diversity of Amdoparvoviruses remains to be discovered, and the few studies to date that examine Amdoparvovirus-associated disease – including studies in this dissertation – suggest that they can be significant pathogens. In this context, it is critical that we determine the range of possible outcomes of infection, and the factors mediating host range and virulence. For

a critically endangered species like the red panda, such studies are immediately valuable for species conservation goals, in addition to their value as models for comparative studies. For an abundant, free-ranging wildlife species like the striped skunk, these studies are opportunities to evaluate viral dynamics unfettered by the captive setting, and in a species with significant opportunities to transmit infections (to conspecifics or potentially other species) in rural, suburban, and even urban settings. The studies presented in this dissertation provide foundational information for future studies of amdoparvoviral phylodynamics and pathogenesis.

The Chapahamaparvoviruses have recently risen to prominence thanks to the discovery of Mouse Kidney Parvovirus (MKPV). MKPV is now the recognized cause of renal lesions in laboratory mice that, despite careful scrutiny, remained enigmatic for decades. That this virus remained undetected for so long, and in a population under such vigilance, underscores the insidious nature of these persistent pathogens. As a complement to the Amdoparvovirus studies, this dissertation also includes a study describing the discovery and initial characterizations of a novel Chapahamaparvovirus and a novel Circovirus in free-ranging black bears. The studies are linked thematically by the shared goal of characterizing the significance of novel, persistent, and potentially pathogenic viruses in wildlife.

Chapter 2 describes the basic epidemiological context of Red Panda Amdoparvovirus (RPAV) in US zoos. Prior to this study, RPAV had only been reported in a single zoological collection. By prospectively sampling feces from across the US zoo-housed population, we established that RPAV infections are widespread in red pandas throughout this population. RPAV was detected in samples from 52/104 apparently healthy red pandas, representing 25/37 zoological cohorts tested. Further, by repeated sampling from red pandas of an RPAV-positive

cohort, we demonstrated consistent shedding of viral nucleic acid over a four-year period. Taken together, these findings suggest that RPAV infections are likely persistent and generally carried asymptomatically in individual hosts. Phylogenetic analysis of viral sequences from these samples demonstrated the presence of three distinct RPAV lineages, with multiple lineages sometimes present in the same cohort. Although it remains to be demonstrated definitively, this finding suggests the strong likelihood of three independent introductions into the zoo-housed population, possibly from three different asymptomatically infected, wild-caught founder animals, with infections transmitted among cohorts when red pandas are transferred between institutions for breeding or management purposes. Evaluation of additional historical samples from zoo red pandas, and testing of free-ranging red pandas from their native habitat, would help to clarify the natural history of RPAV and its patterns of spread throughout the zoo population.

Chapter 3 presents a parallel consideration of the epidemiology of Skunk Amdoparvovirus (SKAV) in free-ranging animals across North America, with consideration of its evolutionary dynamics and routes of transmission. We investigated the prevalence and phylogenetic relationships of SKAV in multiple, distant sites in the US and Canada. With an overall rate of detection of 79.2%, and with infected animals detected in every region tested, we significantly expanded the known range of SKAV in North America. Indeed, SKAV appears to be endemic throughout the striped skunk population, with a high degree of genetic variation and local diversification due to genetic drift, suggesting a long-term virus-host association. SKAV phylogenies are also influenced by recombination, as demonstrated by multiple well-supported breakpoints throughout the genome, mainly localized within three ‘hot spots.’ We demonstrated differing evolutionary pressures in the nonstructural (NS) and capsid (VP) genes, characterized

by a higher percentage of positively selected sites in NS and an overall greater genetic diversity in NS than in VP. This relative conservation of antigenic capsid sequences has been suggested as a possible indication of a distinct mechanism of pathogenesis, wherein conserved VP epitopes promote immune detection and subsequent antibody-dependent enhancement of infection (ADE). This remains to be demonstrated conclusively.

Chapters 4 and 5 describe efforts to characterize pathologic manifestations of RPAV and SKAV, respectively. Having demonstrated that both viruses occur at high prevalence in asymptomatic animals, our assignment of causality relied on the colocalization of virus with lesions. Using RPAV- or SKAV-specific probes in chromogenic *in situ* hybridization (ISH) assays on formalin-fixed, paraffin embedded tissue sections, we identified a spectrum of lesions that are likely attributable to Amdoparvovirus infection in both species. Similar manifestations were noted in red pandas and skunks, and Amdoparvovirus-associated lesions in both species were largely reminiscent of those typical of Aleutian Mink Disease Virus (AMDV) infection in mink, with some exceptions. RPAV and SKAV both appear to be associated with myocarditis, arteritis, chronic tubulointerstitial nephritis, interstitial pneumonia, and oral mucosal inflammation/ulceration. In red pandas, a distinct manifestation involving multisystemic pyogranulomatous lesions was observed in several cases. Notably, while AMDV-infected mink often develop membranoproliferative glomerulonephritis (MPGN) – attributed to antigen-antibody complex deposition – MPGN was not a common feature in the red pandas or skunks examined in these studies. Heavily plasmacytic inflammatory infiltrates colocalizing with virus-specific probe hybridization were noted in some cases, reminiscent of the exuberant humoral response in mink with AMDV, but whether a similar type 3 hypersensitivity reaction occurs in

these species – and the potential contribution of antigen-antibody complex deposition to the development of lesions – remains to be determined. Tissue targets of Amdoparvovirus infection in red pandas and skunks appear to include both epithelium (oral mucosa, renal tubular epithelium) and mesenchymal cells (endothelium, leukocytes). Despite the evidence of asymptomatic infections in both species, these studies provide strong support for the role of RPAV and SKAV in causing significant disease. The factors mediating virulence – potentially including host immunity, viral genotype, and co-pathogens – remain to be determined.

Chapter 6 incorporates concepts from the previous chapters in assessing the significance of several novel viruses – in particular a novel Chapahamaparvovirus and a novel Circovirus – as they relate to a syndrome of idiopathic encephalitis in free-ranging black bears. These presumably persistent viruses were discovered by metagenomic analyses, and subsequently evaluated for prevalence and association with lesions. *Ursus americanus* Parvovirus (UaPV) was only detected in a single case, and while it was not apparently associated with the clinical presentation and lesions in question, the discovery expanded the known host range of Chapahamaparvoviruses, some of which are known to cause disease. *Ursus americanus* Circovirus (UaCV) was detected in 10/16 cases, and expands the known host range of the *Circoviridae*. Because of this high rate of detection, cases were evaluated for an association with lesions by ISH. Positive probe hybridization was observed in multiple tissues, including brains of bears with and without diagnoses of encephalitis. Although a clear correlation with lesions was not established, the demonstration of virus in these sections – generally associated with blood vessels and the perivascular space – was intriguing and warrants further evaluation.

Future directions:

Impactful follow-up studies should focus on expanding our understanding of viral infection dynamics, including molecular mechanisms of infection, effects on individual hosts, and – particularly in the case of the red panda – epidemiological factors that may influence conservation goals.

An important question, as yet unanswered, is whether Amdoparvoviruses are indeed species-specific. Examples of apparent cross-species infections are reported, but most studies that suggest multi-host tropism have relied on serological methods rather than specific sequence identification. Determining the specificity of serological methods for distinct Amdoparvovirus species would paint a clearer picture of the potential distribution of viruses across multiple hosts. (I.e., in studies that detected "anti-AMDV antibodies" in multiple hosts, were the detected infections in fact all AMDV, or rather a variety of Amdoparvoviruses that are specific in their respective hosts?) Also critical in understanding species specificity is the question of how Amdoparvoviruses behave upon infection of a potentially novel host. One suggestion is that the apparent specificity of infections could be attributable to adaptation via intra-host evolution. This could only be rigorously tested in an experimental setting, for example by infecting a potentially susceptible species with various amdoparvoviruses and tracking infection status and sequence distribution over time. The observation of consistent viral evolutionary changes (e.g., RPAV sequences becoming more AMDV-like in experimentally infected mink) could support the hypothesis that Amdoparvoviruses can infect a range of species and rapidly adapt to novel hosts.

Determining the impact of viruses on individual animals is, of course, critical for understanding pathogenesis. Several potential lines of inquiry are possible in this regard. One important next step is to more specifically identify cellular targets of infection, which, as

demonstrated in this thesis, likely include leukocytes, endothelial cells, dendritic cells of the spleen and lymph nodes, and various types of epithelium. Co-labeling studies in archived tissues, combining ISH and cell-specific immunohistochemical markers, could help to define this more clearly. Correlating viral distribution by ISH and markers of cellular activity (such as markers for mitosis and apoptosis) will also be useful for understanding consequences of infection at the cellular level. Single cell RNA sequencing of blood samples from infected animals would also provide useful data in this regard. In particular, identifying the immune cell targets of infection – and subsequently interrogating any perturbation of their function when infected – would be very useful in determining immunological consequences of infection. Serial quantitative serological assessments would be helpful for determining whether a non-neutralizing humoral response contributes to the pathogenesis of other Amdoparvoviruses, as it does for AMDV.

Additionally, building upon the sequence and pathology data produced in this thesis, archival samples could be evaluated to determine whether particular disease manifestations are correlated with specific viral sequences. It is clear that multiple viral clades can be associated with a given disease manifestation. Identifying specific viral mutations that are associated with particular outcomes will be difficult given the high degree of genetic variation observed within viral species, but such analyses may be possible if a sequence data and lesion distribution are evaluated from a more robust archive of necropsy material. Assessing intra-host viral diversity, by comparing sequence data from lesions and from putative sites of persistence, may also be helpful in this regard.

For the critically endangered red panda, a clearer picture of RPAV epidemiology is needed. In the zoo-housed population, extensive record-keeping and the availability of archival samples would enable a detailed social network analysis that could track the spread of infections

throughout the population, potentially even identifying infected founder animals, and could be integrated with husbandry/management data and animal demographics. This would be helpful for identifying risk factors associated with infection and disease, and determining whether management changes are necessary or possible to decrease the prevalence or even eradicate RPAV from the population. Investigations in free-ranging red pandas are also needed to determine the prevalence (if any). Ultimately, a prophylactic vaccination program would be ideal, but vaccinations (for AMDV) have so far been unsuccessful due to the non-neutralizing nature of the antibody response and subsequence antibody-dependent enhancement of infection. Significant progress has been made in the area of vaccine development, particularly with mRNA-based vaccines during the SARS-COV2 pandemic. Novel vaccination strategies could be tested in non-endangered species, such as striped skunks, and adapted for use in red pandas if determined to be safe and effective.

In summary, the studies presented in this dissertation aimed to characterize the impact of novel, persistent viruses – particularly parvoviruses – in several free-ranging and zoo-housed wildlife species. Studies of viral persistence are challenging, as disease manifestations may vary markedly depending on extrinsic factors such as host immunity and co-infection. This challenge is compounded by the difficulties inherent in studying natural disease in wildlife, where sample availability, sample quality, and conservation status can limit the scope of investigations. Nevertheless, these studies significant expand our collective understanding of a growing but heretofore underappreciated group of potential pathogens. The hope is that these studies can provide a stepping stone for future work, aiming to advance our understanding of viruses and their pathogenesis, to promote wildlife health (and all health), and to help save species.